Freie Universität Berlin

Analysis of telomere length in patients with chromosomal instability syndromes, particularly Nijmegen Breakage Syndrome (NBS) and its mouse model by complementary technologies

Inaugural-Dissertation
to obtain the academic degree
Doctor rerum naturalium (Dr. rer. nat.)

Submitted to the Department of Biology, Chemistry and Pharmacy
of Freie Universität Berlin

By

Raneem Habib

From: Lattakia, Syria

Date of birth: 24-10-1980

Year of submission: 2012

2008 – 2012

Supervisor

Prof. Dr. Karl Sperling

Institute of Medical and Human Genetics

Charité University-Berlin, Germany

1st Reviewer: Prof. Dr. Karl Sperling

2nd Reviewer: Prof.Dr. Rupert Mutzel

Date of defence: 20.07.2012

Table of contents

Abbreviations:

ABI	Applied Biosystem
ALT	Alternative Lengthening of Telomeres
AT	Ataxia telangiectasia
bp	Base pair
BrdU	Bromodeoxyuridine
DAPI	Diaminophenylindolhydrochlorid
cDNA	complementary Deoxyribonucleic acid
CGH	Comparative Genomic Hybridization
Ct	Cycle threshold
Cy3	Indocarbocyanin dye 3
dH_2O	Distilled water
ddNTPs	Dideoxynucleotides triphosphates
DAPI	Diaminophenylindolhydrochlorid
DNA	Deoxyribonucleic acid
DSBs	Double strand breaks
dNTP	Deoxynucleotide triphosphates
EBV	Epstein–Barr virus
FA	Fanconi anemia
FB	Fibroblasts
FISH	Fluorescence in situ hybridization
G1	Gap 1
Gy	Gray
HR	Homologous recombination
hTERT	Human telomerase reverse transcriptase
Ig	Immunoglobulin
Kb	Kilo base pairs
LCLs	Lymphoblastoid cells lines
µg	Microgram
ml	Millilitre
µl	Microlitre
NBS	Nijmegen breakage syndrome
NHEJ	Non-homologous end joining
P	Passage
POT	Protection of telomeres
Q-PCR	Quantitative polymerase chain reaction
RNA	Ribonucleic acid
SB	Southern blot
SCEs	Sister chromatid exchanges
SV40	Simian virus 40
TRF	Telomeric repeat binding factors
UV	Ultraviolet
WCP	Whole Chromosome Painting
WS	Werner syndrome
WT	wildtype
XP	Xeroderma pigmentosum

1. Introduction

What do protozoa, such as *Tetrahymena* and human cancer cells, e.g. HeLa cells, have in common? In principle, they can divide indefinitely or in other words: They are potentially ''immortal". In contrast, fibroblast cultures derived from human skin have only a limited capacity to proliferate before they undergo ''senescence". Moreover, the number of cell divisions in culture is negatively correlated with the age of the donor. The underlying, common principle between these observations is the length of telomeric DNA. Telomeric DNA is an evolutionary highly conserved repetitive sequence which plays a crucial role both in cellular senescence and in carcinogenesis. In addition, a number of human genetic disorders have been identified which are characterized by dysfunctional telomeres, a defective DNA damage response, limited cell proliferation capacity *in vitro* and a highly increased cancer risk. Thus, telomere biology is directly linked to basic biological phenomena such as aging, tumorigenesis, maintenance of DNA integrity and chromosomal instability. Recent investigations have focused on shortening of telomeres, which is one of the hallmarks of the aging process. Telomeres are located at the ends of chromosomes and have an essential role in maintenance of genome stability in all eukaryotes. Shorter telomeres have been associated with an increased incidence of diseases and poor survival. The speed of telomere shortening can be increased or decreased by certain environmental factors. Healthy diet and sporty activities can reduce the rate of telomere shortening, which delays onset of age-associated diseases and increases lifespan.[1]Telomeres are nucleoprotein structures that protect chromosome ends from extensive shortening by exonucleolytic degradation, prevent inter- and intra-chromosomal fusion, and reduce chromosomal instability.[2] Telomeres become shorter with every cell division due to the end replication problem which will be discussed later in this thesis. The length of telomeres can be used to determine the cell's age and how many more times the cell can divide. They can be considered a cellular clock, which defines the number of cellular divisions and protects the cells from uncontrolled proliferation. When telomeres become too short, the cell stops replicating and enters into a phase known as cellular senescence. This process leads to cells aging and death by apoptosis. When somatic cells escape apoptosis, this can result in oncogenic transformation leading to the development of cancer. The investigation of the molecular mechanisms of aging could lead to a new treatment strategy for various age-associated diseases, such as neurodegenerative diseases, cancer as well as lifestyle-related diseases.[3]

The recent study of telomere length revealed that in most human tissues telomere shortening is correlated with age, except for brain and myocardium tissue. Yearly telomere length reduction in various tissues was shown to be in the range of 20–60 base pairs (bp) which is equivalent to only one round of mitosis. [4]

1.1. An early history of telomere biology

The story of telomere started in 1938 when the American geneticist Hermann Muller (1890-1967, Nobel laureate 1946), who had studied the genetic effects of radiation (X-ray mutagenesis) in the fruit fly *Drosophila*, noticed that the irradiated chromosomes never exhibited free ends. Muller considered the natural chromosome ends as terminal "genes" which might have an important function in sealing the end of chromosome. At that time he was unaware of the nature of these chromosome ends. He coined the term "telomere" from the Greek *telos* meaning "end" and *meros* meaning "part".[5,6,7]

Around the same time, the American scientist, Barbara McClintock (1902-1992, Nobel laureate 1983) observed in maize that X-ray induced or spontaneous chromosome breaks resulted in fusion of their ends. McClintock noticed that the intact chromosome ends, the "natural ends", had a unique function which is different from broken chromosome ends caused by X-ray irradiation or mechanically (e.g. breakage–rejoining–bridge cycle of ring chromosomes), as the broken ends never fused with the "natural ends".[8, 9] This observation in plants was in agreement with Muller's results in animals. They both showed that the ends of eukaryotic chromosomes are capped by special structures called telomeres or ''natural ends" , which play a crucial role in the integrity of chromosomes. Their discovery laid the foundation for the modern telomere biology. However, the molecular nature of the telomeres was unknown at that time.

The sequence of telomeric DNA tandem repeats was determined in 1975 by Elizabeth Blackburn and Joseph Gall. These two biologists studied DNA in the macronucleus of the single-celled ciliate *Tetrahymena* at the University of Yale. Like other ciliates *Tetrahymena* has a conventional micronucleus and an unusual macronucleus where the chromosomes are fragmented into thousands of gene-sized pieces. Blackburn and Gall isolated the fragments containing the genes for ribosomal RNA (rDNAs). The ends of these rDNA fragments contained tandem arrays of the hexanucleotide sequence 5'$(CCCCAA)_n$3', where *n* was between 20 and 70.[10]

In the 1980s, Jack Szostak, a molecular biologist at Harvard Medical School, designed a linear plasmid that allowed Blackburn and Gall to clone the budding yeast telomeres and to map their sequences.[11] It was still unclear how these repeats prevented the loss of DNA from the telomere after each round of DNA replication. However, they realized that the replicated plasmids had a greater length than expected. Blackburn and Szostak suggested that the telomere elongation was due to the activity of an unknown enzyme capable of synthesizing telomere repeats.[12] Blackburn and her student Carol Greider spent years to prove that in the macronucleus of *Tetrahymena* (with its 40.000 telomeres) the repeats were added to chromosome ends by a special enzyme. Finally in 1989, they identified the enzyme which adds the short repeats to the 3' ends of the DNA molecules and called it ''telomerase''.[13] For their discovery of telomeres and telomerase, Elizabeth Blackburn, Jack Szostak and Carol Geider were awarded the Nobel Prize in 2009.

1.2. The structure and function of telomere

Telomeres are specialized non-coding regions of DNA which form, in association with various proteins, the ends of chromosomes. In vertebrates, including humans, the telomeric DNA is comprised of a long tract of double-stranded (TTAGGG)n repeats (hexameric TTAGGG in the leading strand and CCCTAA in the lagging strand in humans) which extends for 5-15 kilobases (kb). Each chromosome end contains approximately 1000 to 2000 telomeric repeats. [14,15,16] Vertebrate telomere ends consist of a G-rich single stranded (ss) 3'overhang.[17] The 3' end seems to terminate randomly, but a high fraction of the 5' strands end with the sequence CCAATC-5', suggesting that a nuclease with high specificity processes the 5' strand.[18] The double stranded (ds) part of the telomere is invaded by the 3' end, thereby creating ring structures of a duplex T-loop and a smaller, ss displacement loop (D-loop) [19, 20] (Fig. 1).

A variety of proteins are associated with the telomeres, six of them collectively referred to as the shelterin multiprotein complex. These shelterin proteins are TRF1, TRF2 (telomeric repeat binding factors), TIN2, RAP1, POT1 (protection of telomeres 1) and TPP1 (or PTOP). TRF1, TRF2 and POT1 are bound directly to the TTAGGG repeats. Together with the three other shelterin subunits, they allow the cells to distinguish the telomeres from DNA double strand breaks. In addition, shelterin affects the structure of the telomere terminus and controls the synthesis of telomeric DNA by the telomerase (Fig. 2).[21, 22, 23]

Telomeres have an essential role in protecting the ends of chromosomes, and without these special caps, the chromosome ends would be recognized by the DNA repair machinery as

DNA double strand breaks (DSB). In addition, telomeres prevent chromosomal ends from degradation, fusion, and rearrangements of chromosomes.[24] Thus the telomere is an important structure whose function is to prevent chromosomes instability and allow cells to divide without losing genes due to chromosome shortening associated with the phenomenon of the ‘‘end replication problem’’.

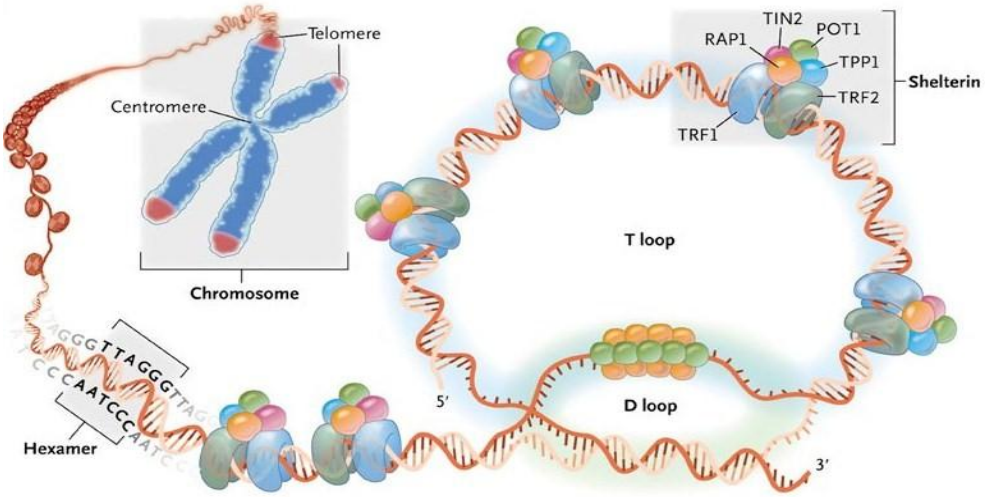

Figure 1: Human telomere structure associated with the shelterin multiprotein complex. The hexameric repeat TTAGGG characterizes the leading strand and CCCTAA the lagging strand. The 3' end of the telomeric leading strand terminates as a single-stranded overhang which folds back and invades the double-stranded telomeric helix, forming the T loop. (from Young, 2010). [25]

1.2.1. The “end replication problem”

James Watson and Francis Crick revealed the structure of DNA in 1953. Their double-helical model with two unwinding strands of DNA was revolutionary. It proposed a definition for the gene in chemical terms and paved the way for the understanding of gene action and heredity at the molecular level. The Watson - Crick DNA model also threw light on the mechanism of DNA replication. The replication of the double-stranded DNA is semiconservative; the double helix is made up of two single strands which serve as templates for the polymerization of free nucleotides by the enzyme DNA polymerase. This enzyme adds new nucleotide only to the 3' ends. Thus, the polymerization of the 3’ strand is continuously the leading strand. The opposite lagging strand is oriented in the 5' to 3' direction.[26] The lagging strand is elongated in short stretches, which are called Okazaki fragments.[27] Synthesis of the leading strand and every Okazaki fragment is primed by a short RNA primer. Thus, at the end of each round of DNA replication RNA primers must be removed and replaced by DNA. Consequently, at the 5’ end, the terminal DNA has a

gap after each round of replication by at least the length of one RNA primer and thus becomes shorter, a phenomenon called “end replication problem”. The “end replication problem” leads to shortening of all eukaryotic chromosomes, which are linear DNA molecules. Most prokaryotic and viral DNA genomes are circular, thereby circumventing this difficulty.

James Watson and Alexsei Olovnikov independently recognized this problem and pointed out that the newly formed DNA molecule will be left with a single stranded tail. Moreover, it was postulated that such incomplete replication would lead to a shortening of chromosomes over time (Fig. 2), resulting in reduced viability.[28] Olovnikov also pointed out the possible link between chromosome shortening and the limited replicative lifespan of human somatic cells observed in culture, [29,30] which can lead to cellular senescence or carcinogenesis. [31,32] The discovery of telomerase solved the “end replication problem”. The mechanism by which telomerase extends telomeres will be explained in details in chapter 1.3.

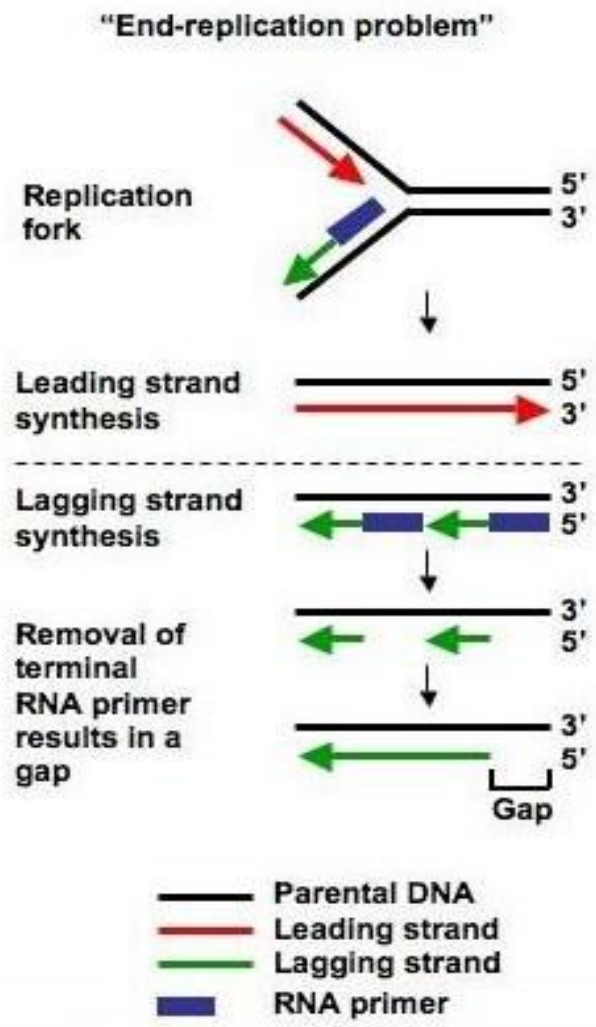

Figure 2: End replication problem: The leading strand (red) is continuously synthesized in the direction from 5' to 3' by DNA polymerase. The synthesis of the lagging strand (green) is initialized by RNA primers (blue). When RNA primers are removed, a gap is left at the 5' end of the lagging strand. (/http://gallus.reactome.org/cgibin/eventbrowser?DB=test_gallus_reactome_release_2_myisam&ID=157579&/).

1.2.2. Telomere binding proteins

A large number of proteins are associated with the telomeres. Six of them TRF1, TRF2, TIN2, RAP1, POT1 and TPP1 (PTOP) form the shelterin complex, which plays an important role in keeping telomeres away from DNA damage checkpoints and therefore protects chromosome ends from triggering the DNA repair pathways. Besides shelterins, additional proteins bind to the telomeres including DNA repair proteins (e.g. ATM, ATR, the NBS1/MRE11/RAD50 complex, DNA PKs, Apollo, Ku 70/80, WRN, BLM, ERCC1/XPF, RAD54, RAD51D and XRCC3) as well as proteins associated with the telomerase complex (e.g. TANK1, TANK2, DKC1) [33] (Fig. 3). The telomeric DNA binding proteins are also components of the double-stranded break (DSB) repair machinery

and can distinguish natural chromosome ends from DSBs and thereby protect chromosome termini from inappropriate end-to-end fusions. Additionally, telomere binding proteins recruit and regulate the activity of telomerase to ensure an appropriate length of telomere DNA, which is maintained as a buffer against loss of genetic information, stored in genes located close to the ends of linear chromosomes.[34] The task of telomere binding proteins in maintaining telomere function suggests their role in regulating cellular senescence, as well as cancerogenesis and aging. There are several genetic disorders associated with mutations in genes encoding telomere binding proteins involved in DNA damage repair, which will be discussed later.

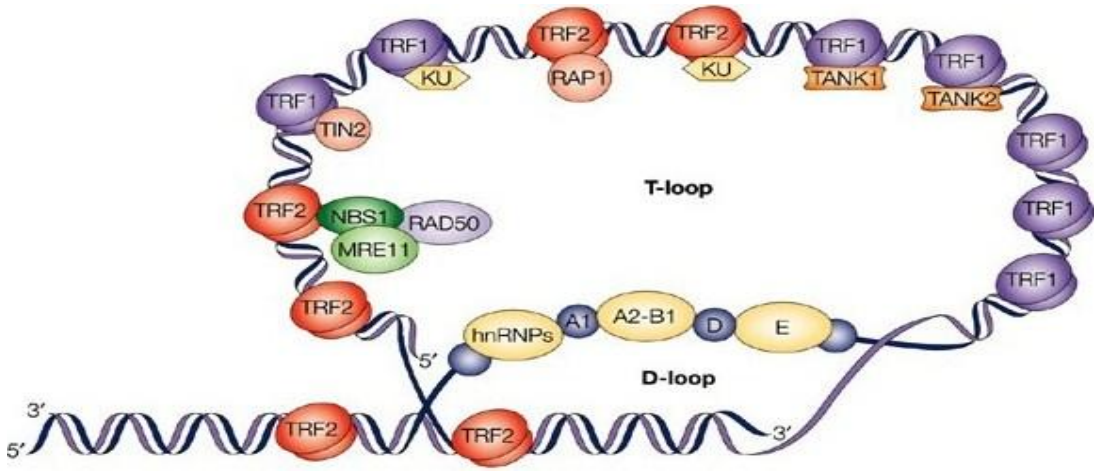

Figure 3: Telomeric DNA and protein assembly: T-loop and D-loop with the associated telomere binding proteins. (from Neumann and Reddel, 2002).[35]

1.3. Telomerase and telomere maintenance

Telomerase is present at the blastocyst stage of embryological development. It is expressed in human stem cells, human germ lines and the majority of primary human tumors. [36,37,38] It is not detectable in most normal somatic cells. The telomerase enzyme is a reverse transcriptase, which is responsible for the synthesis of telomere DNA by adding short repeats to the 3' ends of DNA strands.[39] The activity of telomerase was demonstrated for the first time in the extracts of mating *Tetrahymena*, where it added telomeric repeats TTGGGG to the 3' end of DNA strands. This enzyme recognizes the ending sequence of the oligonucleotide which needs to be elongated. For example, if the oligonucleotide ends with TTG, telomerase first adds GGG and then starts the next round of TTGGGG addition.[40] Accordingly, it was confirmed that telomerase is a specialized DNA polymerase and the main positive regulator of telomere length. It elongates the telomere terminus to compensate natural telomeric loss.

The composition of human telomerase was identified in 2007 by Scott Cohen working at the Children's Medical Research Institute in Australia.[41] Telomerase consists of two subunits of human telomerase reverse transcriptase (TERT), telomerase RNA (TER or TERC), and dyskerin (DKC1) [42,43,44,45] (Fig. 4).

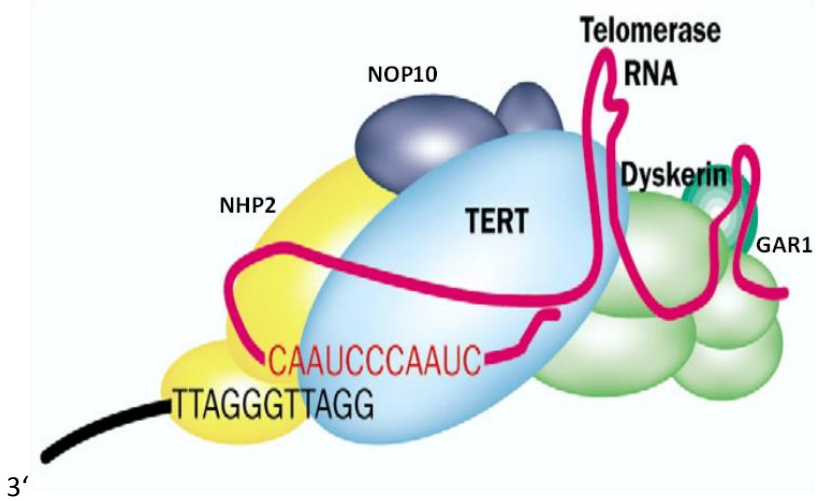

Figure 4: The human Telomerase ribonucleoprotein complex: telomerase RNA component (TERC), telomerase reverse transcriptase TERT is associated with dyskerin protein and other proteins, such as NHP2, NOP10 and GAR1, constitute the telomerase ribonucleoprotein complex. Additional subunits may be required to mediate interaction of telomerase with the telomeric repeats at the chromosome 3'end. (from Wong and Collins, 2003).[46]

In all vertebrates, including humans, the RNA sequence 3'-AAUCCC-5' acts as the template for the synthesis of 5'-TTAGGG-3' repeat unit by a mechanism shown in Figure 5. Briefly, telomerase RNA anneals to the 3' DNA overhang, which is then extended by telomerase's RNA. Telomerase's RNA serves as a template and the polymerase elongates the telomere's terminus. After the addition of a few nucleotides to the 3' overhang, the telomerase RNA moves along the newly synthesized DNA and the synthesis is continued by TERT. Primase and DNA polymerase use very long 3' overhangs as a template to generate a complementary DNA strand.[47]

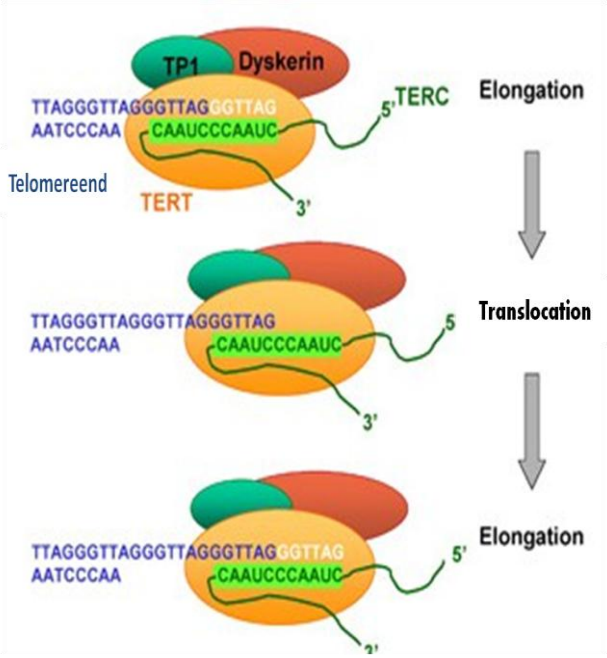

Figure 5: Telomere elongation by telomerase. Telomerase anneals to telomere via its RNA template and adds nucleotides to the end of the telomere. Telomerase translocates to the next binding site without falling off the telomere. Telomerase components TERT: telomerase reverse transcriptase (orange), TERC: telomerase RNA component (green line), the dyskerin protein (red),TP1: The RNA-binding subunit (green).(/http://www.uke.de/kliniken/medizinische-klinik-1/index_43074.php /).

There is a positive correlation between telomere length and telomerase activity. Telomerase activity is regulated at different molecular levels, including transcription, mRNA splicing, transcript maturation and modification of hTERC and hTERT. The hTERT, which contains binding sites for a large number of regulatory factors, including activators and repressors, is responsible for the catalytic activity of telomerase.[48 ,49 ,50]

1.3.1. Telomeres, telomerase and cancer

Telomerase activity is very low in most normal somatic cells. However, it can be detected at very high levels in cancer cells. About 90% of cancer cells contain short telomeres but high levels of telomerase activity make these cancerous cells “immortal” and increase their proliferation capacity. For example, 75% of oral carcinomas, 80% of lung cancers, 84% of prostate cancers, 85% of liver cancers, 93% of breast cancers, 94% of neuroblastomas, 95% of colorectal cancers, and 98% of bladder cancers have detectable telomerase activity.[51] It remains to be elucidated whether telomerase could be used as a sensitive biomarker for diagnosis, early detection, and prognosis of cancer or as potential target in the development of anti-cancer therapy.

Telomeres act as an internal mitotic clock and limit the number of cell divisions. Gradual telomeres shortening leads to the induction of senescence associated with the activation of

a number of cell-cycle checkpoint pathways. Under normal conditions, the cell cycle is arrested and cells undergo apoptosis. When the cell-cycle arrest checkpoint is bypassed, telomeres continue to shorten and are recognized as DNA double-stranded breaks. The activation of proteins involved in DNA-damage response leads to homologous recombination or non-homologous end joining of the chromosomes. Cells with unstable and aberrant chromosomes undergo apoptosis. [52,53] However, cancer cells bypass the cell-cycle checkpoints and do not undergo apoptosis. This leads to further shortening of telomeres until activation of the telomerase. Thus, in cancer cells telomeres are stabilized at a constant length, which allows the unlimited proliferation.[54,55] Aneuploidy and chromosome instability are considered hallmarks of solid tumors.[56,57] This instability can result from erroneous chromosomal segregation during cell division as well as uncontrolled telomere shortening or defects in its maintenance (Fig. 6, 7).

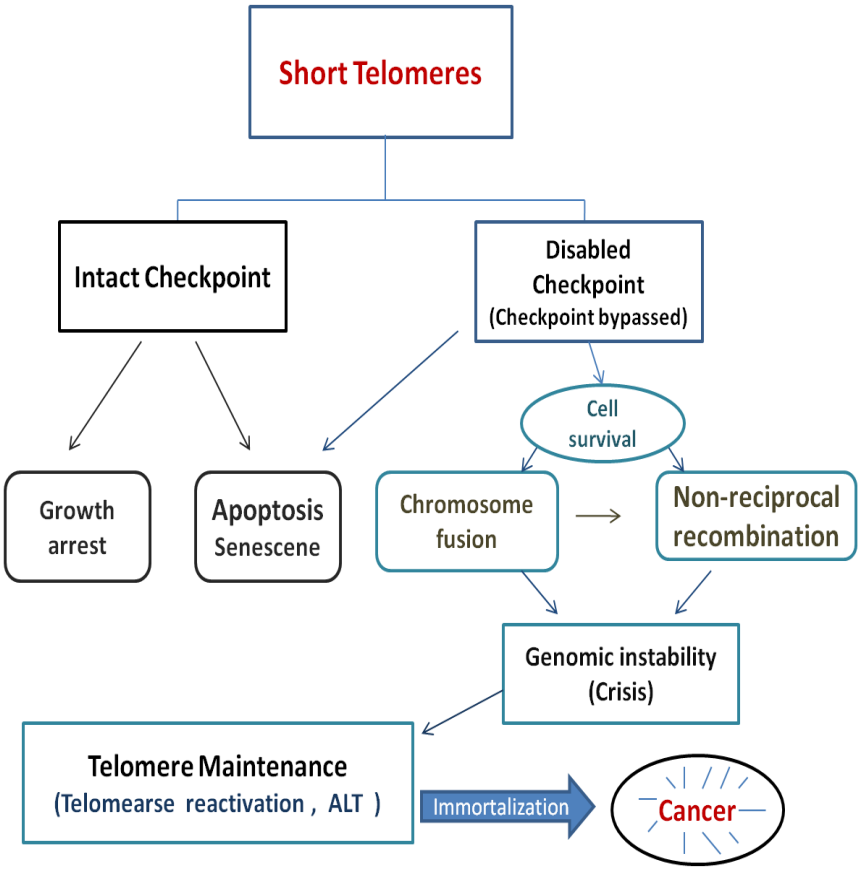

Figure 6: Cell responses to telomere shortening (telomere associated pathways). Critical short telomeres trigger either senescence or apoptosis (intact checkpoint) in normal somatic cells. In cells with disabled checkpoints, short dysfunctional telomeres trigger chromosome instability, perpetuated through recurrent breakage-fusion-bridge cycles. Few cells through reactivation of a telomere maintenance mechanism (usually telomerase or alternative lengthening telomere (ALT)) stabilize telomere length and chromosome ends resulting in cell immortalization. The cells continue dividing, which gives rise to a tumor.(after Callen and Surralles, 2007).[58]

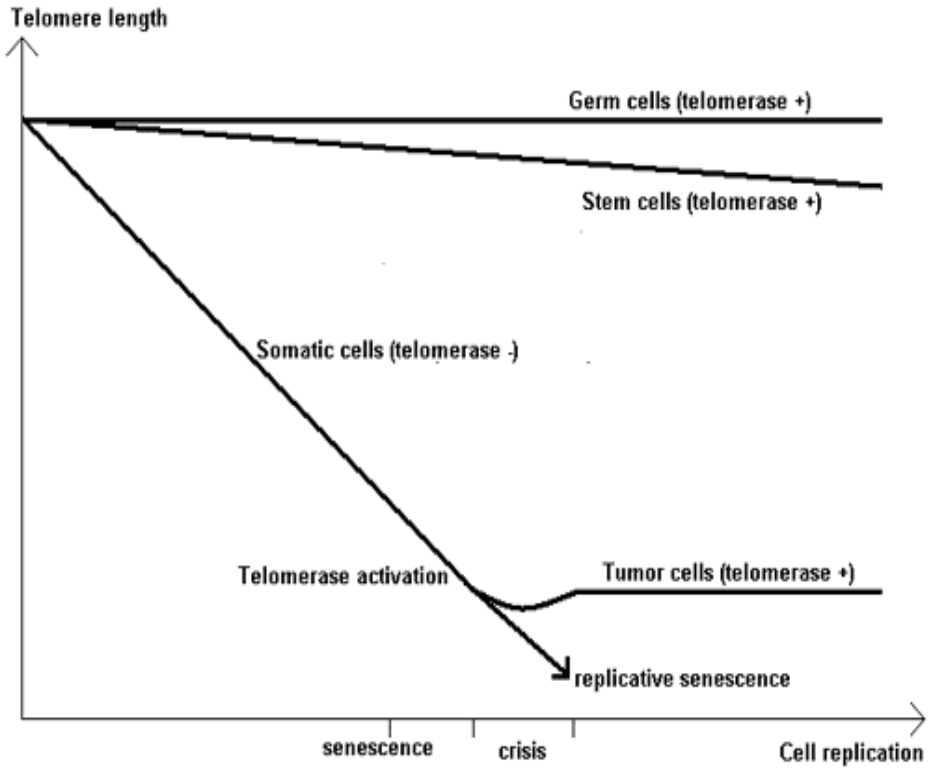

Figure 7: Telomeres-telomerase hypothesis. The two-steps hypothesis of cellular senescence and immortalization: normal somatic cells in culture have a limited proliferative life span before they undergo a permanent growth arrest, termed "replicative senescence" or "mortality" and become inactive. Telomerase is normally active in stem and germ cells but not somatic cells which require the reactivation of the telomere lengthening enzyme telomerase. However, some cells bypass the growth arrest. These cells can gain an additional lifespan and then undergo a crisis situation and proliferate indefinitely as immortal cells. (from Wai, 2004).[59]

1.3.2. Telomerase and cancer therapy

The measurement of telomerase activity could be a new diagnostic method for cancer detection. Since almost all human tumors express telomerase activity, inhibition of this enzyme has been suggested as a general mechanism in cancer therapy. Down regulation of telomerase activity can be achieved by introducing a dominant negative hTERT in immortalized cell lines. As a consequence, the telomeres become shorter and the cells enter apoptosis.[60] Thus, many pharmaceutical companies attempt developing drugs that selectively target cancer cells by inhibiting telomerase activity. However, before such inhibitors are commercially available, they must be tested *in vitro,* in model organisms and finally in clinical trials with respect to their efficiency and their side effects. There are many studies focused on targeting telomerase in cancer therapy. [61,62,63]

Moreover, if telomerase activity could be controlled, it could be used to generate stem cells. Such cells could be used for transplantation and treatment of many kinds of diseases, e.g. in diabetes by replacement of insulin-producing cells. [64, 65]

1.3.3. Alternative lengthening of telomeres

As previously explained, most cancer cells start unlimited proliferation by the activation of telomere maintenance mechanisms. The best known is the activation of telomerase. However, some cancer cells do not require telomerase to maintain their telomere lengths. In these cells, a telomerase-independent telomere maintenance pathway has been identified, the so-called alternative lengthening of telomeres ALT (Fig. 8). [66,67] Cells with ALT activity accumulate nuclear bodies called PML bodies (these react against SP100 auto-antibodies observed in promyelocytic leukemia, PML; also referred to as ALT-associated PML bodies or APBs),[68] which are found exclusively in telomerase-negative tumors. The ALT cells contain extra chromosomal telomeric DNA, telomere-specific binding proteins, and proteins involved in DNA recombination and replication. Activation of ALT during immortalization involves recessive mutations in genes that are so far unknown. A correlation was found between telomere length and the presence of nuclear bodies. The formation of these bodies might be an alternative way for cells to lengthen telomeres in the absence of telomerase. [69,70]

Since both telomere length maintenance mechanisms are crucial for immortalization of cells, it has been hypothesized that they may contribute to cancer and ageing,[71] and help to understand telomere elongation and cellular immortalization. [72]

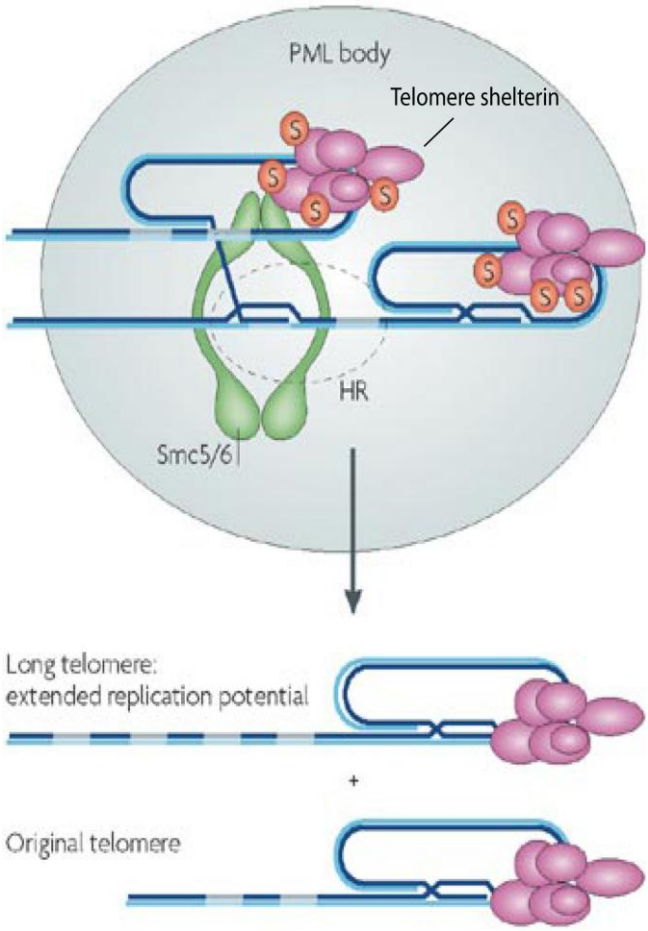

Figure 8: The Alternative Lengthening of Telomeres (ALT): PML: Promyelocytic leukemia body, SMC5/6: the structural maintenance of chromosomes localizes to APBs, In ALT cells, the Smc5/6 complex and HR (homologous recombination*)* proteins associate with PML bodies in G2 phase, **S**: sumoylation of shelterin recruits or maintains telomeres at APBs and promotes telomere HR. (from Murray and Carr, 2008).[73]

1.4. Telomere impairment in chromosomal instability syndromes

Chromosomal instability refers to inherited conditions associated with genome instability and DNA breakage, which is associated with an increase in rate of spontaneous and clastogen induced chromosomal alterations. Cancer risk is the hallmark of almost all chromosomal instability syndromes, such as Ataxia telangiectasia (AT), Werner syndrome (WS), Bloom syndrome (BS), Fanconi anemia (FA) and Nijmegen breakage syndrome (NBS). The underlying genes play a crucial role in different cellular pathways, such as DNA damage repair, DNA processing, cell cycle regulation and apoptosis. In addition, some of the proteins are also involved in telomere maintenance. [74,75,76] Figure 9 shows an integrated view of the interplay between chromosome instability syndromes and telomere biology.

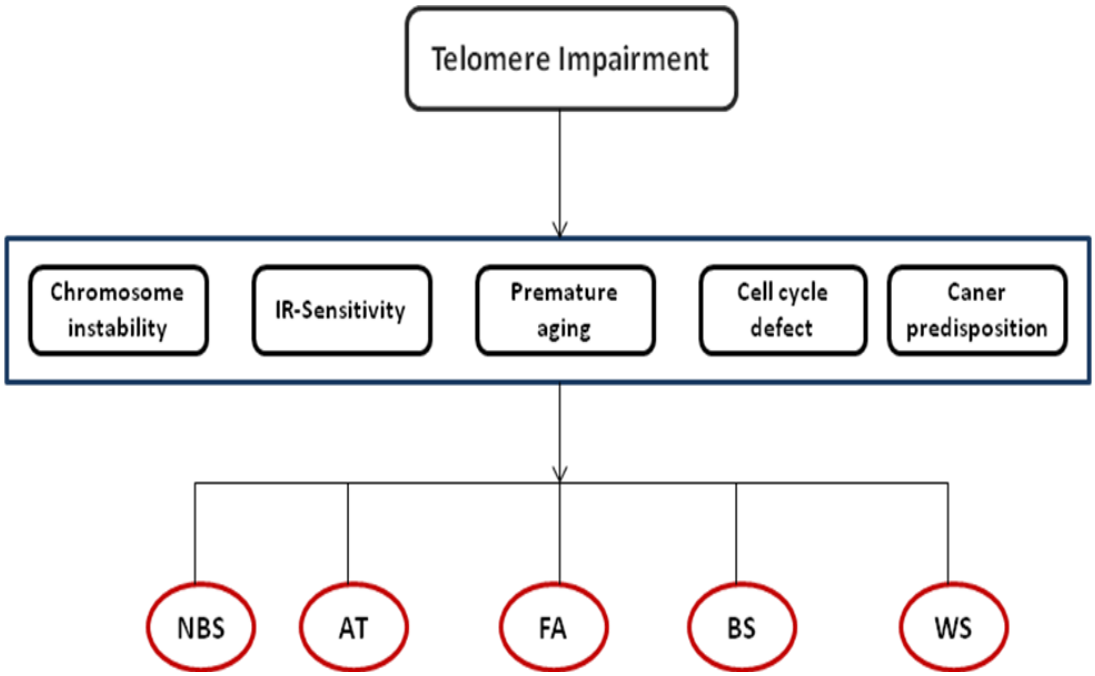

Figure 9: An integrated view of the interplay between chromosome instability syndromes and telomere biology. IR = Ionizing radiation, NBS (Nijmegen Breakage Syndrome), AT (Ataxia telangiectasia), FA (Fanconi anemia), BS (Bloom syndrome), WS (Werner syndrome). (from Callén and Surrallés, 2004).[77]

1.4.1. Nijmegen Breakage Syndrome

Nijmegen breakage syndrome (NBS), also called Berlin Breakage Syndrome, Seemanova Syndrome II and Ataxia-Telangiectasia Variant 2,[78] is a rare human genetic disorder. NBS belongs to the group of chromosome instability syndromes and is an autosomal recessive disorder. The name comes from the Dutch city Nijmegen, where the condition was first described by Weemaes et al. in 1981.[79] This syndrome is caused by mutations in the *NBN* (previously known as *NBS1*) gene that encodes the protein nibrin (also known NBS1, p95 or NBN). [80] Most NBS patients are from Central and Eastern Europe, notably Poland, the Czech Republic and Slovakia. Some NBS patients were also diagnosed in Germany and Ukraine. NBS has also been reported in Italy, France, Great Britain, Spain, Bosnia, Croatia, Turkey, Russia, Morocco, Argentina, Chile, and New Zealand. Malignancy is the most common cause of death in NBS patients.

The clinical features of NBS patients as well as the cellular consequences of relevant gene mutations will be briefly described below.

1.4.1.1. Clinical cellular, and genetic characteristics of NBS patients

NBS patients are clinically characterized by microcephaly, a distinct facial appearance with slightly upward-slanting forehead, palpebral fissures, small chin, short stature, and immunodeficiency. The intelligence seems to drop with age and mental retardation is

evident by the age of 7 years. Other features associated with NBS are growth retardation, strong predisposition to lymphoid malignancies, skin pigmentation abnormalities, such as café au lait and/or vitiligo spots, and minor limb abnormalities. The craniofacial characteristics of NBS become more obvious with patient age, probably because of progressive microcephaly in addition to a relatively long nose and a receding mandible.[81,82] Moreover, different types of ovarian failure and the associated hypergonadotropic hypogonadism are hallmark manifestations in most girls and young women with NBS.[83] Figures 10, 11 and 12 present clinical features in patients with NBS.

Figure 10: A clinical manifestation of a 6-month-old infant with Nijmegen breakage syndrome with microcephaly and other facial features such as slightly upward-slanting, palpebral fissures and small chin. (/http://emedicine.medscape.com/article/1116869-overview/).

Figure 11: Progressive vitiligo in a patient with Nijmegen breakage syndrome. (/http://emedicine.medscape.com/article/1116869-overview/).

Figure 12: Typical facial features (craniofacial characteristics) in a 9-year-old girl with Nijmegen breakage syndrome; microcephaly, markedly upward-slanting palpebral features, relatively long nose and receding mandible. (/http://emedicine.medscape.com/article/1116869-overview/).

Cells derived from NBS patients show spontaneous chromosomal instability, a sensitivity to ionizing radiation (IR), defective cell cycle checkpoint control, and failure to activate the p53 protein. Moreover, the NBS gene is also involved in the rearrangement of immunoglobin genes, which explains the high rate of rearrangements, especially of chromosome 7 and 14 in lymphocytes as well as the immunodeficiency. [84,85] Table 1 presents clinical and cellular characteristics of NBS.[86]

Table 1: Clinical and cellular characteristics of Nijmegen Breakage Syndrome

Characteristics of NBS	
Clinical features	Presence
Predisposition to malignancy	++
Radiosensitivity	+
Immunodeficiency	+
Ovarian dysgenesis	+
Hyperpigmentation	+
Growth retardation	+
Microcephaly	+
Mental retardation	(+)
Distinctive face	+ -
Cerebellar degeneration	-
Elevated α-fetoprotein	-
Cellular features	Presence
Chromosome breakage	++

Radiosensetivity	+
Radioresistant DNA synthesis	+
Defective cell cycle checkpoint control	+
Reduced p53 response	+

Nijmegen breakage syndrome has been considered for a long time as a variant of ataxia-telangiectasia (AT) because some of its characteristic abnormalities are similar to those observed in AT. However, these two diseases are genetically different.[87]

The *NBN* gene belongs to a group of DNA double-strand break repair genes. The gene is located on chromosome 8 at 8q21and consists of 16 exons, which span a region of more than 50 kb. The *NBN* gene encodes a protein called nibrin (also referred to as p95 or NBS1).[88,89] Nibrin is a 95-kDa protein, which forms a multiprotein complex with hMRE11 and hRAD50 (MRN). The MRN complex plays a role in several critical cellular functions, including cell cycle checkpoint control, DNA repair and telomere maintenance. Nibrin protein consists of 754 amino acids. The N-terminus contains two specific domains: FHA (fork-head associated) domain and BRCT (breast cancer carboxy terminal) domain.[90,91] The FHA and BRCT domains are likely to have a crucial role for both binding to histone H2AX and for relocalization of the MRN complex to the DSBs.[92] These domains seem also to be involved in cell cycle checkpoints and the process of DNA damage repair. [93,94] The C-terminal domain contains a MRE11-binding site, and this interaction is required for the nuclear localization of the MRN complex.

More than 90% of NBS patients are of Slavic origin and homozygous for the founder mutation, 657del5, a 5 bp truncating mutation in exon 6 of the *NBN* gene.[95] The remaining patients are either heterozygous for 657del5 and a second unique mutation (compound heterozygotes) or homozygous for one of nine unique mutations observed in various ethnic groups. [96,97,98,99,100] Some NBS patients were diagnosed first as FA. They had the homozygous mutation 1089C>A.[101,102] The rarer mutations are located between nucleotides 657 and 1142. A schematic diagram of the *NBN* gene with the mutation sites found in NBS patients is presented in Figure 13.

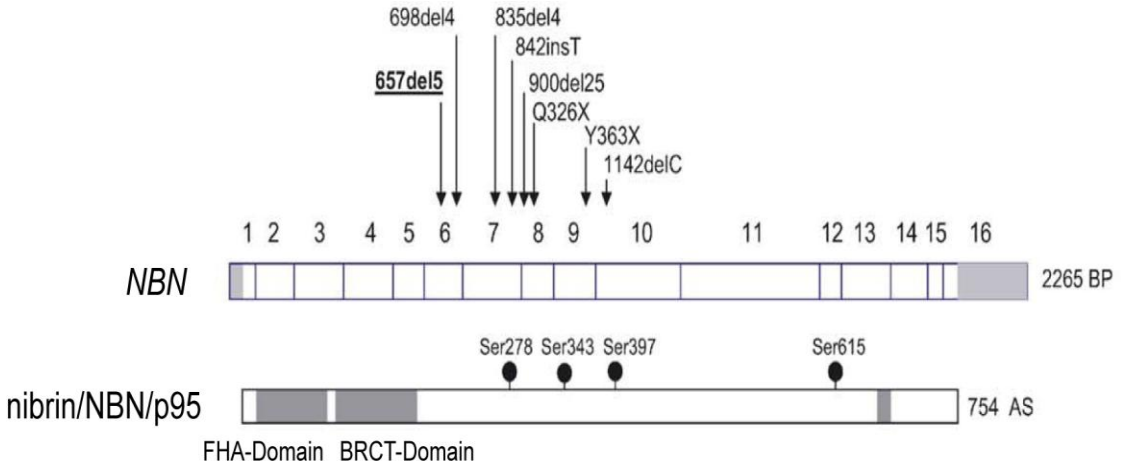

Figure 13: The *NBN* gene and its protein, nibrin/Nbs1/p95.
The exons of the *NBN* gene are shown together with the sites of some mutations found in NBS patients. Below the gene, the protein product nibrin/NBN/p95 is shown with the known domains and sites of serine phosphorylation by ATM (Ser 278, Ser 343 and Ser 397). (after Digweed and Sperling, 2004).[103]

1.4.1.2. The role of nibrin in DNA-damage repair, cell cycle integrity and telomere maintenance

Nibrin together with RAD50 and MRE11 form the MRN complex (Fig. 14). The presence of nibrin is essential for the function of this complex, which clearly has a crucial role in the viability of proliferating cells and is responsible for DNA double-strand break repair, cell cycle checkpoint signalling and telomere maintenance.[104]

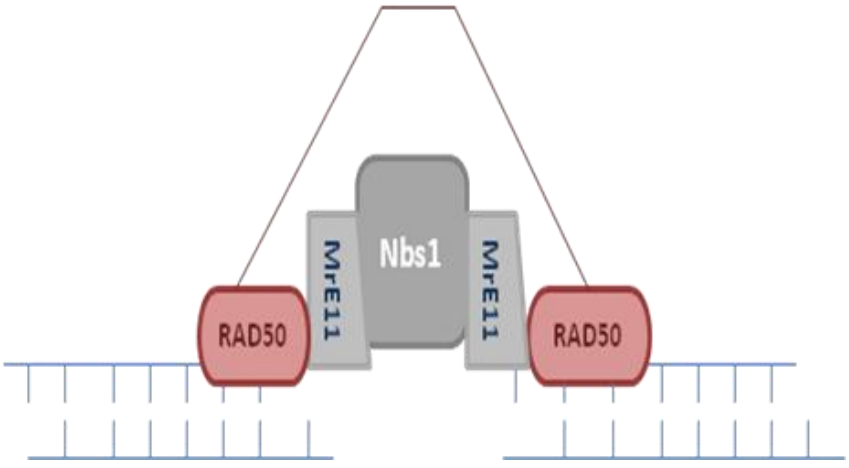

Figure 14: A general diagram of the architecture of the MRN complex. MRE11with RAD50 and nibrin attach as a complex to the broken DNA ends. As is shown here, two RAD50 molecules bridge the DSB and keep the ends together. (after Zhang, Zhou and Lim, 2006).[105]

1.4.1.2.1. Function of nibrin in double-strand break repair

DNA double-strand breaks (DSB) can arise spontaneously or due to the damaging action of the reactive oxygen species (ROS), generated as a by-product of normal cellular metabolism, and of environmental factors such as ionizing radiation. All DNA lesions must be repaired before entry into mitosis to maintain genomic integrity.[106] There are two major mechanisms of double-strand breaks repair: Nonhomologous end joining (NHEJ) and homologous recombination (HR).[107] NHEJ is an error-prone process that repairs double-strand breaks by removing some nucleotides and ligating the broken ends together. Many proteins, such as Ku70, Ku80, DNA LigIV, Artemis, XRCC4, DNA PKcs and nuclease with endo- and exonuclease-activity, are involved in this pathway. [108,109] In the HR pathway the homologous chromatid serves as a template to ensure correct repair. This process takes place after S-phase when a sister chromatid is available. It depends on a group of proteins such as RAD50, RAD51, RAD52, MRE11, BRCA1, BRCA2 and RPA.[110] The MRN complex is considered the first sensor of DSBs and is involved in the activation of DNA damage-response kinases such as ATM (ataxia telangiectasia mutated), ATR (ataxia telangiectasia Rad3-related) and DNA-PKcs (DNA-dependent protein kinase catalytic subunit) which in turn phosphorylate various proteins of the NHEJ and HR repair pathways. These proteins are transducers of the DNA damage signal and act as activators of the repair pathways.[111, 112,113,114 115,116.117, 118]

Moreover, it was demonstrated that nibrin also plays a role in the VDJ recombination process, based on DSBs, in which the immunoglobulin (Ig) and T cell receptors (TCR) genes are recombined to generate functional T- and B-cells. Therefore, lymphocytes from NBS patients are characterized by their massive chromosome instability, and consequently a high predisposition to lymphoma. Nibrin and the phosphorylated histone H2AX have been found localized to the sites of class switch recombination in B lymphocytes. [119,120,121]
In addition, it was demonstrated that nibrin affects gene conversion and sister chromatid exchanges, which possibly result from unusual crossover events, suggesting that nibrin is essential for HR pathway, at least in vertebrate cells [122,123] (Fig. 15).

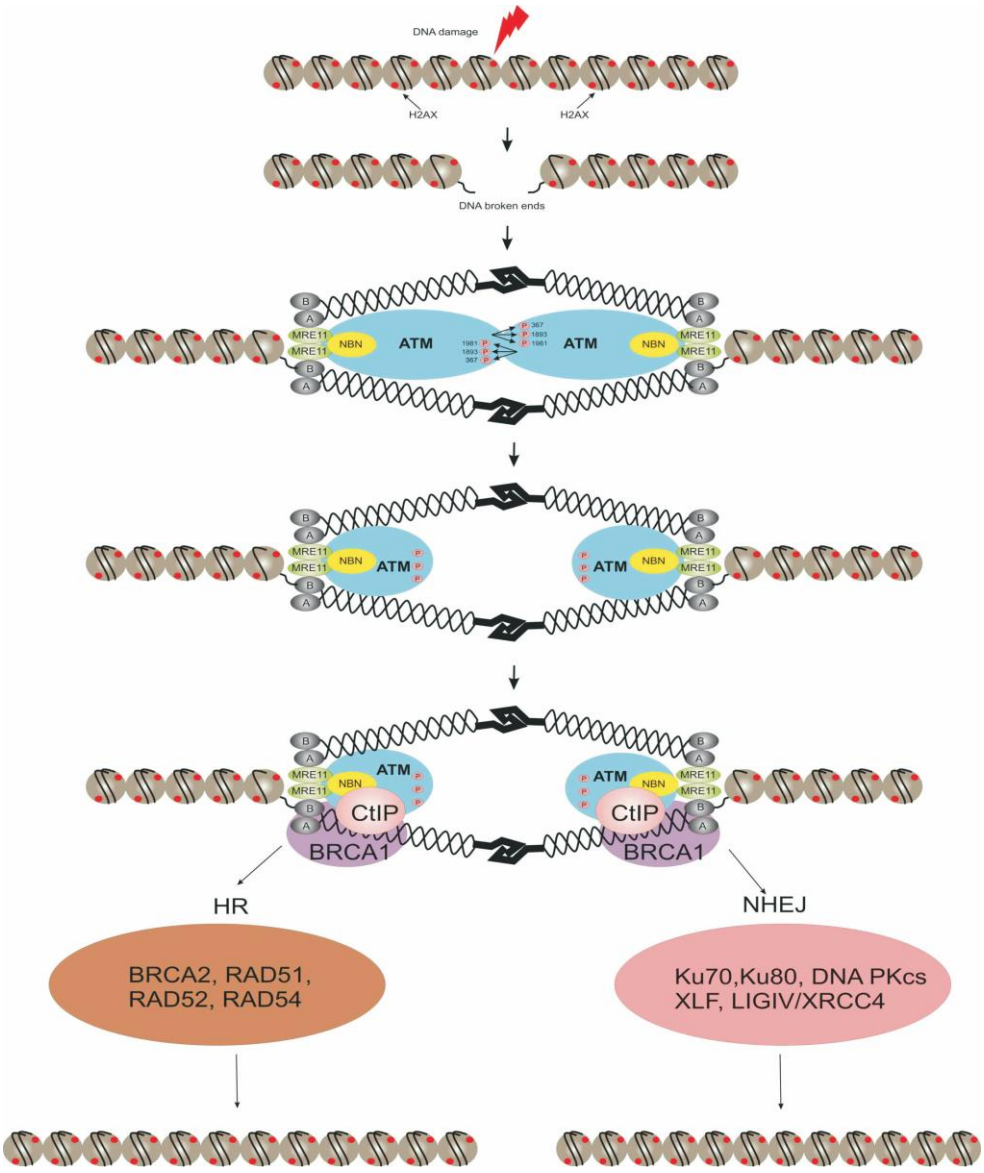

Figure 15: Schematic representation of DNA repair mechanism and the role of nibrin (NBN protein in yellow) in DNA repair machinery. H2AX: Histone H2AX is phosphorylated in an ATM-dependent manner in response to replication stress, A and B: domains of RAD50, MRE11 and NBS1 associate with these Walker A and B domains of RAD50, P: phosphorylation. Homologous recombination (HR) and non-homologous end joining (NHEJ), in addition to the MRN complex, also BRCA1 and CtIP (C-Terminal Binding Protein Interacting Protein) are involved in the activation of HR-mediated repair of DNA in the S and G2 phases of the cell cycle. (from Czornak, Chughtai and Chrzanowska, 2008).[124]

1.4.1.2.2. The function of nibrin in cell cycle checkpoint control

Various types of DNA damage which are caused by X-ray radiation, UV light, gamma irradiation, and chemical agents activate the checkpoint signaling cascades. There are three distinct checkpoints that recognize the presence of damaged DNA and arrest the cell cycle at different stages: G1/S, intra-S-phase, and G2/M. [125,126,127] The balance between cell cycle arrest and damage repair on one hand and the initiation of cell death on the other hand,

determines if the cell continues dividing or enters apoptosis. Nibrin seems to be a main modulator of cell cycle checkpoints.[128] When DNA damage occurs MDC1 (mediator of DNA damage checkpoint protein 1) directly binds to nibrin and targets it to the sites of DNA damage. The MDC1–nibrin interaction is required for the intra-S-phase cell cycle checkpoint control after DNA damage.[129] Disruption of the MDC1–nibrin interaction results in failure of nibrin accumulation at DNA double-strand breaks and the intra-S checkpoint activation. In addition it was demonstrated that nibrin was required for the activation of the ATM-CHK2 pathway that modulates the initiation of the intra S-phase checkpoint after exposure to IR. This process is activated by phosphorylation of a series of cell cycle signaling kinases. Thus, nibrin can be considered as an important factor involved in regulating the intra-S-phase checkpoint control.[130] It was shown that the expression of proteins involved in the G1 checkpoint such as p21 and p53 were reduced in NBS fibroblasts as well as in NBS lymphoblastoid cells after IR, indicating a defective or attenuated G1 arrest.[131,132,133] Thus, nibrin is also involved in the G1 checkpoint control. Phosphorylated nibrin promotes the phosphorylation of many target molecules through activation of ATM, which in turn activates CHK2 which then modulates proteins involved in the G2 checkpoint control.[134] Unlike normal cells, irradiated NBS lymphoblastoid cells have an inactive CHK2 protein and consequently a G2/M checkpoint defect. [135,136]

1.4.1.2.3. The function of nibrin in telomere maintenance

Nibrin plays an important role in telomere maintenance and extension. DNA DSB repair proteins which are involved in the NHEJ pathway such as DNA-PKcs, Ku70, Ku80, XRCC4 and Artemis, have an important role in telomere capping and in protecting the chromosome ends from inappropriate DNA repair.[137,138,139,140] Nibrin works as a modulator for ATM activation which in turn activates DNA repair proteins (as explained previously). In addition, nibrin was found to associate with TRF2, one of the shelterin proteins of the telomere, which binds exclusively to the telomere and participates in T-loop formation and stabilization. Nibrin modulates telomere function through the formation of the T-loop, which is required specifically in S-phase. The transient recruitment of nibrin to telomeres in S-phase suggests a role of nibrin in telomere replication. [141],[142] NBS patients' primary fibroblasts have short telomeres and show premature senescence during *in vitro* culture.[143] This could be corrected by transfection of the defective cells with both hTERT and nibrin.[144] Nibrin was also found to be involved in ALT, which works in the absence of telomerase, exclusively in telomerase-negative tumors as described in chapter 1.8. Nibrin co-localized with the PML bodies and was associated by the BRCT-domain with the PML-

binding protein and SP100. In addition, nibrin plays a role in recruiting recombination proteins such as RAD50, MRE11 and BRACA1 to PML nuclear bodies. [145],[146] The role of nibrin in telomere maintenance is presented in Figure 16.

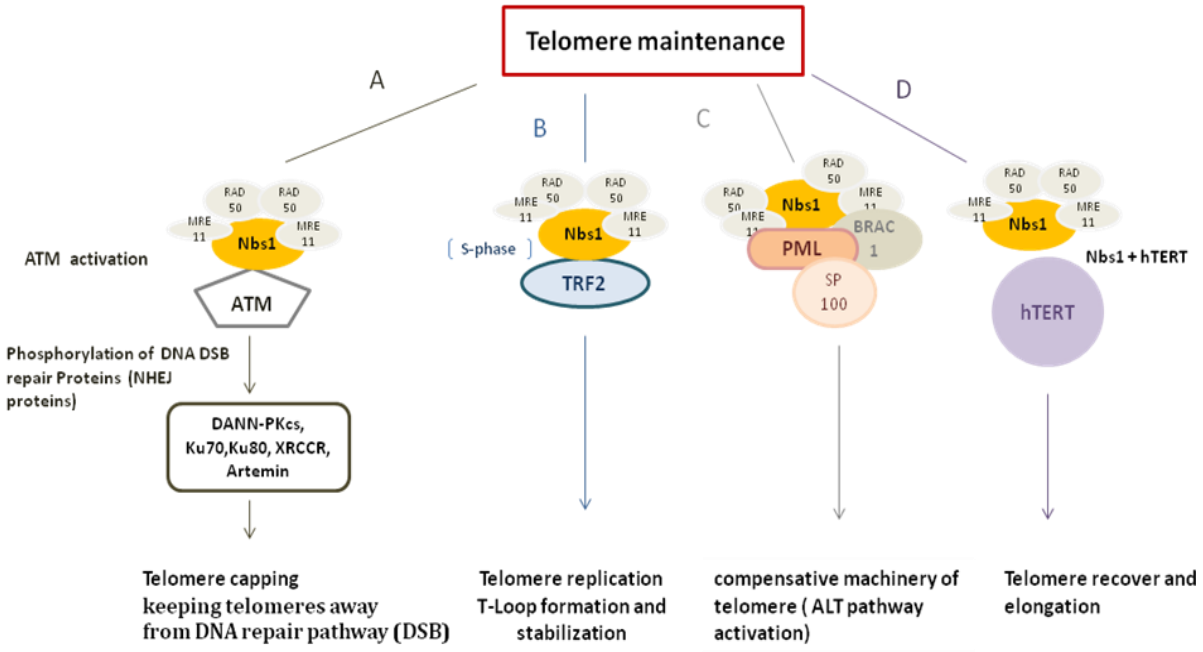

Figure 16: The role of nibrin in telomere maintenance. A: Nibrin activates the ATM kinase by phosphorylation, the activated ATM kinase modifies the DSB repair proteins such as DNA-PKcs, Ku70, Ku80, XRCC4 and Artemis, which were also found to cap telomeres in order to protect the chromosome ends from inappropriate DNA repair. **B:** Nibrin was found to associate with the shelterin protein TRF2. TRF2 binds exclusively to telomeres and participates in T-loop formation and stabilization. The nibrin-TRF2 association takes place in S-phase. **C:** Nibrin is involved in ALT through association with the PML-binding protein, SP100. Nibrin recruits other proteins, such as RAD50, MRE11 and BRACA1, to the PML nuclear body **D:** both hTERT and nibrin are able to recover telomere defects and extend the length of telomeres.

1.5. Aims of the thesis

Aim of this thesis is the analysis of telomere length in chromosomal instability syndromes, particularly in the autosomal recessive disorder Nijmegen Breakage Syndrome (NBS). The patients are homozygous for the common founder mutation. This allele is also present in a humanized Nbs mouse which serves as a mouse model of the disease. The underlying *NBN* gene is directly involved, amongst others, in telomere maintenance. Three different complementary methods to measure telomere length will be applied: Q-PCR), to measure the relative total length of telomeric repeats, Q-FISH, to determine the relative length of individual telomeres, and TRF analysis, to estimate the total absolute length of telomeric DNA. In vivo studies will be performed on in blood DNA (and other tissues) from individuals of different ages, as well as in vitro studies on various cell lines after different passages. Special attention will be given to changes which occur during cultivation and might be related to the high cancer risk in chromosomal instability syndromes.

2. Materials and Methods

2.1.Materials

2.1.1. Instruments

Instrument	Company
Biological safety cabinet	BIOHAZARD
Centrifuge	Megafuge 1.0
Incubator	Biosafe ece
Tissue culture Flasks	TPP
Pasteur pipette	WU-MAINZ
Pipettes, 10ml sterile	Falcon
Pipettes, automatic	Eppendorf
Pipette tips	Eppendorf
Phase Microscope	ZEISS
Slides	Thermo
Water bath	Köttermann
Coverslips, 24x60 mm	Langenbrinck
Drying oven	MELAG
Karyotype system	Meta system
Oil immersion	ZEISS
Phase microscope, HBO 50 camera	ZEISS
Slides	Thermo
Software karyotype software	Ikaros (Metasystems)
Coverslips, 24x60 mm	Langenbrinck
Coverslips, 18x18 mm	Menzel
Fluorescent microscope with CCD camera	ZEISS Axioskop
Glass bottle 1000ml,100ml	SCHOTT
PCR machines	Eppendorf AB Applied Biosystem
Tips	Eppendorf
Telomere analysis Software	Isis and Ikaros (Metasystems)
Water Bath	GFL 1083
Biological safety cabinet	BIOHAZARD
Black light lamp	MAZDAFLUOR TFWN20
Drying oven	MELAG
Fluorescent microscope with CCD camera and software	ZEISS Axioskop Ikaros and Isis software (Metasystems)
Vortex	VWR Heidolph Reax 2000
Water bath	GFL
Filter 0.2 µm	Millipore
Heating block	Lab 4 you
Magnetic Stirrer	IKA
Minifuge	VWR
Phase microscope	ZEISS

Agarose electrophoresis set	Renner
UV transluminator	UVP
Warm plate	Medax
Conical tubes	Falcon
Eppendorf tubes	Eppendorf
Eppendorf tubes centrifuge	Biofuge 15
Heating block	Lab 4 you
DNA - Sequencer ABI prism 3730	Applied Biosystem
PCR 0.5ml tubes	Eppendorf
PCR tubes, ultra thin 0.2 ml	Biozym
Sequencing plate (96 PCR plate)	Thermo Scientific
SeqPilot Software	Applied Biosystem
Balance	Sartorius
Camera	Polaroid
Electrophoresis power supply	GIBCO BRL
Fity Combs	Renner GmbH
Microwave	Siemens
Transilluminator, UV	UV, INC
Adhesive Q-PCR Seal	Thermo
96-well q-PCR Plates	ABI Prism®SDS 7500
Corcial bottle 100ml	SCHOTT
Gel electrophoresis equepment	GIBCO BRL
Glass bottle 1000ml	SCHOTT
Hybridization oven	BACHOFER
Microcentrifuge	Eppendorf
Nylon gel membrane (Membrane optimized for nucleic acid transfer)	GE Healthcare -Amersham Hybondtm-N
Pipettes 10ml	Falcon
Shaking water bath	GFL
X-ray film	Kodak
Centrifuge, 4ºC	Biofuge-Heraeus
Eppendorf tubes	Eppendorf
Gel-electrophoresis set	GIBCO BRL
Ice or cold block	Eppendorf

2.1.2. Chemicals and reagents

Reagent	**Company**
Acetic acid 100%	Merck
Amniomax™-C100 medium	Gibco
Amniomax™-C100 medium supplement (Gentamici sulfate, L-glutamine supplement)	Gibco
KaryoMax®Colcemid®Solution (10 µg/ml)	Gibco
KCl	Merck

Fetal Bovine Serum	Biochrom AG
Methanol	J.T.Baker
Penicillin /streptomycin antibiotic solution	Gibco
RPMI-1640+ glutamax™ medium	Gibco
Trypsin /EDTA 0.05 %	Gibco
Giemsa	Dr.K.Hollborn
KH_2PO_4	Merck
Mount media (Vitro-clud)	R.Langenbrinck
NaCl	Merck
Na_2HPO_4	Merck
Trypsin 2.5 %	Gibco
DAPI (0.1 µg/ml)	Sigma
Ethanol serial 70%, 85%,100%	Merck
Florescence mounting solution	VECTASHIELD®)
Formaldehyde 37 %	Merck
Pre-treatment solution(Proteinase K) (2000x)	DAKO
TBS (Tris-Buffered Saline, pH 7.5)	DAKO
Telomere PNA-Probe /Cy3	DAKO
Rinse solution (x50)	DAKO
Wash solution (x50)	DAKO
Bromodeoxyuridine (BrdU) 10mM	SERVA
Hoechst 33258	SERVA
1xPBS	BIOCHROM AG
Phosphate Buffer pH 6.8	BRAND
Chromosome painting probes	XCP

DAPI stock (200 µg/ml)	Sigma
SSC	Sigma
DAPI stock (200 µg/ml)	Sigma
Dextransulfat	Eppendorf
Ethanol	J.T.Baker
Formamid	Fluka
NaCl	Merck
NaOH	Merck
NP-40 (Igepal)	Sigma
Sodium citrate dihydrate	Merck
RNAse A	Roche
SSC	Sigma
Chloroform	Merck
Ethanol 70%	Merck
PBS	BIOCHROM AG
2-Propanol	Merck
5x Big Dye	ABI
Big Dye® mix (v3.1kit)	ABI
Dynabeads Sequencing clean up	Invitrogen
Agarose 2%	Invitrogen
DNA molecular weight marker (100 bp)	Invitrogen
Ethidium Bromide (10 mg/ml)	Boehringer Mannheim
Loading Dye (20g Saccharose)	Merck
SYBR® Green qPCR Mix	Solis Biodyne
Anti-DIG-AP	Roche

Control-DNA(Southern blot)	Roche
Detection buffer (10x)	Roche
DIG easy Hyb	Roche
DIG molecular weight marker	Roche
Digestion buffer (5x)	Roche
*Hinf*1(40U/µl)	Roche
*Ras*1(40U/µl)	Roche
Substrate solution	Roche
Telomere probe (DIG-labeled)	Roche
Washing buffer (10x)	Roche
Water,nuclease-free(1.1ml)	Roche
Working buffer (10x)	Roche
Chloroform 99.0%	J.T Baker
DEPC-treated water	Invitrogen
TRIzol	Invitrogen

2.1.3. Buffers and solutions

Aqueous solutions were prepared using autoclaved Millipore water. For sterilization, solutions were autoclaved or passed through a 0.2 µm filter (Millipore).

Solution	**Components**
KCl 0.4%	0.4g KCL in 100 ml dH_2O
Fixative	Acetic acid 100% : Methanol (1 : 3 volume)
Trypsin Solution 2.5%	22ml NaCl 0.4% + 2.5 ml trypsin
NaCl 0.9%	0.9g NaCl in 100ml dH_2O
Giemsa solution	90ml Giemsa + 10ml Phosphate buffer 0.025M pH 6.8
Phosphate buffer 0.025M pH 6.8	11.13g $Na_2HPO_4x2H_2O$ + 8.5g KH_2PO_4
TBS Buffer	One package of TBS powder in 1L pure water

Pre-treatment solution	10µl pre-treatment solution 1:2000 in 20 ml TBS buffer
DAPI stock (200 µg/ml)	1 mg 4,6-diamidino-2-phenylindol 2HCl in 5 ml dH_2O
DAPI staining solution	150 ul DAPI stock (200 µg/ml) in 60 ml 2x SSC
Rinse solution	10 ml Rinse solution in 490 ml pure water
Wash solution	10ml wash solution in 490 ml pure water
Hoechst 33258 buffer	2.38 mg Bisbenzimide H 33258 (100mg) +24 ml dH_2O
BrdU solution	30.7mg BrdU 10mM + 100ml dH_2O
1xPBS	9.55g PBS + 1L dH_2O
20x SSC	175.3 g NaCl 88.2 g Na Citrat Dihydrat in 1000 ml dH_2O
2x SSC	50 ml 20x SSC in 450 ml dH_2O
SpectrumGreen (0.2 mM)	50 nM SpectrumGreen in 50 µl dH_2O
SpectrumOrange (0.2 mM)	50 nM SpectrumOrange in 50 µl dH_2O
NaOH (0.035 N)	3.5 ml 1N NaOH in 97.5 ml dH_2O
2x SSC/0.1% NP-40	500 ml 2x SSC in 500 ml NP-40
0.4x SSC/0.3% NP-40	100 ml 2x SSC 1.5 ml NP-40 in 400 ml dH_2O
RNase A stock 20 mg/ml	100 mg RNase A 100 ul 1M TrisHCl 150 ul 1M NaCl up to 10 ml dH_2O
RNase A 1:200	5 ul RNase A (stock 20 mg/ml) 995 ul 2x SSC
Solution B (cell lysis)	400 mM Tris-HCL; 60 mM EDTA; 150 mM NaCl, 1% SDS
Solution C (Deproteinization)	5M Na perchlorate (Merck 1.06564.0100)
TE pH 8.0	10 mM Tris HCl pH 8.0; 1 mM EDTA pH 8.0
1x TBE buffer	10x TBE (10x TBE: 108 g Tris + 55g Boric acid + 9.3g Na_2 EDTA-H_2O Triplex)
Denaturation solution	0.5 M NaOH, 1.5 M NaCl
Loading Dye (20g Saccharose)	0.125g Bromphenol Blue, 50ml dH_2O

TAE buffer	0.04 M Tris-acetate,0.001 M EDTA,pH 8.0
1xWashing buffer (Southern blot)	Dilution 1:10 : 1xwashing buffer with dH_2O
1xBlocking buffer (Southern blot)	Dilution 1:10 : 1xbolcking buffer with maleic acid buffer
Maleic acid buffer (Southern blot)	Dilution 1:10 : maleic acid buffer with dH_2O
Detection buffer (Southern blot)	Dilution 1:10 : detection buffer with dH_2O

2.1.4. Kits

Kit	**Company**
Telomere PNA FISH KIT/Cy3	DAKO (K5326, DakoCytomation, Denmark)
CGH Nick Translation Kit	Abbott
c-DNA synthesis kit	Invitrogen
Southern blot, *T*elo *TAGGG* Telomere length assay kit	Roche

2.1.5. Primers

Primers for telomere length measurement

Name of primer	**Sequence**
TEL-F	5´-CGGTTTGTTTGGGTTTGGGTTTGGGTTTGGG-3´
TEL-R	5´-GGCTTGCCTTACCCTTACCCTTACCCTTACCCTTAC-3´
HBG_qPCR_F	5´-GCTTCTGACACAACTGTGTTCACTAGC-3´
HBG_qPCR_R	5´-CACCAACTTCATCCACGTTCACC-3´
36B4-F	5´-CAGCAAGTGGGAAGGTGTAATCC-3´
36B4-R	5´-CCCATTCTATCATCAACGGGTACAA-3´
Tel_mouse_F	5´-CGG TTT GTT TGG GTT TGG GTT TGG GTT TGG GTT-3´
Tel_mouse_R	5´-GGC TTG CCT TAC CCT TAC CCT TAC CCT TAC CCT-3´
36B4_mouse_F	5´-ACT GGT CTA GGA CCC GAG AAG -3´
36B4_mouse_R	5´-TCA ATG GTG CCT CTG GAG ATT -3´

Primers for RNA detection (gene expression)

Name of primer	**Sequence**
hTERT_F	5´-CGGAAGAGTGTCTGGAGCAA-3´
hTERT_R	5´-GGATGAAGCGGAGTCTGGA-3´
GAPDH_F	5´-TCCACCACCCTGTTGCTGTAG-3´
GAPDH_R	5´-GACCACAGTCCATGCCATCACT-3´
HPRT_F	5´-GAGGATTTGGAAAGGGTGTTTATTC-3´
HPRT_R	5´-ACAATGTGATGGCCTCCCA-3´

Primers for DNA sequencing (*NBS* founder mutation)

Name of primer	Sequence
NBS_Ex6_F	5´-CAGATAGTCACTCCGTTTACAA-3´
NBS_Ex6_R	5´-CATGATCACTGGGCAGGTC-3´

2.1.6. Cell cultures

Most of the cell lines were established at the Institute of Medical and Human Genetics-Charite- Universitätsmedizin, Berlin. The fibroblast cell lines were propagated in Amniomax medium with gentamicin sulfate and L-glutamine supplement. Cells were grown in incubators maintained at 37°C and 5% CO_2**.** Lymphoblastoid cells (LCLs) were cultured in Roswell Park Memorial Institute (RPMI) medium with L-glutamine (RPMI+glutamax™) supplemented with 15% FBS (Fetal Bovine Serum), and 1% penicillin /streptomycin (10.000 µg/ml). Cells were grown in incubators maintained at 37°C and 5% CO_2. The cells were fed twice per week and split regularly.

Cell lines,

ID	Tissue	Age (years)	Sex	Status
94P0112 96P0048	Fibroblasts	5 7	Male Female	NBS-Homozygote
94P0496	Fibroblasts	9	Male	NBS-Homozygote
09P0285 09P0752	Fibroblasts	4 9	Male Female	Controls
GMA7166	Fibroblasts	20	Female	NBS -Homozygote
GMV7166	Fibroblasts	20	Female	NBS -Homozygote (SV40-transformed)
GMV7166+nbs	Fibroblasts	20	Female	NBS–Homozygote (SV40-transformed and transfected with the NBS wildtype gene)

97P0614	Lymphoblastoid cells	3	Male	NBS-Homozygote (EBV-transformed lymphoblastoid NBS cell lines)
94P0307		2	Male	
96P0616		12	Female	
95P0182		14	Female	
89P0319		9	Female	
Rozd		11	Female	
06P0131	Lymphoblastoid cells	5	Male	Controls
96P0125		15	Male	
07P0370	Blood	32	Female	Controls
01P0614		32	Female	
10P0287		32	Male	

2.1.7. DNA probes

DNA was isolated at the Institute of Medical and Human Genetics, Berlin,

Blood DNA of NBS-Heterozygotes:

Number	ID	Age (years)	Sex
1	5343	1	F
2	10130	2	M
3	4328	3	M
4	8296	3	M
5	3221	4	M
6	3223	5	F
7	10133	5	F
8	10131	5	M
9	10123	7	M
10	7234	8	F

11	6017	8	M
12	3224	10	M
13	10120	12	F
14	4787	19	M
15	8295	22	F
16	3222	25	F
17	10124	25	M
18	508	27	F
19	6024	30	F
20	466	30	M
21	7235	30	M
22	7824	33	M
23	7823	35	M
24	6025	40	M
25	4786	40	M
26	464	50	F
27	463	54	M

Blood DNA of NBS-Homozygotes:

Number	**ID**	**Age (years)**	**Sex**
1	13720	1	M
2	12207	1	M
3	13424	1	F
4	6645	1	F
5	5342	1	M
6	6018	2	F
7	7105	2	F

8	3769	2	M
9	3772	2	F
10	7694	3	F
11	11766	3	F
12	8294	3	F
13	13607	5	F
14	13028	6	M
15	3426	6	F
16	8165	6	M
17	9990	6	M
18	11348	7	F
19	5202	7	F
20	3201	7	F
21	4530	7	F
22	8304	8	M
23	12557	8	-
24	5700	9	F
25	11154	10	M
26	7822	10	M
27	9028	10	F
28	5546	10	M
29	6023	12	F
30	13921	12	M
31	2552	13	M
32	3197	13	M
33	3205	14	M
34	3316	15	M

35	5567	15	M
36	5450	18	F
37	10376	19	F
38	5431	20	F

Blood DNA of other chromosomal instability syndromes:

Number	**ID**	**Age (years)**	**Sex**	**diagnosis**
1	10703	1	M	NBS-Like
2	12641	1	F	NBS-Like
3	12755	1	F	NBS-Like
4	12439	1	F	NBS-Like
5	11694	2	M	NBS-Like
6	11207	3	M	NBS-Like
7	12446	3	F	NBS-Like
8	11785	4	F	NBS-Like
9	10889	5	F	NBS-Like
10	11947	5	F	NBS-Like
11	10462	5	M	NBS-Like
12	7690	5	F	NBS-Like
13	10362	6	M	NBS-Like
14	11153	6	M	NBS-Like
15	9414	7	M	NBS-Like
16	11118	7	F	NBS-Like
17	10603	9	M	NBS-Like
18	10604	10	M	NBS-Like
19	10116	11	M	NBS-Like
20	12329	12	F	NBS-Like

21	12129	14	M	NBS-Like
22	56661	15	M	NBS-Like
23	11170	27	M	NBS-Like
24	06714	28	F	NBS-Like
25	10272	30	F	NBS-Like
26	8348	-	-	NBS-Like
27	7236	-	-	NBS-Like
28	MAW	-	-	NBS-Like
29	FA	-	-	NBS-Like
30	AT15	60	M	AT
31	AT17	5	F	AT
32	L6	9	F	AT
33	L15	9	M	AT
34	88P0326	7	M	FA
35	I, G	7	F	FA
36	B, M	4	M	FA
37	HSC62	2	M	FA

DNA probes extracted from different cell types:

DNA sample (ID)	**Tissue**	**Age (years)**
07P0670 (control) 04P0143 (control) 96P0048 (NBS-homozygote) BR14 (NBS-homozygote)	Fibroblasts	6 months 3 months 7 1
GMA7166 (NBS- homozygote) GMV7166 GMV7166+nbs	Fibroblast SV40-transformed NBS-fibroblast	20

97P0614, 94P0307 ,96P0616 ,95P0182 89P0319 and Rozd (NBS-homozygote) 06P0131, 96P0125 (controls)	Lymphoblastoid cells	3 -15
06P0565 (NBS-homozygote)	Fibroblast, brain, colon, heart, lungs, spinal cord, skin, small intestine, stomach, thymus, adrenal gland, liver, kidney, spleen and umbilical cord	Fetus (abortion at 34 weeks)
07P0370,01P0614,10P0287 (controls)	Blood, Lymphoblastoid cells , CD3 and CD19	32

Blood DNA of controls (1-10 years)

Number	**ID**	**Sex**
1	04P0523	F
2	04P0862	F
3	05P0586	M
4	05P0509	F
5	04P0535	F
6	01P0888	M
7	02P0153	M
8	04P0216	M

Blood DNA of controls (11-20 years)

Number	**ID**	**Sex**
9	112	F
10	204	F
11	166	F

12	17	F
13	443	F
14	444	M
15	210	F
16	365	F
17	247	F
18	47	F
19	293	-
20	193	M
21	390	M
22	431	M
23	423	M
24	11	M
25	161	F
26	420	F

Blood DNA of controls (21-30 years)

Number	**ID**	**Sex**
27	02	M
28	440	F
29	143	F
30	448	F
31	129	F
32	169	F
33	164	F
34	13	M
35	413	F

36	223	F
37	163	M
38	40	F
39	188	F
40	241	M
41	246	M
42	470	M
43	280	F
44	262	F
45	191	F
46	328	M
F	333	F
48	471	F
49	464	M
50	284	F
51	150	F
52	330	F
53	292	M
54	01	F
55	425	F
56	49	F
57	165	F
58	189	M
59	323	M
60	90	F
61	320	F
62	93	F

63	41	F
64	388	F
65	147	F
66	303	F
67	445	F
68	430	F
69	102	F
70	32	M
71	313	F
72	160	M
73	472	F
74	347	F
75	146	M
76	222	F
77	Ra	F
78	305	F
79	383	F
80	207	F
81	37	M
82	187	M
83	73	M
84	104	F
85	23	-
86	31	F
87	269	F
88	1	M
89	271	F

90	372	M
91	27	-

Blood DNA of controls (31-45 years)

Number	**ID**	**Sex**
92	595	M
93	188	M
94	596	M
95	192	M
96	597	-
97	194	F
98	584	-

Blood DNA of controls (46-80 years)

Number	**ID**	**Sex**
99	591	F
100	592	M
101	579	M
102	590	M
103	570	M
104	574	M
105	588	F
106	572	F
107	580	M
108	587	M

Mouse DNA,

Mouse specimen	Tissue	Date of birth	Status
68	Heart, Brain, Liver and Kidney	09.10.2009	humanized NBS mouse (hNBN del)
92	Heart, Brain, Liver and Kidney	20.04.2010	humanized NBS mouse (hNBN del)
87	Heart, Brain, Liver and Kidney	04.02.2010	humanized NBS mouse (hNBN del)
95	Heart, Brain, Liver and Kidney	24.01.2010	humanized wild-type mouse (hNBN wt)
98	Heart, Brain, Liver and Kidney	29.01.2010	humanized wild-type mouse (hNBN wt)

2.2. Methods

2.2.1. Chromosome preparation

The basic techniques used in human cytogenetics, such as tissue culture and differential staining of human chromosomes, karyotyping and analysis of the replication pattern after BrdU incorporation, as well as in situ hybridization, are described by Verma and Babu 1989.[147]

2.2.1.1. Trypsinization and cell culture harvesting

Cell cultures were incubated with 25µl of colcemid solution (10µg/ml) at 37°C for 90 min. Thereafter, the medium was transferred from the flask to a sterile 15ml tube. The cells were trypsinized in 0.5ml of 0.05 % Trypsin/EDTA. Then, the cell suspension was transferred with a 1ml Pasteur pipette to the 15ml tube containing the medium. The tube was centrifuged at 1000g for 10 min. After centrifugation, the supernatant was removed and the pellet was carefully resuspended in the remaining fluid. The Colcemid treated LCL cells were directly transferred to the 15 ml conical tubes.

2.2.1.2. Hypotonic treatment and fixation of the cells

Five ml of 0.4 % KCl hypotonic solution, prewarmed to 37°C, were added to the trypsinized cells followed by incubation at RT for 10 min. The tube was centrifuged at 1000g for 10 min. The supernatant was discarded, the cells resuspended, and 5ml of a cold

fixative solution (1:3 acetic acid: methanol) were slowly added and gently mixed. The tube was centrifuged at 1000g for 10 min and the supernatant was carefully removed. The fixation step was repeated three times. After the last centrifugation the cell suspension was kept at -20°C.

2.2.1.3. Preparation of slides

One to two drops of the fixed cell suspension were transfered onto a cold wet glass slide. The cells were spread on the glass slide using a hot steam from a water bath and dried under a lamp or on a heating plate. The quality of the chromosome spread was monitored under a phase contrast microscope.

2.2.2. Giemsa-banding

After Giemsa-banding each chromosome pair can be identified by its characteristic light and dark bands. Prior to banding, the slides were incubated overnight at 65°C. Then, they were incubated in a trypsin solution (2.5%) for several seconds, the exact time varied between 8 -30 seconds, thereafter the slides were washed under running cold water. Then they were stained in freshly prepared Giemsa solution for 6-15min depending on the slide preparation conditions. Finally, the slides were washed with distilled water and air dried. Coverslips (24x60 mm size) were mounted with mounting medium. Metaphases were studied under the light microscope at 1000x magnification, documented with a HBO 50 camera and analyzed with the Ikaros Karyotype software from Metasystems. For Giemsa staining without banding the slides were incubated directly in Giemsa solution without trypsin treatment.

2.2.3. Quantitative fluorescence in situ hybridization of telomere repeats (Q-FISH)

This is the method of choice for measuring the telomere length of individual chromosome arms. The fluorescence intensity of single telomeres (T) is measured relative to a constant repetitive region in the centromeric region of chromosome 2 (C). The T/C ratio reflects the relative length of individual telomeres. The method was performed according to Perner et al., 2003. [148] The chromosome preparation was checked under a phase microscope and a region of approximately 20x20 mm with many well spread metaphases was marked with a diamond pen on the back of the slide. Pre-treatment was performed by immersion of the slide in six glass coplin staining jars containing: TBS for 2 min, 3.7% formaldehyde for 2 min and four jars with TBS for 5min each. Thereafter, the slides were immersed in cold ethanol (70%-85%-100%) and dried at RT.

Denaturation and hybridization steps were performed by adding 7µl of Telomere PNA probe /Cy3 onto the marked area of the slide. The area was covered with an 18x18mm coverslip and sealed with glue in order to prevent evaporation of the probe. The slide was kept for 3 min at 80°C to denature the PNA probe and then incubated at RT for 50 min in the dark (hybridization). After removing of the coverslip, the slide was washed at 65°C in the wash solution. DAPI staining was performed in the dark for 14min followed by washing in distilled water. The slide was air-dried at RT. Finally, a coverslip (24x60mm) was mounted with two drops of vectashield medium.

2.2.3.1. Quantitative image analysis

Metaphases are captured and karyotyped using a florescence microscope with individual filter sets (DAPI in blue color and Cy3 in red, Fig. 17), and linked to Isis and Ikaros software from Metasystems. The image of each metaphase is filtered and non-chromosome objects are deleted, then chromosomes are transferred into the karyotype window.

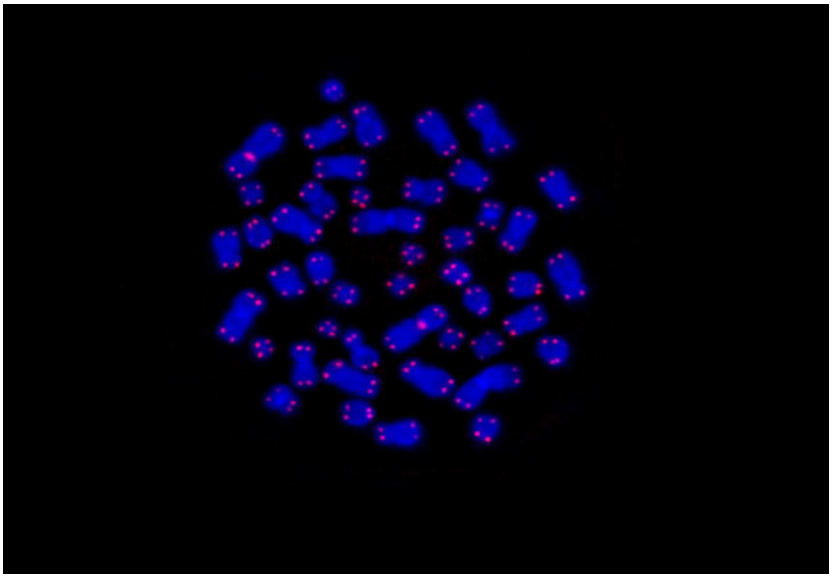

Figure 17: Typical human image after Q-FISH. Blue color: DAPI staining of the chromosomes, red color: (Cy3) telomeres signals and centromere of chromosome 2.

The telomere measurement algorithm displays two horizontal lines overlaid to each chromosome in the karyogram, which define the telomere measurement areas for p- and q-arms of each chromosome (Fig. 18).The measurement area of the reference probe is equally displayed as two horizontal lines on the respective chromosome. For the initial line

positions, the software uses default parameters. Within the measurement area the integrated fluorescence intensity in the Cy3 channel is measured.

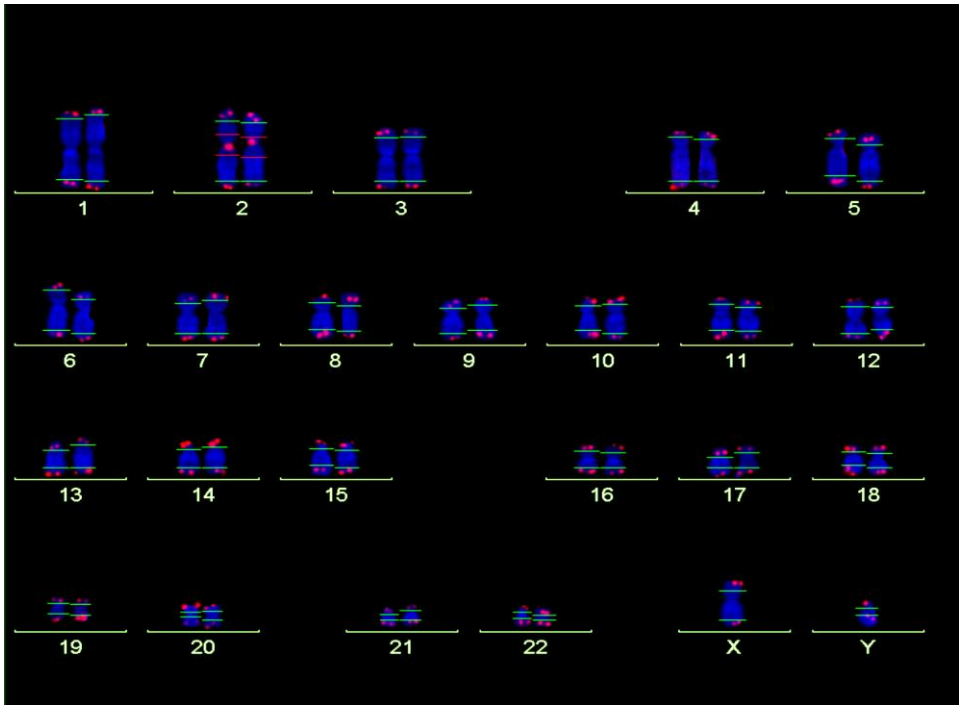

Figure 18: Karyogram with thresholds. Chromosomes are stained with DAPI (Blue). Red thresholds enclose the reference signal on chromosome 2. Green thresholds mark the limits of upper and lower borderline of the telomere signals on the chromosomes.

The normalized data are derived by calculating the ratio of the absolute telomere intensities and the absolute reference signal intensities. As the analysis is repeated for additional metaphases (15 metaphases are analyzed for each case), the telomere data are appended to the result file and statistical parameters are automatically calculated and displayed: The mean of telomere intensities of the p- and q-arms of each chromosome, standard deviations, the median (T/C %-value) and the interquartile range representing the range between the first and the third quartile of measured intensities.

2.2.4. Bromodeoxyuridine labeling (BrdU)

BrdU is a synthetic thymidine analog that is incorporated into the newly synthesized DNA strand during S-phase. The quenching of Hoechst33258 fluorescence allows cells that have incorporated BrdU to be distinguished from those that do not have.[149] One cycle of BrdU incorporation results in unifilar substitution, two cycles result in bifilar substitution with

sister chromatid differentiation, and three or more cycles result in various patterns of substitutions. Briefly, 20µl of the 10mM BrdU solution were added to the cell culture in the dark because BrdU is a photosensitizer. The following staining steps were performed in subdued light. The flasks were wrapped with black cover and incubated for 36 or 72 hours respectively at 37°C and 5% CO_2.Colcemid was added for the last two hours. Then the cells were harvested and chromosome preparation was performed as described above. The slides were incubated overnight in the drying oven at 65°C. Thereafter, the slides were stained with 1.5ml Hoechst 33258 buffer, washed with distilled water and rinsed in 1x PBS buffer. Then, they were covered with 24x60 mm coverslips, dried under a black lamp at 58°C for 10min and rinsed with distilled water. Finally, the slides were stained with Giemsa as described above. The metaphases were analyzed at 1000x magnification, documented with a HBO 50 camera and analyzed with the Ikaros Karyotype software (Metasystems).

2.2.5. Whole Chromosome Painting (WCP)

WCP is a cytogenetic technique used to detect and localize the presence or absence of specific DNA sequences on chromosomes. It is also used for the analysis of the chromosome translocations and chromosome identification. This technique requires special probes that bind to the chromosomes, which have a high degree of sequence similarity to the probes. The WCP probes consist of libraries of different sequences stretching over the entire length of the relevant chromosome.[150] It was performed here to identify the aberrant chromosomes of the NBS fibroblast cell line (94P0496) and characterize the translocation between chromosomes 6, 13 and 20. After chromosome preparation, the slide was immersed in cold ethanol (70%-85%-100%) and dried at RT. The hybridization and denaturation steps were performed by adding 8µl of each chromosome painting probe (#6, #13 and #20 in total volume of 24µl). Then, the hybridization area was covered with a 24x32 mm coverslip and sealed with glue in order to prevent evaporation of the probe. The slide was exposed for 5min to 75°C and then transferred and incubated at RT overnight.

Next day, slide was washed at 73°C in 0.4 SSC wash buffer and 2xSSC solution buffer for 2min each. Staining was performed with DAPI solution in the dark for 10min followed by rinsing in distilled water. Then, the slide was air-dried at RT. Finally, the slide was covered with a 24x60 mm coverslip and mounted in subdued light using two drops of vectashield medium. The slide was evaluated using a florescence microscope with individual filter sets (Axioscope) and the Ikaros and Isis software (Metasystems).

2.2.6. Comparative Genomic Hybridization (CGH)

This method was used to test if the chromosomal changes found in the above NBS-fibroblasts (94P0496) were accompanied with an unbalanced karyotype. The procedure was performed according to Tönnies H et al, 2001.[151] After chromosome preparation, the hybridization area with high quality metaphases was marked with a diamond pen on the back of slide. RNAse A treatment was performed by adding 2x SSC. 150µl of RNase A solution onto the glass slide and mounted with a coverslip. The slide was incubated at 37°C for 30 min. After incubation, the coverslip was removed and the slide was washed three times in 2x SSC for 4min. Denaturation of DNA was performed in 0.1% SSC at RT for 1min, followed by incubation in 2x SSC at 70°C for 30min. The slide was transferred for 1min into 0.1% SSC kept at RT followed by immersion in fresh solution of 0.035 N NaOH for 50 sec.

Washing steps were performed in 0.1% SSC at 4°C for 1min, followed by immersion in 2x SSC at 4°C for 1 min. Dehydration was performed by immersion in ethanol series 30%, 50%, 70%, 85% and 100% (one min each). The slide was dried for 10 min on a hotplate at 45°-50°C.

Preparation of hybridization probes. Nick-translation was performed by a PCR reaction using the VYSIS-KIT. In brief, control DNA (1µg) was mixed with 2.5µl spectrum orange (0.2mM), 5µl 10x buffer, 10µl AGC-mix (each nucleotide 0.3mM), 5µl dTTP-mix (0.3mM) and 8µl of CGH-NT enzyme. Patient DNA (500 ng) was mixed with 1.75µl spectrum green (0.2mM), 2.5µl 10x buffer, 5µl AGC-mix (each nucleotide 0.3mM), 2.5µl dTTP-mix (0.3mM) and 4µl of CGH-NT enzyme. The sample was centrifuged and the PCR reaction performed for 100 min at 15°C followed by 10min at 70°C. Samples were kept on ice. The results of nick-translation reaction were checked by standard 1% agarose gel electrophoresis. The control-DNA (250µg) and patient-DNA (250µg) obtained after nick-translation were mixed in an eppendorf tube with 1µl of glycogen, 15µl of Cot-1-DNA (1µg/µl), 3M sodium acetate (1:10) and cold 100% ethanol. The sample was centrifuged at 4°C for 25min at 14.000 rpm. Supernatant was removed and 1ml of 70% ethanol kept at RT was added to the pellet. The pellet was quickly vortexed and centrifuged at 4°C for 15 min at 14.000 rpm. After centrifugation, the supernatant was removed and an additional short spin was performed in order to spin down the remaining ethanol. Ethanol was carefully removed by pipette. The pellet was dried by placing the open tube at 37°C for 5 min. 5µl formamide solution was added to the dry pellet followed

by incubation at 37°C for 1 hour. Then, 5µl of the master mix were added to the tube with mixing by vortexing. Denaturation step was performed at 73°C for 6 min. After denaturation, the sample was centrifuged at 10.000 rpm, vortexed and placed on a freshly prepared CGH slide. The sample was covered with a coverslip and sealed with glue. The glass slide was kept at 37°C in a humid chamber for 3 days. After incubation, the coverslip was removed and the glass slide was immersed for 2 min in 0.4x SSC/0.3% NP-40 at 73°C, followed by short wash in 2x SSC/0.1% NP-40 at RT. After washing, the counterstain was performed by immersion of the slide for 14 min in DAPI solution in darkness, followed by two washes in dH_2O. The slide was transferred into falcon tube and centrifuged for 2 min at 1.000 rpm in order to remove water. Finally, the dry slide was covered with two drops of anti-fade solution and covered with a coverslip and analyzed under the fluorescent microscope. (This method was kindly provided by Mrs. Antje Gerlach- Institute of Human Genetic-Charite, Berlin).

2.2.7. X- irradiation

The cell culture (NBS-fibroblast 94P0496) was split into four parallel cultures. After 24 hours, the cells were exposed to two different doses of X-rays at RT. The first culture was exposed to 0.5 Gy, the second to 1.0 Gy, the third culture was not irradiated (negative control) and the fourth was left to grow normally. The radiation exposure was performed by MagForce Nanotechnologies AG Berlin, Germany using the Muller MG 150 X ray apparatus (U_A, 100 kV; I, 10 mA; filter, 0.3 mm Ni; dose rate 2.1 Gy/min). The cell cultures were transported in a Styropor box at 37°C. After radiation, the cells were incubated at 37°C and 5% CO_2 for four hours including two hours of colcemid treatment (10µg/ml). Then, chromosome preparation was performed as described above. The slides were stained with Giemsa. Metaphases were studied at 1000x magnification, documented with a HBO 50 camera and analyzed by the Ikaros Karyotype software from Metasystems.

2.2.8. DNA extraction

In order to obtain sufficient amount of DNA, the cell cultures were harvested at 80-90 % confluency. The procedure of DNA extraction was performed according to the laboratory manual. The cells were harvested as described above. The cell pellet was washed with 10 ml 1xPBS and centrifuged at 1500 g for 10 min. Then, the pellet was lysed in 1-2ml of solution B (see materials), resuspended and 250-500µl of solution C were added and carefully mixed. Then, one volume of chloroform was added, mixed and centrifuged for 6 min at 1300 g. The upper aqueous phase was transferred to a new tube and then, 0.6-0.8

volume of 2-propanol was added and gently mixed to precipitate the DNA. The precipitated DNA was transferred to an eppendorf tube containing 1ml of 70% ethanol and incubated for 1min at RT. The tube was centrifuged, the ethanol discarded and the DNA washed again in 1ml of 70% ethanol for 10-15 min at RT. Thereafter, the eppendorf tube was centrifuged at 14.000 g for 2 min, all ethanol removed and the DNA pellet dried at 37°C on a heat block. Finally, the pellet was dissolved in an appropriate amount of TE buffer (pH 8.0) and incubated at 37°C over night on a roller. DNA concentration (ng/µl) was measured using the NanoDrop® ND-1000 Spectrophotometer (IMPLEN).The sample was kept at 4C° until further processing

2.2.9. DNA sequencing

DNA sequencing was performed according to the original Sanger's protocol.[152] DNA is prepared as a single strand and the template DNA is mixed with a mixture of all four dNTPs and one of four ddNTPs. Each kind of ddNTP is presented in limiting quantities and labeled with a different fluorescent "tag". DNA polymerase inserts a ddNTP instead of the normal deoxynucleotide (dNTP); ddNTPs are similar to normal dNTPs except that they contain a hydrogen group instead of a hydroxyl group at 3' carbon position. After incorporation of a ddNTP into the newly synthesized DNA strand, the addition of further nucleotides is prevented which results in a series of DNA fragments of different lengths. The DNA fragments, which are labeled with different fluorescent dyes, are separated by electrophoresis based on their size. Finally, the ddNTPs are detected by a standard multiwave fluorescence detector with ABI Prism 3730. The computer program displays the DNA sequence as a graph showing peaks of different colors representing a specific labeled ddNTP.

2.2.9.1. Polymerase chain reaction (PCR) for amplification of the *NBS* gene (Exon-6)

PCR is used to amplify specific DNA fragments. It is based on the enzymatic amplification of a target DNA sequence flanked by oligonucleotide stretches to which specific primers are generated. By PCR it is possible to amplify millions of copies of DNA fragment using several cycles of denaturation of the DNA, annealing of primers and elongation of the product.[153] It requires several necessary components and reagents including: the DNA region to be amplified, a forward and a reverse primer which are complementary to the DNA region at 5´ and 3´ ends of the DNA template, buffer solutions for optimum activity and stability of the DNA polymerase, DNA polymerase such as Taq polymerase or any other heat-stable DNA polymerase, four different deoxyribonucleotide triphosphates

(dNTPs) and Mg^{+2}. Here, PCR was used to amplifying the exon 6 of the *NBS* gene. PCR amplification was carried out in a 15µl reaction volume and PCR master mix was prepared as presented in Table 2. The PCR program used for DNA amplification is shown in Table 3.

Table 2: PCR master mix reactions

reagent	**1x reaction**
Buffer	3µl
dH_2O	23µl
Primer (for)	1µl
Primer(rev)	1µl
Mg^{+2}.	1µl
DNA Taq polymerase	0.2µl
dNTPs	0.4µl
DNA	1µl
Total volume	30µl

Table 3: PCR amplification condition

Temperature	**Time**	**Cycles**
95°C	5 min	1
95°C 53°C 72°C	20sec 30sec 40scc	35
72°C	10sec	1
12°C	∞	

2.2.9.2. Gel electrophoresis

In order to check the results of the PCR reaction, the amplified PCR products (5µl) were checked by electrophoresis on a 2% agarose gel. The agarose gel was prepared by

dissolving two grams of agarose in 100ml 1x TBE-buffer and heated at 60°C in a microwave oven. After that, 5µl ethidium bromide solution (10mg/ml) was added and the agarose was poured into the electrophoresis tray with a comb. The gel was left for 15min to solidify. A mixture of 5µl of PCR product and 5µl loading buffer were loaded onto the gel. 3µl of 1Kb DNA marker were loaded to one of the wells. The electrophoresis was run at 250 V for 15-30 min. The DNA fragments were visualized by UV transilluminator and photographed using a digital camera.

2.2.9.3. PCR–purification

PCR products were used as a template for the sequencing reaction. Since primers and excess of dNTPs can interfere with the sequence reaction, an enzymatic digestion was carried out by addition of two enzymes Exonuclease-1 (Exo1) and Shrimp Alkaline Phosphates (SAP). Exo1 digests the single stranded DNA and the SAP catalyzes the dephosphorylation of 5' phosphate from DNA and dNTP's. Thus, single stranded DNA and remaining primers from the previous PCR reaction can be eliminated while double stranded DNA is maintained in the solution. Table 4 shows the master mixture of PCR-purification solution and the PCR incubation program is shown in Table 5.

Table 4: PCR-purification master mix

Reagent	**1x reaction**
dH_2O	4µl
SAP (5 U/µl)	0.1µl
Exo1 (10 U/µl)	0.05µl
Buffer mix	1µl
PCR product	5µl

Table 5: Incubation program for PCR-purification:

Temperature	Time
37°C 85°C	30sec 15min
12°C	∞

2.2.9.4. Sequencing reaction

The next step after PCR-purification is a sequencing reaction using the ABI BigDye master mix. The mastermix is prepared as presented in the Table 6, the program conditions for sequencing reaction are shown in Table 7.

Table 6: Sequencing reaction mastermix

Reagent	1x reaction
dH_2O	4µl
BigDye mix	0.25µl
Primer F or R	1µl
PCR-Purification product	1µl

Table 7: Program conditions for sequencing reaction

Temperature	Time	Cycles
96°C	1 min	1
98°C 53°C 60°C	20sec 10sec 4min	25
12°C	∞	

2.2.9.5. Sequencing reaction cleaning

The sequence products were cleaned up using a Robot (Dynabeads® Sequencing Clean-Up from Invitrogen). After that the plate was immediately loaded in the ABI 3730 for DNA sequencing.

2.2.9.6. Sequence analysis

The data obtained from ABI 3730 genetic analyser were analyzed by use of the Sequence pilot software (Applied Biosystem). The program allows an automated alignment of the selected patient sequences with reference sequences obtained from the database and displays the differences between patients sequence and reference sequence.

2.2.10. Q-PCR for telomere measurement

Quantitative polymerase chain reaction (Q-PCR) is an advanced technique based on the PCR, to amplify and simultaneously quantify a target DNA molecule. Q-PCR was applied to determine the relative telomere length as described by Cawthon R.M.[154] The *36B4* gene, which is located on chromosome 12 and encodes an acidic ribosomal phosphoprotein PO, was chosen as reference single copy gene because it has already been validated in gene dosage studies. In addition, the β-globin gene (*HBG*) was used to verify the *36B4* in Q-PCR. In all experiments the amount of the single copy gene is compared to the number of telomere copies in order to estimate the relative telomere length (T/S ratio). This ratio should be proportional to the average telomere length and reflects relative length difference in telomeric DNA.

A standard curve was used to test the efficiency of the Q-PCR reaction, in which an endogenous gene and the gene of interest were compared. The assay is first performed with various known concentrations of a reference DNA. Here it was a mix of DNA from five healthy individuals, serially diluted to test the primers of all genes which were used in Q-PCR (Fig. 19).

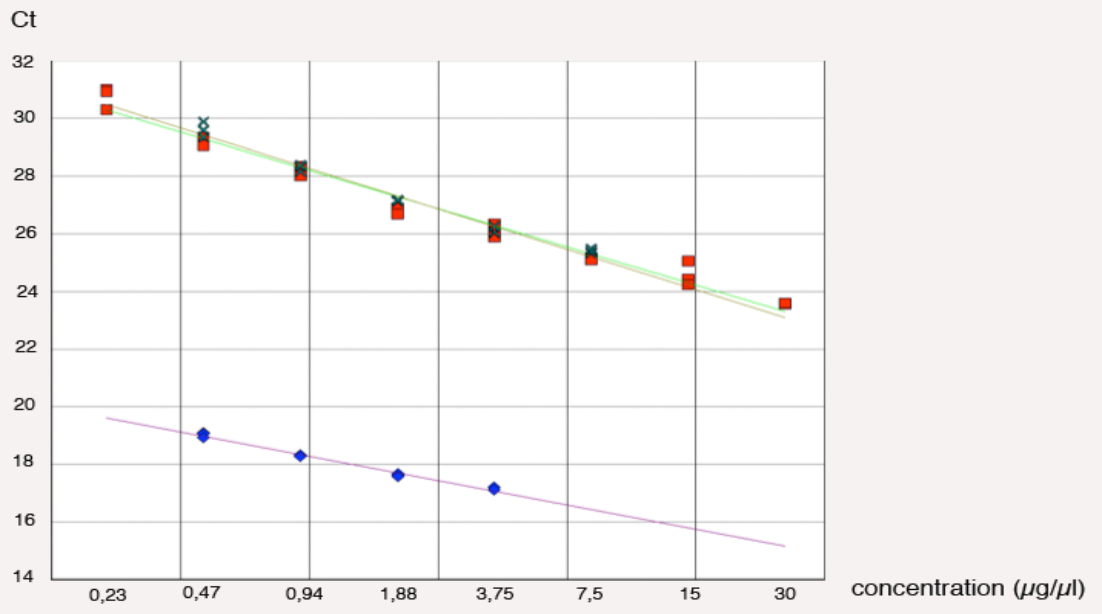

Figure 19: Standard curve used to test the efficiency of the Q-PCR reaction and measurement of the relative T/S ratio. X axis: concentrations of the reference DNA through serial dilutions (1:2), Y axis: C_t (cycle threshold) is the cycle number at which the fluorescence generated within a reaction crosses the threshold line. Telomere: Blue boxes◆, single copy gene *36B4:* red boxes◆ and✤: β-globin gene *HBG*.

For telomere measurement by Q-PCR, three mastermixes of PCR reagents were prepared; the first one with telomere primers, the second with *36B4* (single copy gene) primers and the third with *HBG* primers. 10µl of each master mix were added to each well followed by 10µl of DNA sample in total volume for each well 20µl as shown in Table 8. All samples were diluted to be in the range of mixture DNA reference's concentration and each DNA sample was tested in triplicate.

Table 8: Master Mix for telomere measurement by Q-PCR

reagent	**1x reaction**
dH_2O	4µl
SYBR green mix	4µl
Primer F	1µl
Primer R	1µl
DNA	10µl
Final volume	20µl

Finally, the plate was sealed by an adhesive Q-PCR seal, centrifuged and loaded in the Q-PCR machine to perform the relative quantification test by using an Applied Biosystems prism 7500 (ABI 7500 sequence detection software SDS V1.2.3). The set up of Q-PCR program is presented in Table 9.

Table 9: Q-PCR conditions for the measurement of the relative telomere length

Temperature	**Time**	**replications**
95°C	10 min	1
95°C	15 sec	40
60°C	30 sec	
72°C	46 sec	

The dissociation curve of the PCR products is obtained by performing a slow ramp from low to high temperature (95°C for 15sec, 60°C for 1 min, and slow ramp to 95°C). The increase in temperature causes PCR products to undergo denaturation, a process accompanied by a decrease in fluorescence. The fluorescence signal is continuously recorded on the ABI 7500 SDS, which is used to analyze the fluorescence data and their automated conversion into melt-peaks in the dissociation curve diagram (Fig. 20).

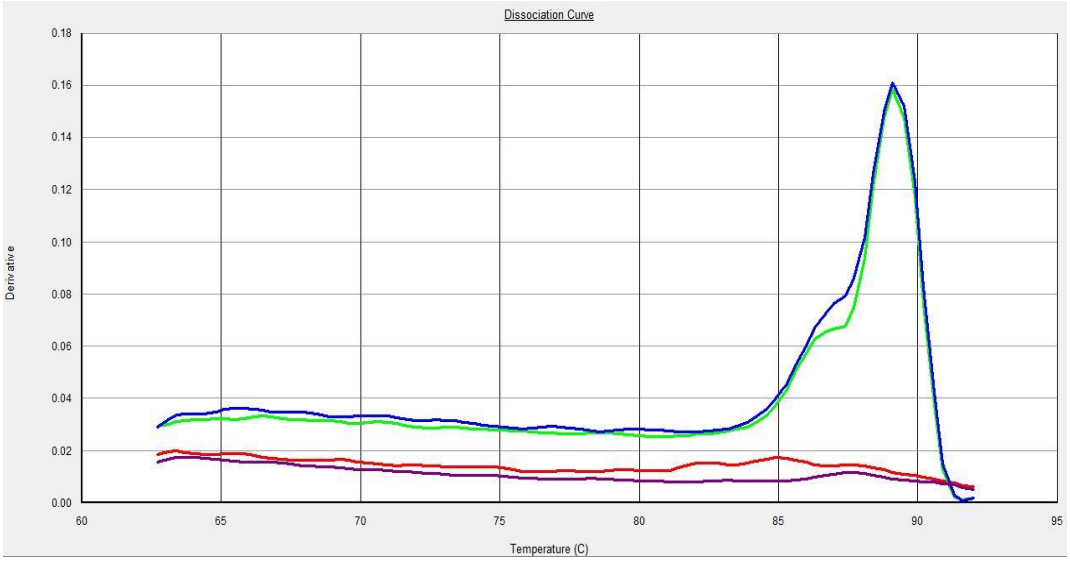

Figure 20: Dissociation curve shows peaks of the melting temperature generated with the Q-PCR product (high blue and green peaks) and in the absence of Q-PCR product (low red and purple peaks), analyzed by ABI 7500 SDS.

2.2.11. TRF analysis

The first technique used to measure telomere length was Terminal Restriction Fragment (TRF) length analysis by Southern blot. The procedure was performed according to the standard manufacture's instruction of Roche (*T*elo *TAGGG* telomere length assay). The protocol involved DNA cutting into fragments by a mixture of frequently cutting restriction enzymes: *Hinf1* and *Rsa1*. The DNA fragments were separated by gel electrophoresis, and then transferred onto a nylon membrane. The blotted DNA fragments were hybridized to a digoxigenin (DIG)-labeled probe specific for telomeric repeats and incubated with a DIG-specific antibody covalently coupled to alkaline phosphate, which provided a visible signal that indicated the location of the telomere probe (TRF) on the blot. Then, the hybridized membrane was incubated in a series of washing solutions with gentle agitation. The solutions included: 1x washing buffer for 5min at 25°C, 1x blocking solution for 30 min at 25°C, anti-DIG-AP working solution for 30min at 25°C, 1x washing buffer for 15min at 25°C, 1x detection buffer for 5min at 25°. After washing approximately 40 drops of a substrate solution were applied immediately to the wet membrane, which was placed in a hybridization bag with a DNA side facing up. The membrane was covered with the second sheet of the hybridization bag and incubated for 5min at 25°C. The substrate solution was discarded and the membrane was exposed to an x-ray film placed inside the sealed bag for 20min at RT. Luminescence continues for at least 24 hours and signal intensity will increase during the first hours (Fig. 21). After exposure of the blot to an X-ray film, an estimate of the mean TRF length can be obtained

by visually comparing the mean size of the smear to the molecular weight marker. Mean TRF length is calculated using the formula: TRF length = ∑(ODi) / ∑(ODi/Li), where ODi is the chemiluminescent signal and Li is the length of the TRF at position i. (This method was performed by Dr. Ilja Demuth-Institute of Human Genetic-Charite, Berlin).

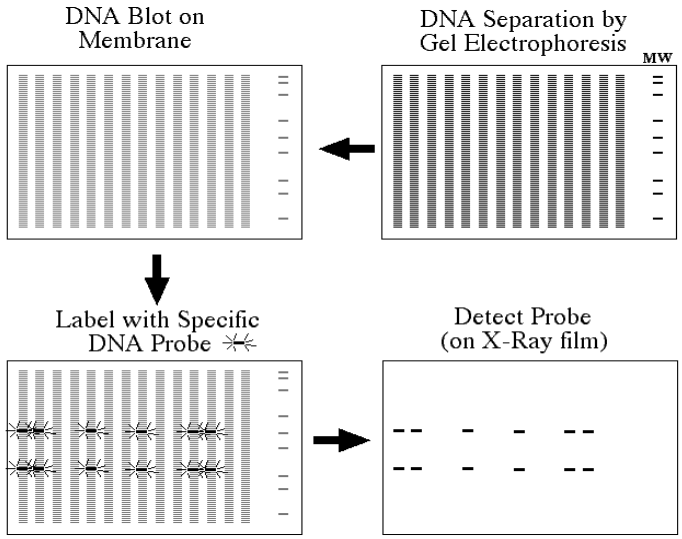

Figure 21: Steps of TRF analysis by Southern blots to determine the molecular weight of a restriction fragment and to measure their amounts in different samples. (http://www.bio.davidson.edu/courses/genomics/method/Southernblot.html).

2.2.12. Gene expression of hTERT (human telomerase reverse transcriptase)

The expression pattern of *hTERT*, the human telomerase reverse transcriptase catalytic subunit gene, is a rate-limiting determinant of the enzymatic activity of human telomerase. The *hTERT* complementary DNA (cDNA) was synthesized from a mature hTERT mRNA template in a reaction catalyzed by the enzyme called reverse transcriptase. The procedures were performed according to the standard manufacture's instruction of Invitrogen.

2.2.12.1. RNA- extraction

Total RNAs was isolated using TRIzol reagent (Invitrogen), involving: homogenization, Phase separation, RNA precipitation, RNA wash, and RNA dissolving.

The cells were washed with 1 ml of 1x PBS, followed by cells lysis with 1 ml TRIzol reagent and mixed well by vortexing until the pellet dissolved completely. 200 µl of chloroform (99.0 %) were added per 1ml of TRIzol and mixed well by vortexing. The mixture was centrifuged at 13000g for 15min at 4ºC. The mixture was separated into 3

phases: lower red, phenolchloroform phase, an interphase and a colourless upper aqueous phase which contained the RNA. The upper aqueous phase was transferred carefully without disturbing the interphase into a fresh tube. The RNA was precipitated from aqueous phase by mixing with 500 µl 2- propanol (99.5 %) and the precipitate was centrifuged at 13000g for 20min. The supernatant was removed completely. The RNA pellet was washed once with 1 ml 75% ethanol and mixed by vortexing followed by centrifugation at 13000g for 5min. The ethanol was removed and the RNA pellet was dried on heat block at 70°C. The RNA was dissolved in 20 µl DEPC-treated water. Finally, RNA pellet was tested by 1% agarose gel-electrophoresis according to the standard procedures at 120 V for 20min. The results were visualised by the use of an UV-transilluminator and documented using a digital camera. RNA concentration (µg/µl) was measured using the NanoDrop®ND-1000 Spectrophotometer (IMPLEN).

2.2.12.2. cDNA synthesis

Typically a 20 µl reaction volume was used for 1ng–5µg of total RNA. Two master mixes were prepared: the first with MMLV-Reverse transcriptase (RT+), the second without MMLV-Reverse transcriptase as negative control (RT-). Table 10 shows the reagents used for cDNA synthesis.

Table 10: cDNA synthesis reaction master mix:

Reagent	**1x reaction**
5x strand buffer	4µl
dNTP's (10mM)	2µl
Random hexamer primers (50ng/µl)	2µl
DTT (0.1M)	1µl
RNAse out (40u/µl)	0.5µl
Final volume	9.5 µl
total RNA	X µl
DECP-H_2O	up to 20µl

Finally, 1µl of MMLV- Reverse Transcriptase (200u/µl) was added only for RT+ reactions. The reagents were mixed by pipetting the required volume of DECP-H_2O into each nuclease-free microcentrifuge tube, and then 5µl of master mix Rt+ or Rt- was pipetted into tubes. All tubes were quickly centrifuged. At this time all RNA probes were heated on a heat block at 65°C for 5min. RNAs probes were kept on ice until needed. All tubes were quickly centrifuged and transferred into a PCR machine. The program of temperatures and incubation times for cDNA synthesis in the PCR machine is presented in Table 11.

Table 11: cDNA synthesis PCR program:

Temperature	**Time**
20°C	10min
42°C	60min
85°C	8 min

2.2.12.3. Q-PCR for gene expression

The expression of the *hTERT* gene (human telomerase reverse transcriptase) was analyzed by Q-PCR. For that three master mixes were prepared each one contained the reagents as shown in Table 12. The master mixes differ from each other in the primers for the specific genes, which were: *GAPDH* (glyceraldehyde-3-phosphatedehydrogenase) as an internal control, *HPRT* (guanine phosphoribosyl transferase) as endogenous control gene and *hTERT* as the tested gene. The 96-well Q-PCR plate was prepared, quickly centrifuged and transferred to the Q-PCR machine. Program conditions for Q-PCR are presented in Table 13. All PCRs were performed on Applied Biosystem prism 7500 (sequence detection software DSD V1.2.3). The Q-PCR products were checked by agarose gel electrophoresis, visualized by UV- transilluminator and photographed.

Table 12: Q-PCR master mix for gene expression

Reagent	**1x reaction**
dH_2O	4µl
SYBR green mix	4µl
Primer F	1µl
Primer R	1µl
cDNA	10µl
Final volume	20µl

Table 13: Q-PCR condition for *hTERT* gene expression

Temperature	**Time**	**replications**
95°C	10 min	1
95°C 60°C 72°C	15 sec 30 sec 46 sec	40

2.3. Statistical tests

The original data were exported to excel 07, GraphPad Prism 5 software and SPSS15.0 software for different statistical analysis such as descriptive tests, graphs and boxplots (whisker diagram) as well as the significance tests: T-Test for independent samples (Mean comparison) ,Wilcoxon statistical test for two related samples (Median comparison), Mann-Whitney statistical test for two independent samples (Median comparison), Fisher's exact test and Chi- square test.

3. Results

3.1. Methodological basis

There are different methods to measure telomere length, which all have distinct advantages and disadvantages.[155] In this thesis, three approaches were applied, which complement each other:

1. Quantitative-PCR (Q-PCR): This is the only technique for high throughput analyses and thus has found widespread application. It is based on the simultaneous amplification of telomeric repeats (T) and a single copy gene (S). The T/S ratio is a relative measure and reflects the average genomic telomere length.

2. Quantitative fluorescence in situ hybridization of telomere repeats (Q-FISH): This is the method of choice for measuring the telomere length of individual chromosomes. The fluorescence intensity of single telomeres (T) is measured relative to a constant repetitive region in the centromeric region of chromosome 2 (C). The T/C ratio reflects the relative length of individual telomeres. In addition, the total relative length of all chromosomes can be calculated.

3. Terminal Restriction Fragment (TRF) length analysis by Southern blot (TRF analysis): This is the first technique established to measure the average genomic telomere length. It is a quantitative approach and can be used to calibrate Q-PCR and Q-FISH. In contrast to Q-FISH, TRF-analysis requires substantial amounts of DNA. Due to the very heterogeneous smear, from which the telomere length is estimated, the sensitivity (accurateness) is limited.

Thus, there is no single technique at present to measure telomere length accurately and quantitatively. The combination of these three complementary techniques is, however, well suited to measure human telomere lengths both *in vivo* and *in vitro*.

3.2. Estimation of telomere length by Q-PCR

3.2.1. Telomere length *in vivo*

3.2.1.1. Estimation of telomere length in healthy individuals (controls) as a function of age

Genomic DNA was extracted from venous blood of 108 healthy individuals ranging in age from 1 to 80 years. The sample was divided into five age groups and relative telomere length was measured by Q-PCR (Fig. 22; Appendix 1). Telomere length becomes shorter with age. The decrease is significant between the age groups from 1 to 20 and 21 to 30 years (P=0.002) as well as from 31 to 45 and 46 to 80 years (P= 0.004). Interestingly, no significant difference is found between 21 and 45 years.

Based on the assumption of a linear relationship between telomere length and age the resulting regression curve shows a negative correlation with r = - 0.59 (Fig. 23).

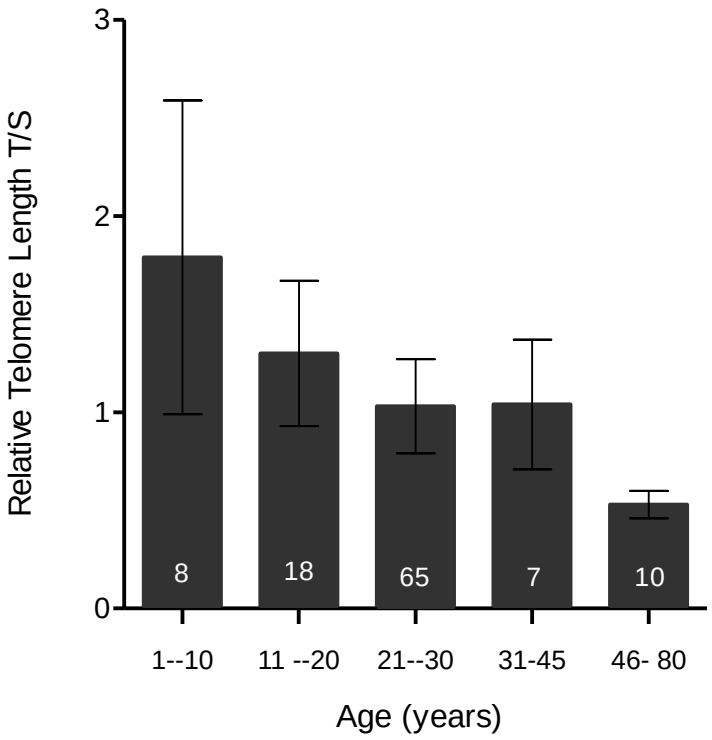

Figure 22: Relative telomere length ± SD in five age groups of healthy individuals (controls) measured by Q-PCR. The numbers in the columns represent the numbers of individuals analysed.

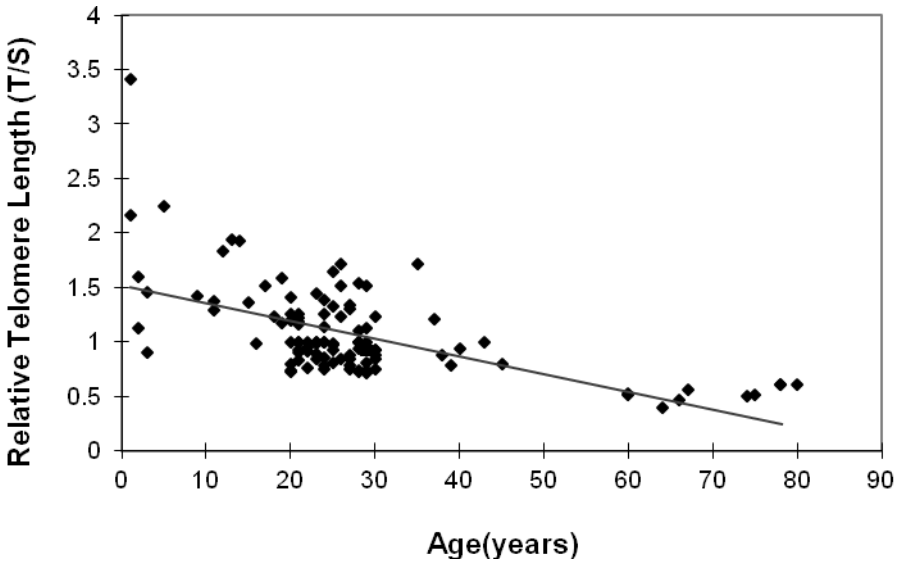

Figure 23: Relation between relative telomere length and age in 108 healthy individuals (controls). The solid line represents the linear regression curve of telomeres as a function of age. The corresponding correlation coefficient is r = - 0.59.

3.2.1.1.1. Comparison of telomere length in healthy individuals (controls) according to gender

This cohort is comprised of 63 healthy females, with an average age of 24.5 and a median age of 24.0 years, and 40 males with an average age of 31.4 and a median age of 25.0 years. Telomere length was measured by Q-PCR (Fig. 24; Appendix 2). The mean relative telomere length of females was significantly longer than that of males ($P<0.05$). In addition, the telomere length of a more homogeneous age cohort (age between 20 and 30 years) was compared. In this case, the average age of females (25.1 years) and males (25.0 years) was almost identical. Here, the mean relative telomere length of females was slightly longer than in males (Fig. 25; Appendix 2), the difference is, however, not significant ($P = 0.1$).

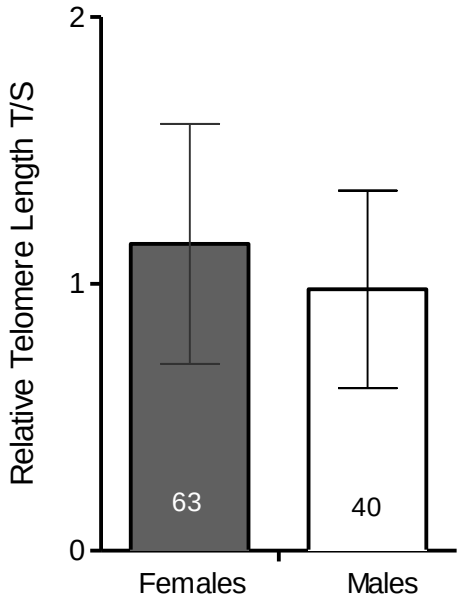

Figure 24: Relative telomere lengths ± SD in 63 females and 40 males of the control group. The mean (median) age was 24.5 (24.0) in females and 31.4 (25.0) in males. The difference is statistically significant (P<0.05). The numbers in the columns represent the numbers of individuals analysed.

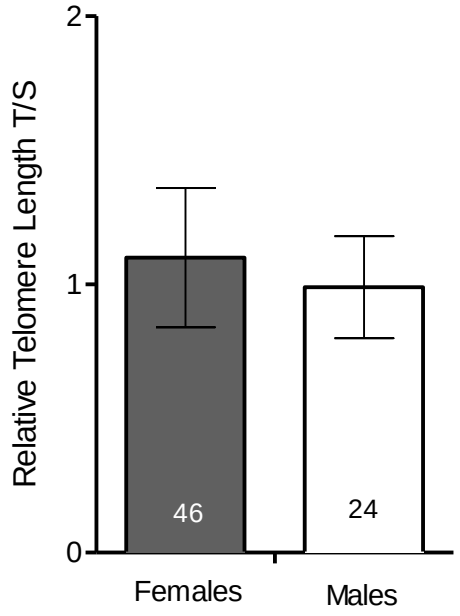

Figure 25: Relative telomere lengths ± SD in 46 females and 24 males of the control group ranging from 20 to 30 years with a mean age of 25.1 and 25.0 years, respectively. The difference is not statistically significant (P=0.1). The numbers in the columns represent the numbers of individuals analysed.

3.2.1.2. Estimation of telomere length between NBS-homozygotes and controls

Telomere length of blood DNA from 38 NBS patients, ranging from 1 to 20 years, was measured by Q-PCR and compared with the relative telomere length of control individuals. The sample was divided in two age cohorts of 1 to 10 and 11 to 20 years (Fig.26; Appendix 3). The mean relative telomere length of controls was significantly longer than that of NBS-homozygotes in both age groups ($P < 0.05$). The regression curve shows an inverse relation between telomere length and age (Fig. 27) with a correlation coefficient of $r = -0.27$.

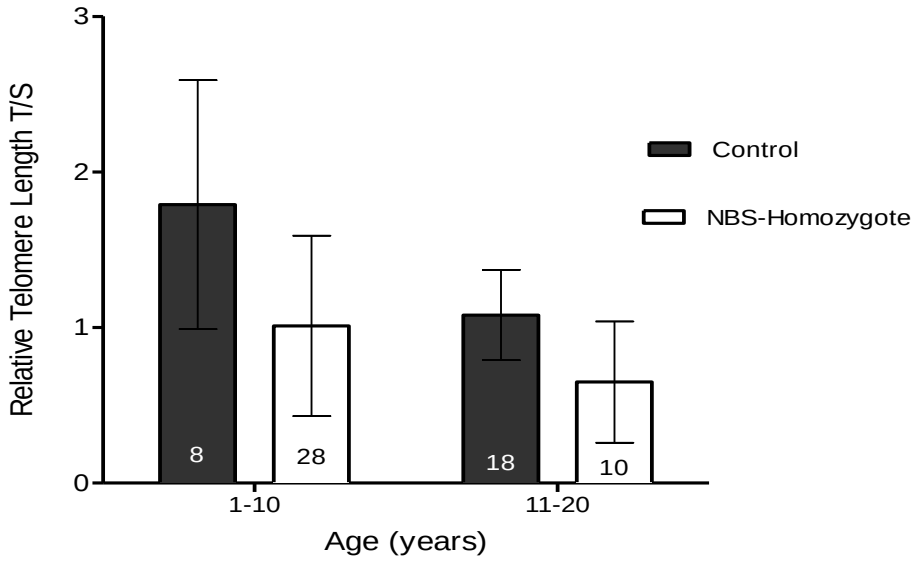

Figure 26: Relative telomere lengths ± SD in NBS-homozygotes and controls in two age groups from 1 to 10 and 11 to 20 years. The numbers in the columns represent the numbers of individuals analysed.

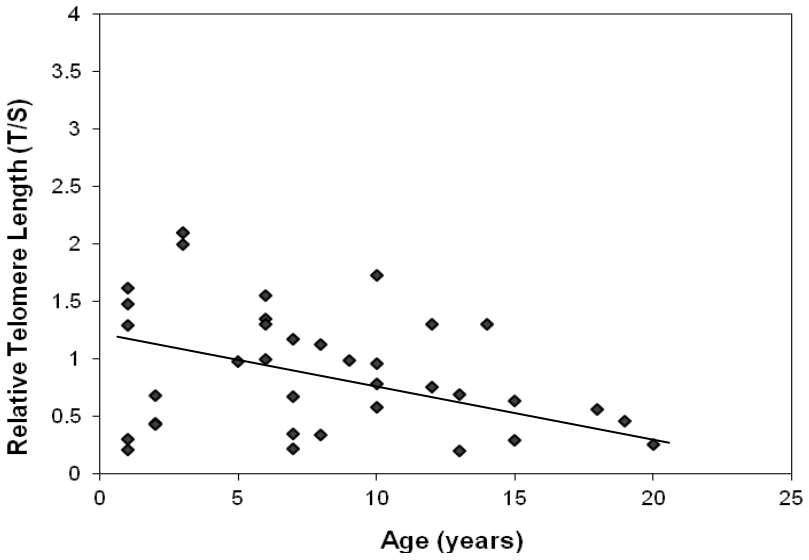

Figure 27: Relation between relative telomere length and age in 38 NBS-homozygotes. The solid line represents the linear regression curve of telomeres as a function of age. The corresponding correlation coefficient is r = - 0.27.

3.2.1.2.1. Comparison of telomere length in NBS-homozygotes according to gender

Twenty female NBS patients with an average (median) age of 7.2 (6.5) years and seventeen males with an average age of 8.4 (10.0) years were compared for telomere length (Fig. 28; Appendix 4). The mean relative telomere length of females was only slightly longer than that of males (P=0.4).

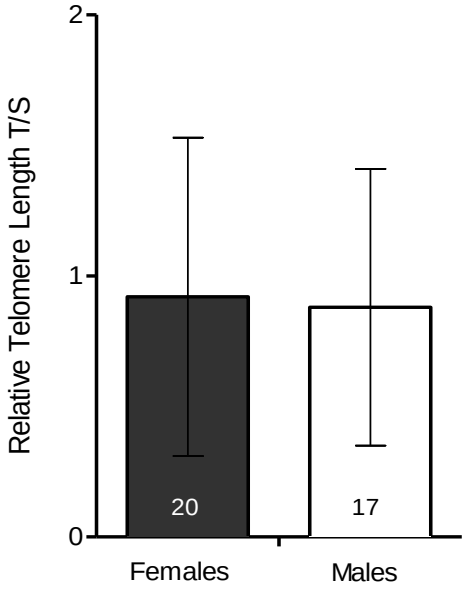

Figure 28: Relative telomere lengths ± SD in 20 female and 17 male NBS-homozygotes with a mean age of 7.2 and 8.4 years, respectively.

3.2.1.3. Estimation of telomere length between NBS-heterozygotes and controls

Telomere length was measured in blood DNA of 27 NBS-heterozygotes ranging from 1 to 54 years of age by Q-PCR (Fig. 29; Appendix 5). A significant difference was observed in the relative telomere length between the controls and NBS-heterozygotes only in individuals older than 30 years (P = 0.01). The average age was 19.8 years in NBS-heterozygotes and 27.4 years in the controls. No significant difference was found in the other age groups (P= 0.2). The relation between age and relative telomere length in the 27 NBS-heterozygotes is also represented by a regression curve, which shows an inverse relation between relative telomere length and age with a correlation coefficient of r = - 0.66 (Fig. 30).

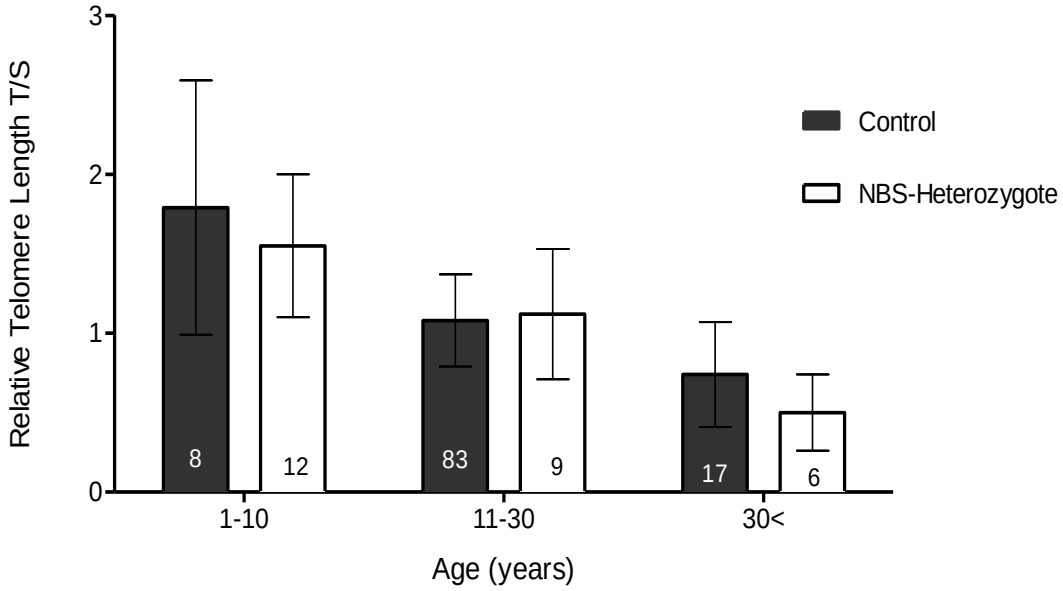

Figure 29: Relative telomere length ± SD in NBS-heterozygotes and controls in three age groups. The numbers in the columns represent the numbers of individuals analysed.

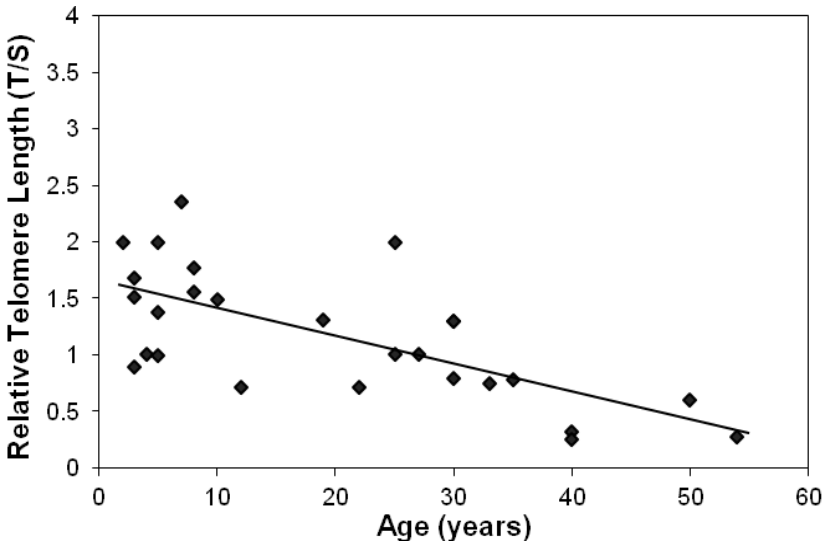

Figure 30: Relation between relative telomere length and age in 27 NBS-heterozygotes. The solid line represents the linear regression curve of telomeres as a function of age. The corresponding correlation coefficient r = - 0.66.

3.2.1.4. Comparison of telomere length as a function of age between controls, NBS-homozygotes and heterozygotes

The linear regression curve of controls, NBS-homozygotes and -heterozygotes showed an inverse relationship between relative telomere lengths and age. The corresponding correlation coefficient was almost the same for controls and NBS-heterozygotes, r = - 0.59 and -0.66, respectively, but much less in NBS-homozygotes with r= -0.27. This is explained by the much greater variability of the individual telomere lengths in the homozygotes (Fig. 31). The decline of the regression curve, reflecting the age-dependent loss of telomeres, is not so different between the three groups. This, however, should not be over interpreted, because it is based on the assumption of a linear relationship between telomere length and age and neglects the great variability. Clearly, the relative telomere lengths were shortest in NBS-homozygotes in comparison with the NBS-heterozygotes and the controls.

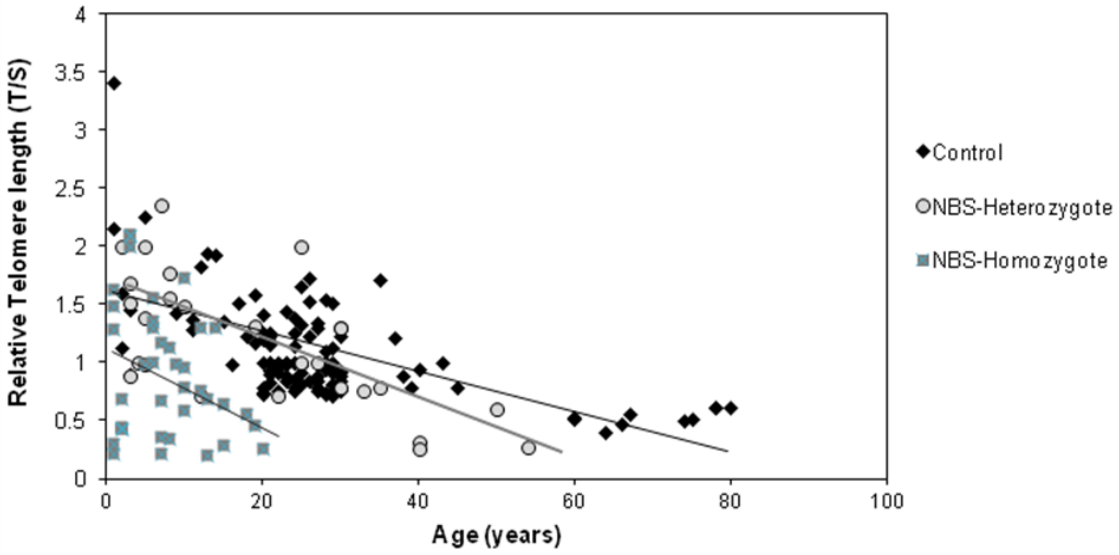

Figure 31: Regression curve of relative telomere length as a function of age between the controls (black), and NBS-heterozygotes (gray) and homozygotes (blue). The corresponding correlation coefficient are r = - 0.59 (control), r= -0.66 (NBS-heterozygotes) and r= -0.27 (NBS-homozygotes).

3.2.1.5. Estimation of telomere length in NBS-like patients and controls

Telomere length was also measured in blood DNA of 29 NBS-like patients ranging from 1 to 30 years of age by Q-PCR (Fig. 32; Appendix 6). The mean relative telomere length of the controls was significantly longer than that of the NBS-like patients. This was found in both age groups, younger than 10 years and from10 to 30 years ($P<0.05$). The average age

in the younger age group was 3.2 years for the controls and 4.9 years for the NBS-like patients, and for the older age group 23.6 years and 19.2 years, respectively.

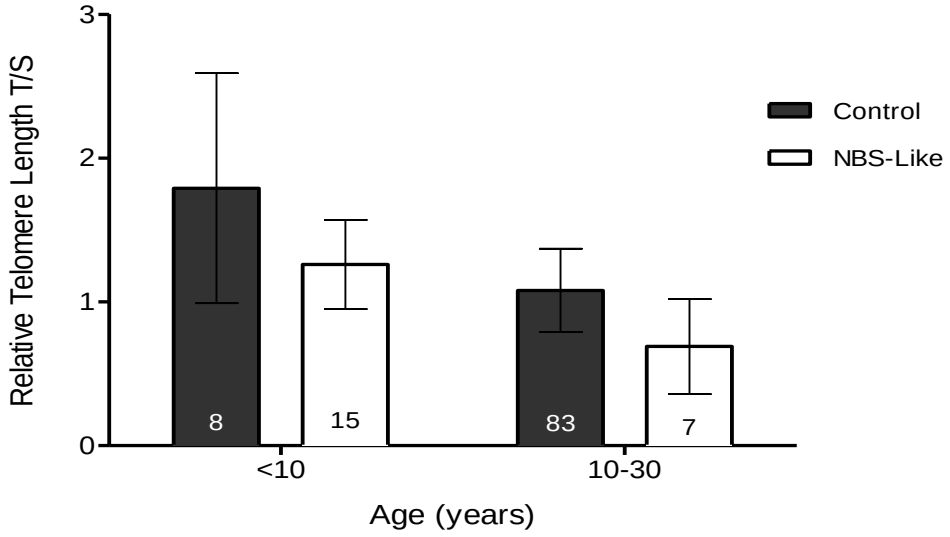

Figure 32: Relative telomere lengths ± SD in NBS-Like patients and controls in two age groups. The numbers in the columns represent the numbers of individuals analysed.

3.2.1.6. Comparison of telomere length in NBS-homozygotes, NBS-heterozygotes, NBS-Like patients and controls

Telomere lengths of NBS-homozygote, NBS-heterozygote, NBS-like patients and controls were compared according to an age range from 1 to 10 years and an age group of younger than 20 years. Mean relative telomere length of controls was significantly longer than that of NBS homozygotes and NBS-like patients in both age groups ($P<0.05$), but not in comparison to NBS-heterozygotes younger than 20 years. NBS-homozygote patients showed the shortest telomere lengths in both age groups (Fig. 33).

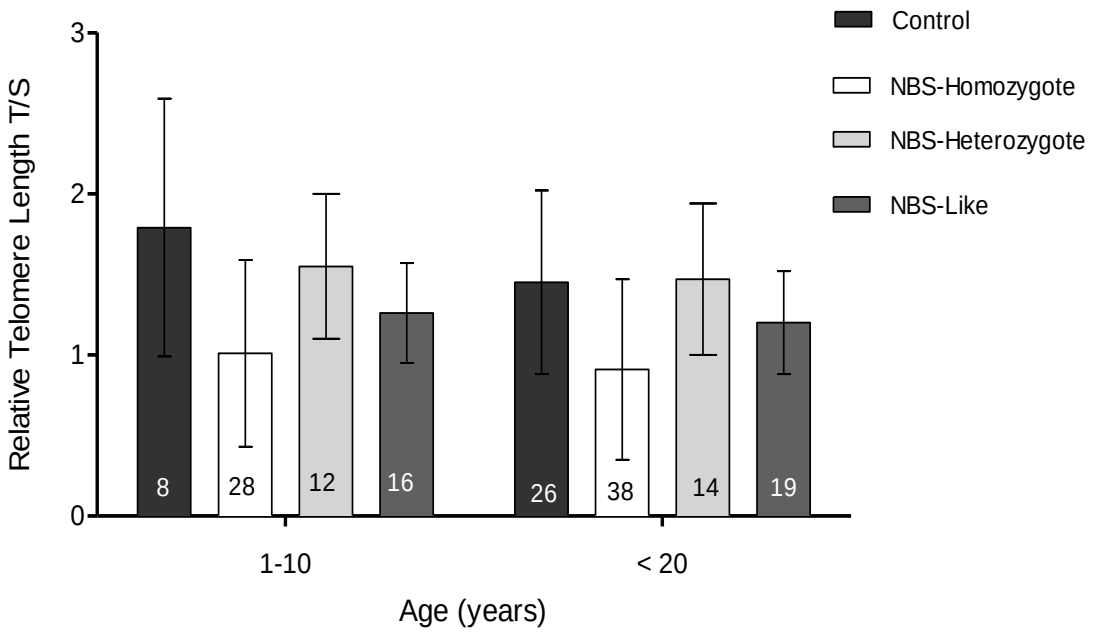

Figure 33: Relative telomere lengths ± SD in controls, NBS-homozygotes, -heterozygotes, and NBS-like patients in two age groups. The numbers in the columns represent the numbers of individuals analysed.

3.2.1.7. Estimation of telomere length in AT and FA patients and controls

Telomere length was also measured by Q-PCR in blood DNA of some patients with other chromosomal instability syndromes such as AT (Ataxia telangiectasia) and FA (Fanconi anemia) ranging from 1 to 10 years, with a mean age of 7.6 (AT), 5.0 (FA) and 3.2 (control) (Fig. 34; Appendix 7). A significant difference was observed in the relative telomere length between the control and AT patients as well as between control and FA patients ($P<0.05$).

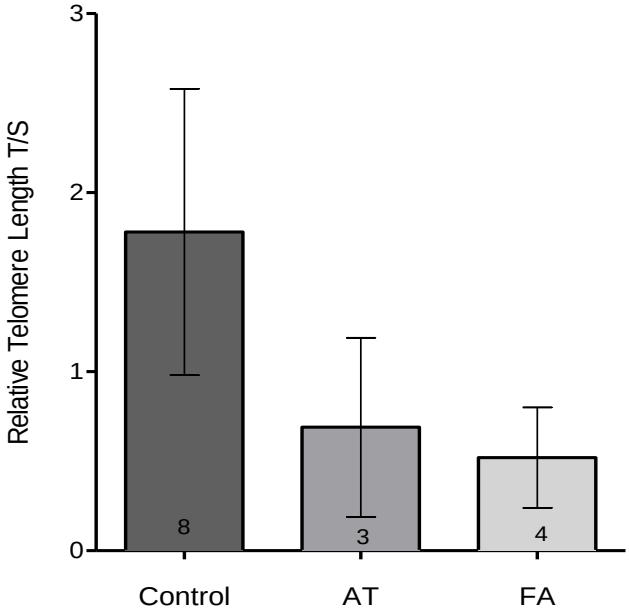

Figure 34: Relative telomere lengths ± SD in control, AT (Ataxia telangiectasia), and FA (Fanconi anemia) patients in age group from 1-10 years. The numbers in the columns represent the numbers of individuals analysed.

3.2.1.8. Comparison of telomere length in isolated B- and T-cells, peripheral blood and LCLs from control individuals of the same age

As reference for the various telomere length measurements a DNA mix of blood DNA from three healthy individuals (two females, one male) of the same age (32 years) was used. The peripheral blood itself is a mixture of mainly B-, T-, granulocytes and natural killer cells. The majority of lymphocyte metaphases obtained after PHA stimulations are derived from T-cells, while the lymphoblastoid cell lines are transformed B-cells. Here, the telomere length of pure B- (CD3) and T-cells (CD19) isolated by Flow Cytometric Analysis was compared with that of the relevant blood DNA and DNA isolated from lymphoblastoid cell lines of the same probands. The isolated B- and T-cells (CD3, CD19) showed shorter telomere lengths than the control mix. For each individual, the relative telomere length in CD19, CD3 cells was almost identical. There was, however, a slight difference between the individuals, because the relative telomere length of 07P0370 was longer than that of the two other controls. On the other hand, the relative telomere lengths of the three single blood probes were very similar (Fig. 35). In contrast to this, the relative telomere length of LCLs was obviously longer than that of the control mix. Here, the relative telomere lengths of the two lymphoblastoid cell lines were almost identical (Fig. 36).

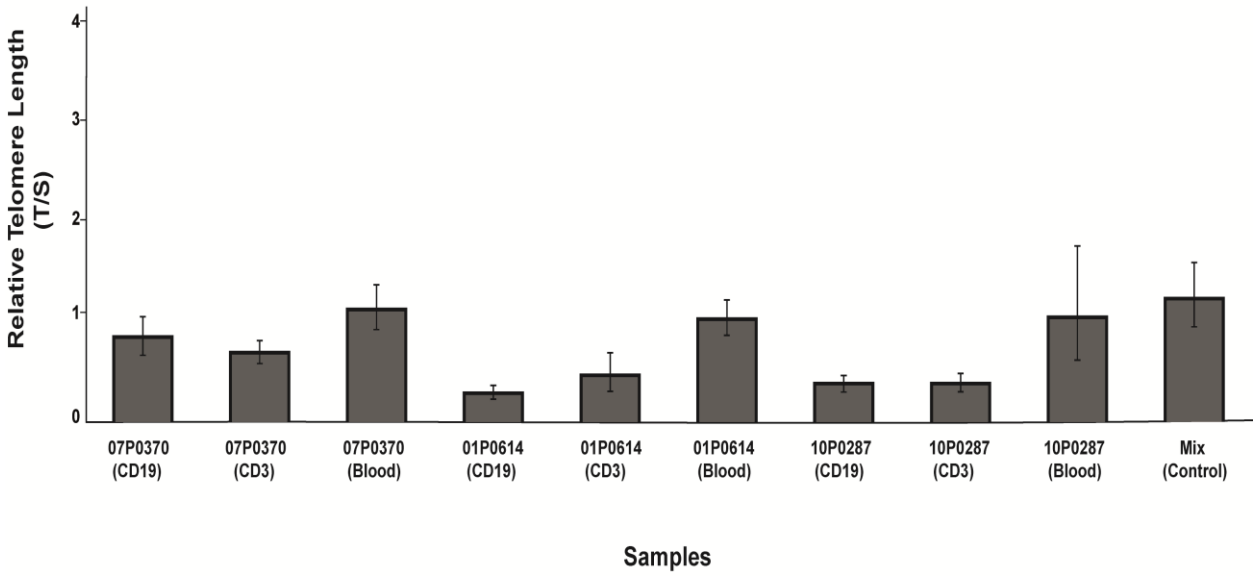

Figure 35: Relative telomere length in CD19 (T-cells), CD3 (B-cells) and blood cells of the three healthy individuals (07P0370, 01P0614 and 10P0287) measured by Q-PCR in comparison to their mixed blood DNA.

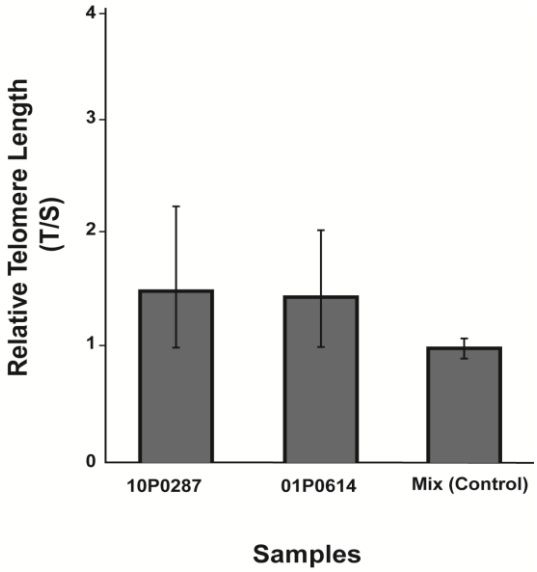

Figure 36: Relative telomere length of two lymphoblastoid cell lines (10P0287 and 01P0614) measured by Q-PCR.

3.2.1.9. Estimation of telomere length in different tissues of the NBS fetus (06P0565)

Telomere length was measured by Q-PCR in 14 different tissues from a NBS-fetus (06P0565) terminated at the 34 week of pregnancy (Fig. 37). The longest relative telomere length was found in spinal cord followed by brain, while the shortest length was observed in the skin.

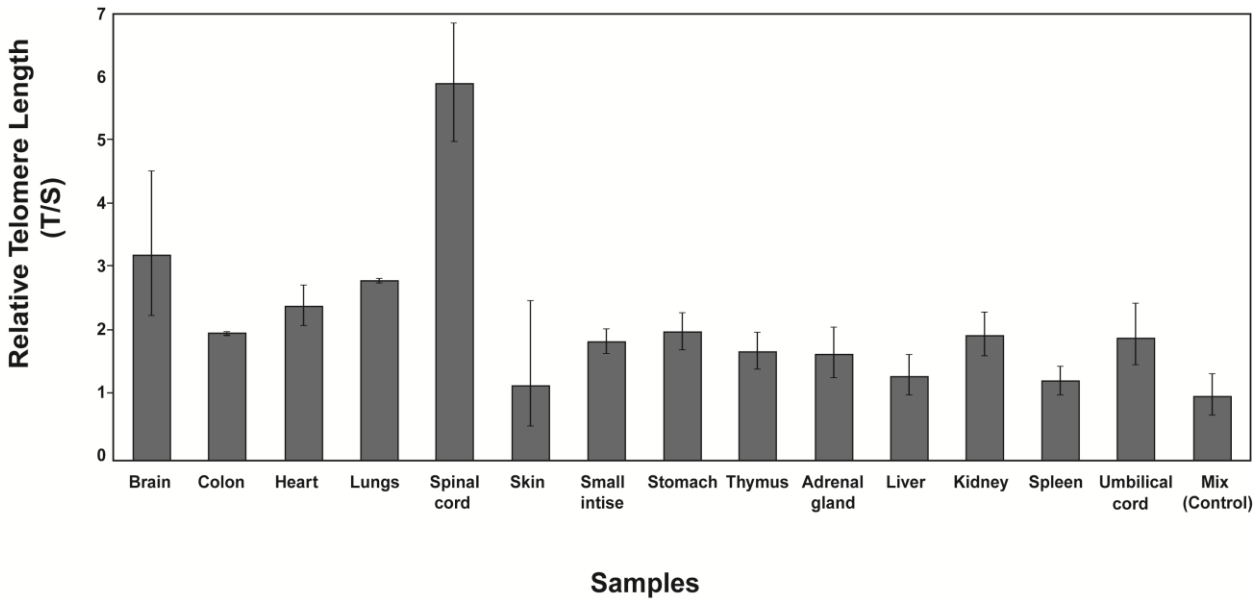

Figure 37: Relative telomere length in different tissues from a NBS-fetus (06P0565).

3.2.2. Telomere length *in vitro*

3.2.2.1. Comparison of telomere length in fibroblasts after different passages

Telomere length was measured in fibroblasts derived from three NBS cases (96P0084, BR14, 06P0565; age at skin biopsy: 7 years, 1 year, 34 week of pregnancy) and two controls (07P0670, 04P0143; age at skin biopsy 6 months and 3 months) after different passages. Relative telomere length decreased as a function of subculturing in all cell lines (Fig.38). As expected, the telomere length of the controls was much longer than that of the NBS fibroblasts. Interestingly, the NBS-fibroblast line BR14 showed a very small loss of telomeres from passage 18 to the last passage 33. It entered the phase of cellular senescence much later than the other NBS lines with P16 and P20. The controls did not reach the final stage of subcultivation.

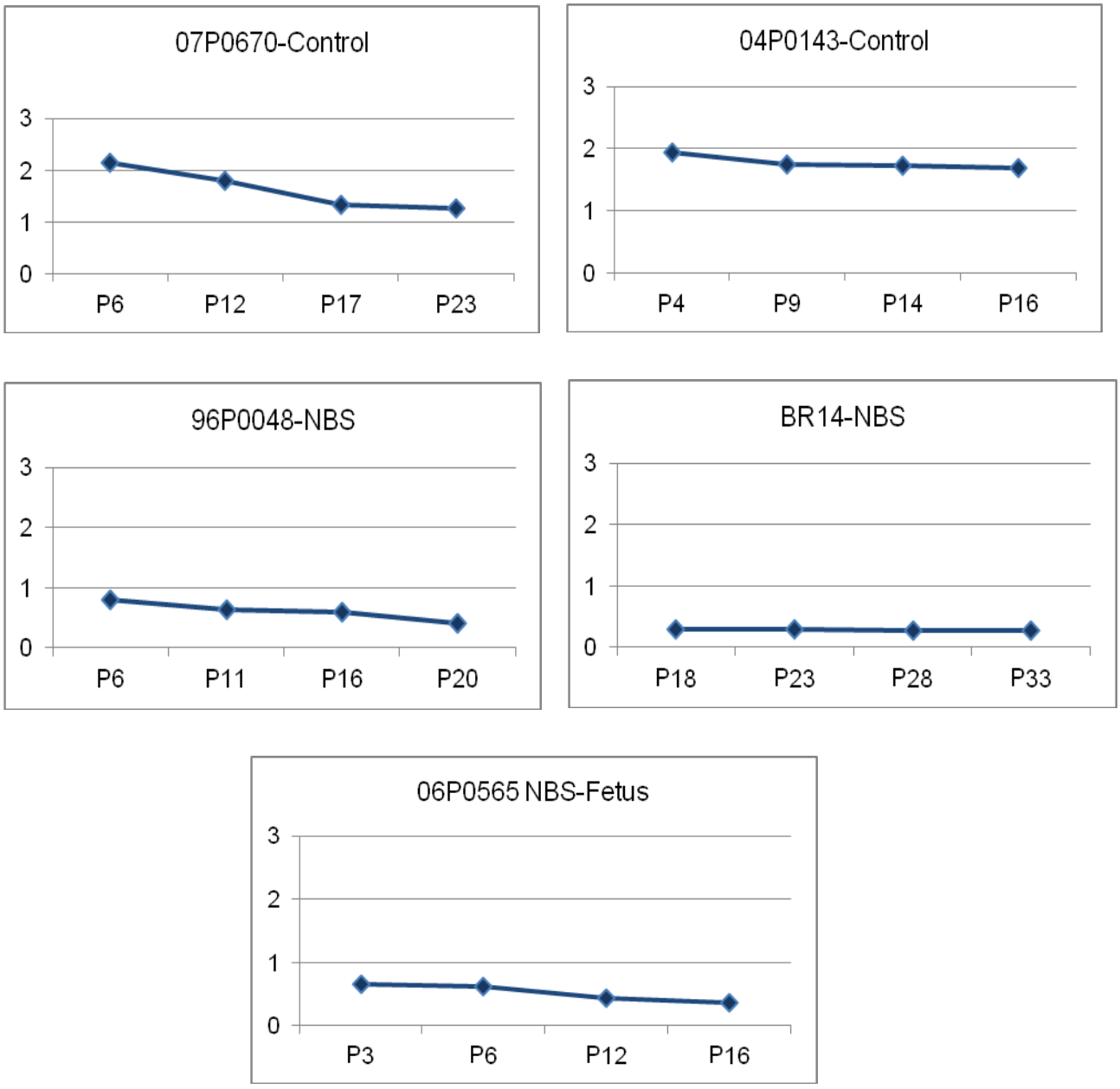

Figure 38: Relative telomere length in NBS-fibroblasts 96P0084, BR14, 06P0565 and controls 07P0670 and 04P0143 after different passages. Y axis represents the relative telomere length, x axis represents the number of passages.

3.2.2.2. Estimation of telomere length in lymphoblastoid cell lines after different passages

Telomere length in 6 NBS-LCLs (95P0182, 94P0307, 89P0319, 97P0614, 96P0616 and Rozd) and two control cell lines (96P0125 and 06P0131) was measured by Q-PCR at two different passages (Fig. 39). The telomere length remained almost constant, in the NBS and the control cell 06P0131. Here again, the relative telomere lengths of the controls were much longer than those of the NBS-LCLs.

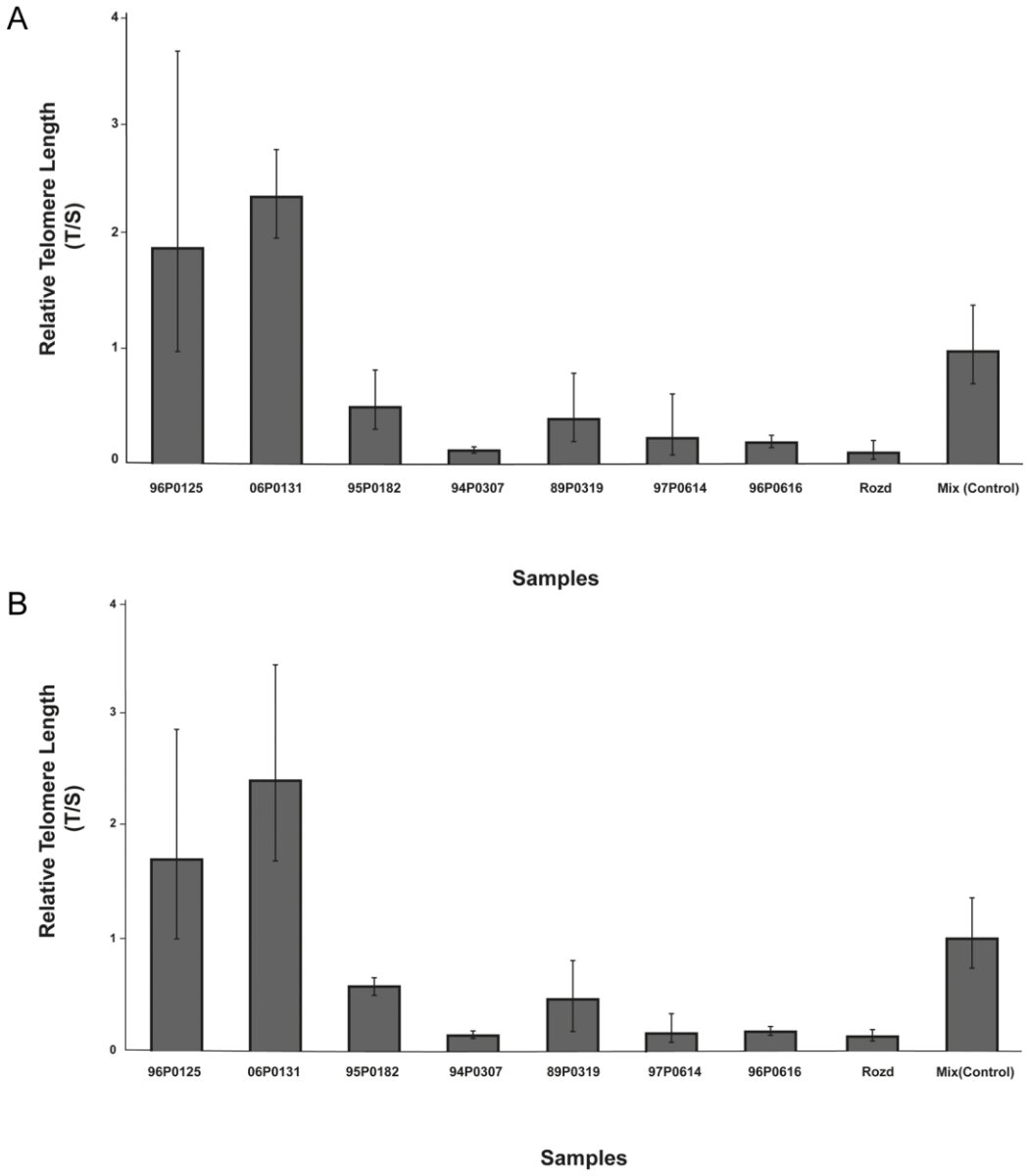

Figure 39: Relative telomere length of NBS-LCLs and two control cell lines 96P0125and 06P0131 (A), and after 6 passages (B).

3.2.2.3. Estimation of telomere length in SV40 transformed NBS fibroblasts after different passages

The diploid NBS fibroblast line GMA7166 was transformed into a permanent cell line by SV40 transfection,[156] and later the defect was corrected by introduction of the NBS wild type allele. The relative telomere length of the original diploid line showed, as expected, a decrease in its length as a function of passages. On the other hand, the telomeres of the derived SV40 transformed cell lines, both with and without the NBS wild type allele,

remained stable at all passages (Fig. 40). Their telomere length was, however, shorter than that of the original diploid fibroblasts line.

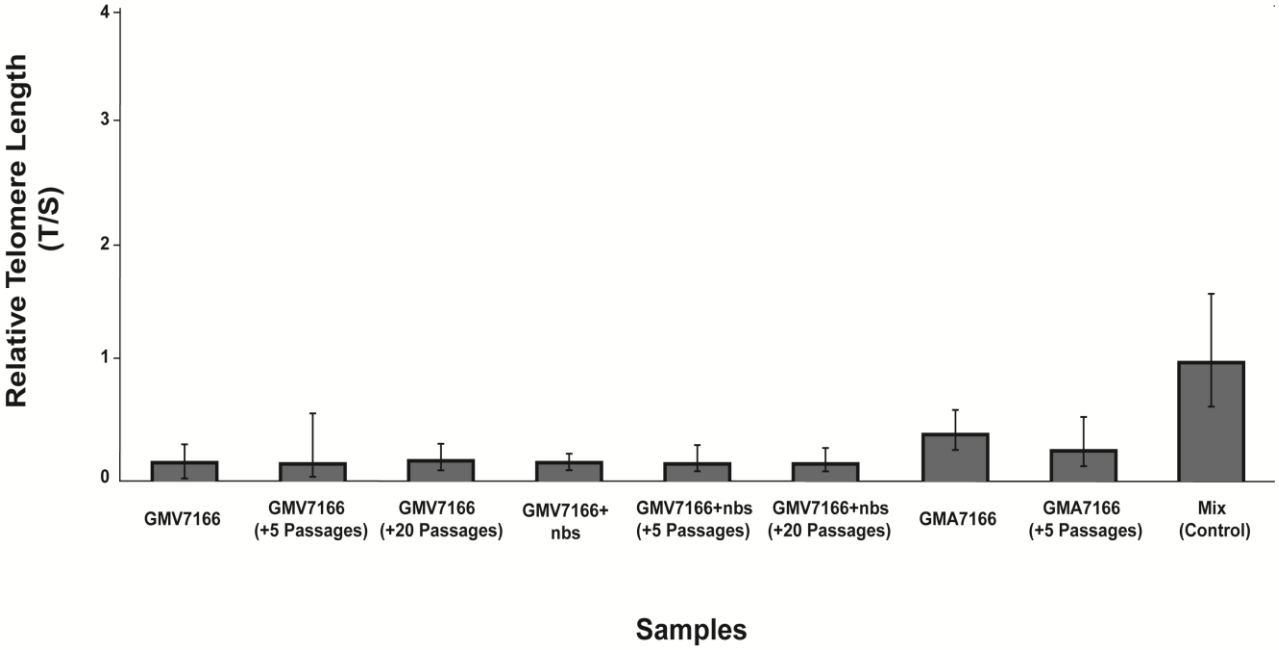

Figure 40: Relative telomere length of the SV40 fibroblast cell lines GMV7166, and GMV7166+nbs (transfected with the NBS wildtype gene) in comparison with the original diploid line from the NBS-patient GMA7166 after different passages.

3.2.2.4. Expression of telomerase in SV40 transformed NBS cell lines and LCLs

The human telomerase reverse transcriptase (*hTERT*) expression was measured at the RNA level by Q-PCR, the *GAPDH* gene served as control. The Q-PCR products were loaded on an agarose gel and separated by gel electrophoresis. A strong expression of *hTERT* was detected in the SV40 transformed NBS cell lines but not in the original diploid line GMA7166. The *hTERT* gene expression was strongly expressed in the lymphoblastoid cell line 96P0182, only weakly in 06P0131 and 94P307, and very low in 96P0614 (Fig. 41). There was no *hTERT* expression in the remaining cell lines. The same results were observed by analysis of the dissociation curves of the Q-PCR products. The height of their peaks corresponds to the amount of the template. (Fig. 42).

A

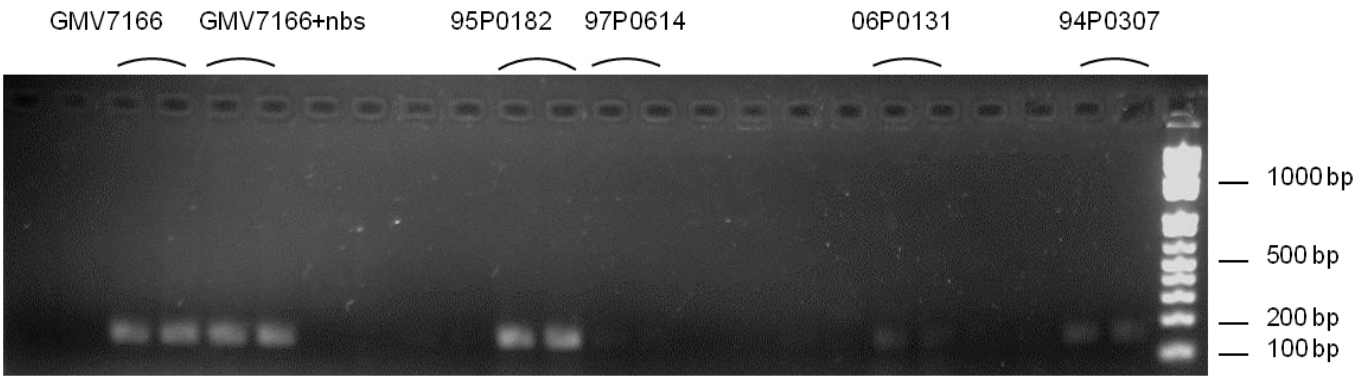

B

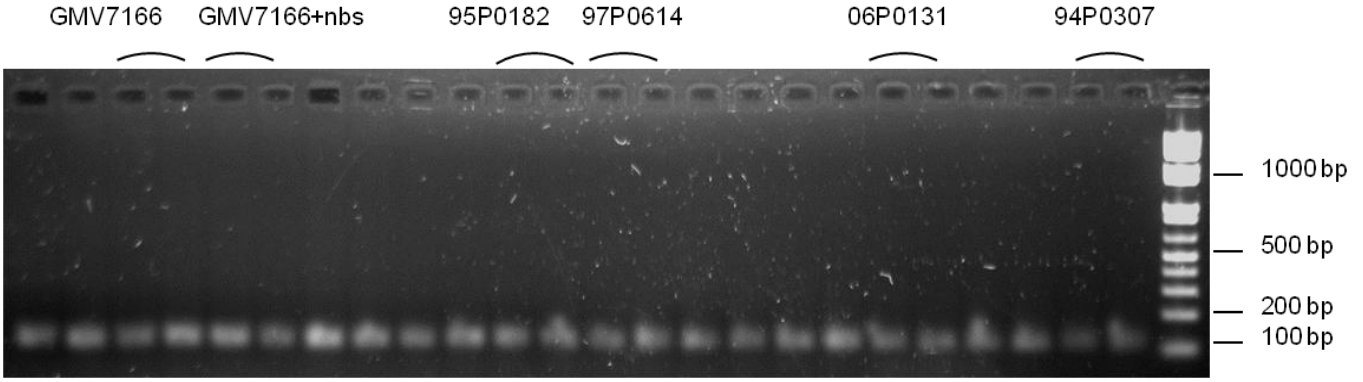

Figure 41: Electrophoresis of Q-PCR products. A: *hTERT* cDNA, B: *GAPDH* cDNA. Each sample was tested twice (two lanes for each sample), which are from left to right: 04P0721 (negative control), GMV7166, GMV7166+nbs, GMA7166, 96P0616, 95P0182, 97P0614, Rozd, 89P0319, 06P0131, 96P0125 and the last two lanes: 94P0307.

A

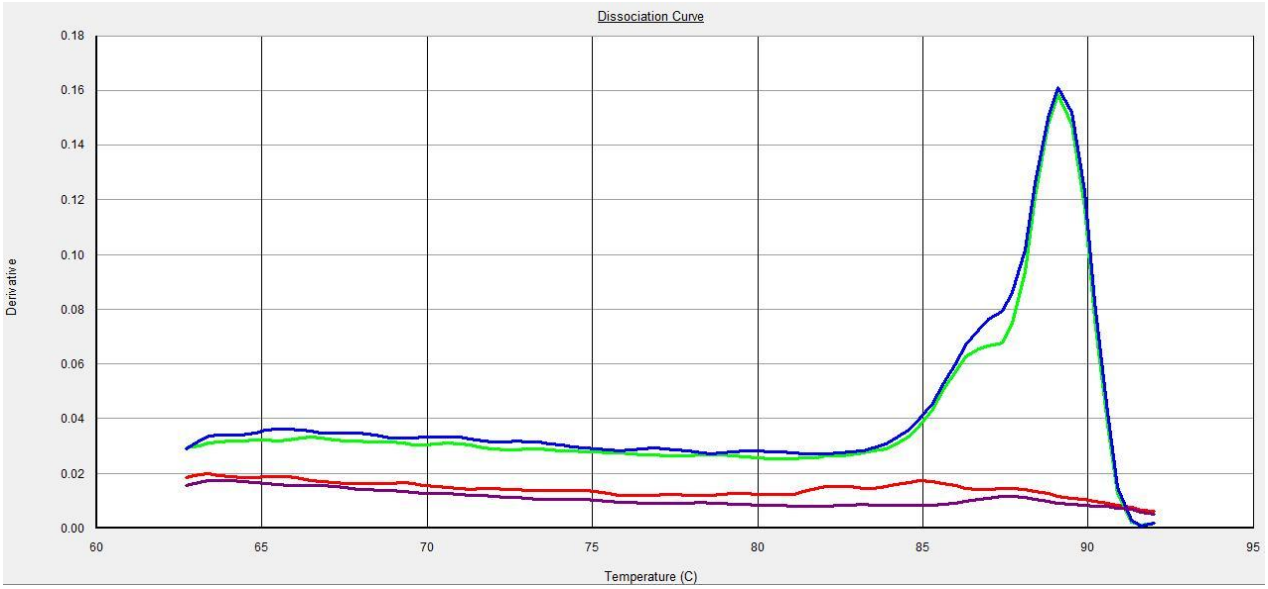

B

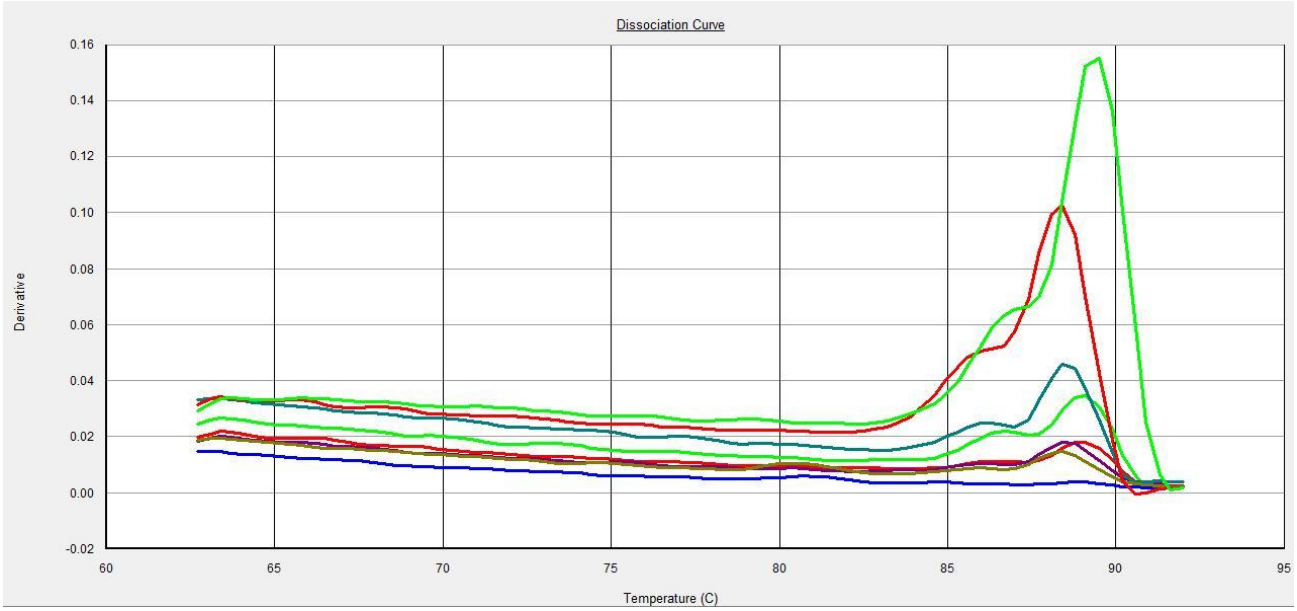

Figure 42: Dissociation curve of Q-PCR for *hTERT* cDNA (template), **A:** The high fluorescent peaks (template) correspond to GMV7166 —, and GMV7166+nbs —, the lower lines (no template) correspond to 04P0721 (negative control) —, GMA7166 —

B: The high fluorescent peaks correspond to 95P0182 (green) —, 94P0307 (red) —, the weak fluorescence peaks correspond to 06P0131—, 97P0614 —, the lower lines (no template) correspond to 89P0319 —, 96P0616 —, Rozd— and 96P0125—

3.2.3. Estimation of telomere length in different tissues of a humanized Nbs mouse model

The humanized Nbs mouse expresses the human NBS gene with the 5pb deletion and can serve as an *in vivo* model, which accurately reproduces the NBS genotype.[157] It is an original approach to improve understanding of NBS pathophysiology and to develop new therapies.[158] This humanized mouse model has been generated by the introduction of the human 5 bp deletion hypomorphic allele (hNBS del5) into NBS-deficient mice. These *hNbs1657Δ5* mice express the C-terminal Nbs p70 protein. [159]

Telomere length was measured by Q-PCR in DNA collected from four different tissues of three humanized Nbs mice with the mutated allele (no 92, 87 and 68), which were about 39, 32 and 41 days of age and two humanized Nbs mice with the human wild-type allele (no 95 and 98),which were both about 32 days of age. Relative telomere length was in all tissues of the mice with the human wild-type allele higher than in those with the mutated allele (Fig. 43). Telomeres in brain tissue showed a higher length than those in the other tissues in both control mice (no 95 and 98) and in one humanized Nbs mouse (no 68). Telomere length had almost the same level in the different tissues of the two other humanized NBS mice (no 92 and 87).

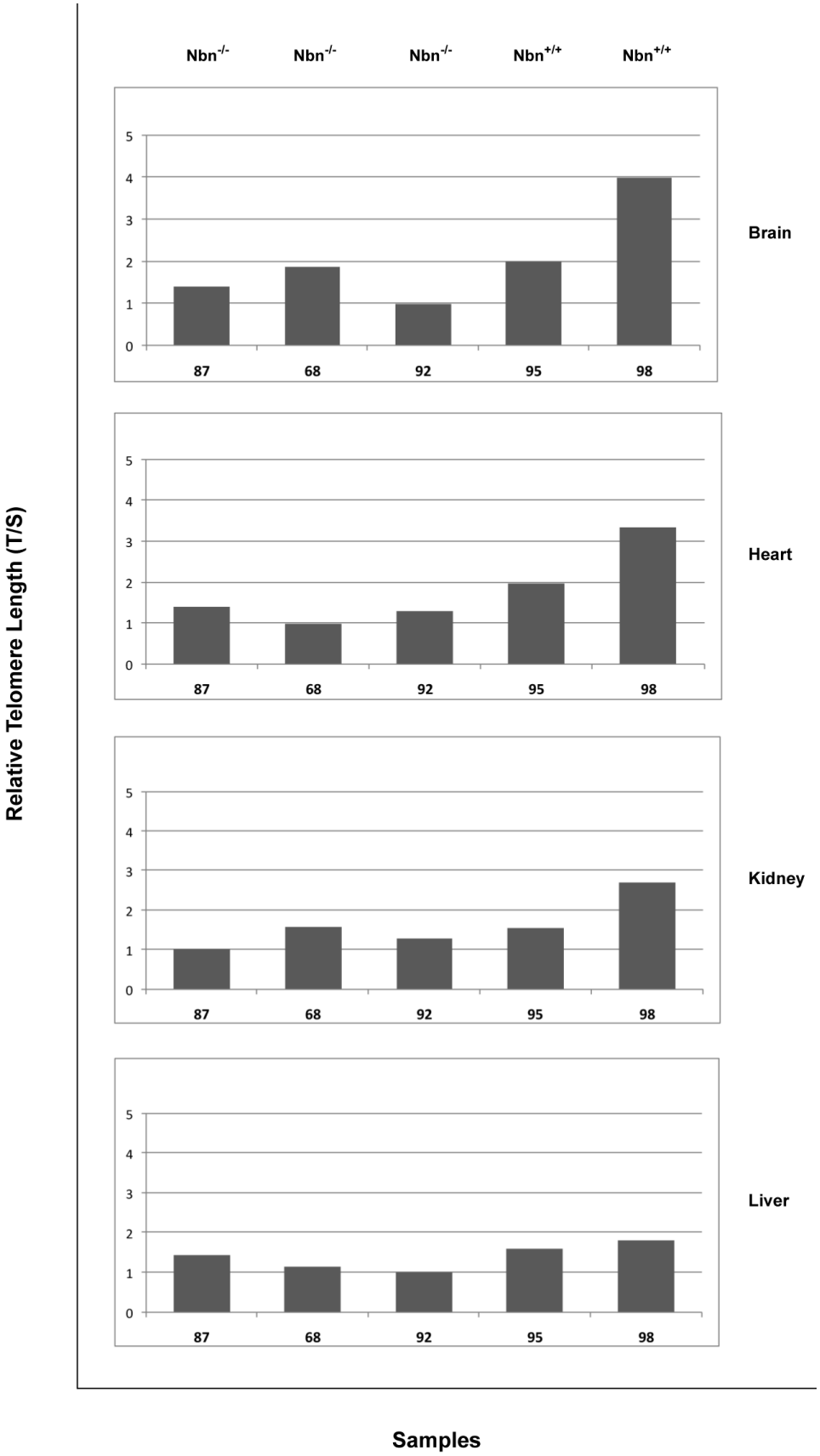

Figure 43: Relative telomere length in brain, heart, kidney and liver tissues of humanized Nbs mice ($Nbn^{-/-}$): 87, 68 and 92, and humanized wild-type mice ($Nbn^{+/+}$): 95 and 98 measured by Q-PCR.

3.3. Estimation of telomere length by Q- FISH

A boxplot is used to visually summarize and compare groups of data. The boxplot uses the median, the approximate quartiles, and the lowest and highest data points to convey the level, spread, and symmetry of a distribution of data values (Fig. 44). It depicts here the distribution of telomere lengths for each sample, with minimum, maximum, Q3: 75% percentile, Q1: 25% percentile and the median: 50% percentile (the T/C value).

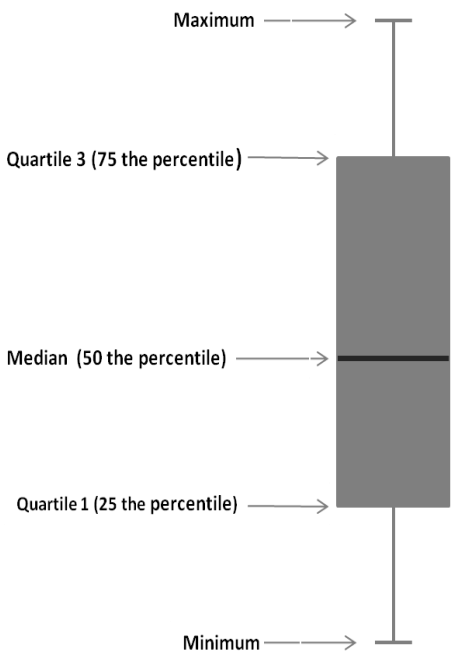

Figure 44: Schematic representation of a boxplot presenting the corresponding values for median, quartile1, quartile 3, minimum and maximum values.

3.3.1. Telomere length in NBS-fibroblast cell lines and controls

Telomere length in three NBS-fibroblasts and two control cell lines was measured by Q-FISH at passage 7. Telomere length was significantly longer in the controls than in the NBS-fibroblasts ($P<0.05$; Mann-Whitney test) with median values (T/C values) of 87.9 and 87.5 for controls, and 61.9, 53.3 and 48.5 for the NBS-cell lines (Fig. 45; Appendix 8). The NBS-cell lines 94P0112 and 96P0048 showed very poor growth. The cell cycle with about 6 to 10 days was much longer than that of the controls with approximately 48 hours. Thus, many attempts to get good quality metaphases from the NBS-fibroblasts failed and only cells of passage 7 could be analysed.

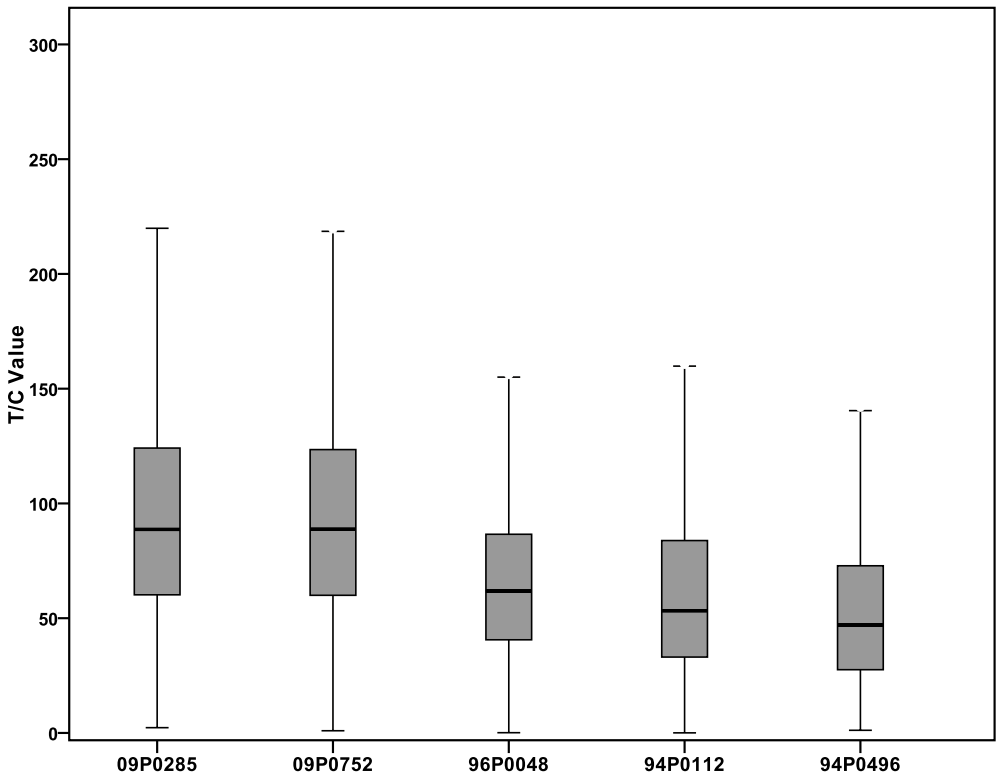

Figure 45: Boxplots of total telomere lengths (T/C value) of NBS-fibroblast cell lines and two controls 09P0285 and 09P0752 at passage 7.

Telomere length was measured in control fibroblast cell line 09P0285 at passage 7 and 24. The median values (T/C values): were 87.9 at passage 7 and 56.1 at passage 24 (Fig. 46; Appendix 9). The telomere length decreased, as expected, and the decrease was significant ($P<0.05$; Wilcoxon test).

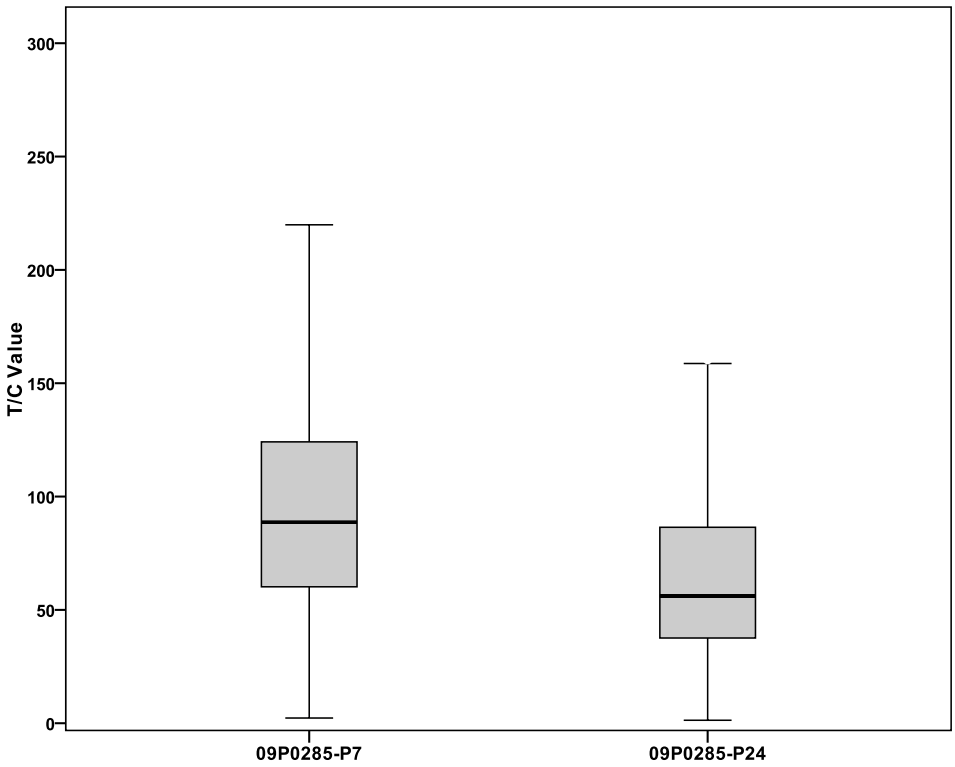

Figure 46: Boxplots of total telomere lengths (T/C value) of fibroblast cell line 09P0285 at passage 7 and 24.

3.3.2. Telomere length in NBS-lymphoblastoid cell lines and control cell lines after different passages

Telomere length (T/C values) of NBS-lymphoblastoid cell lines (LCLs) after different passages was measured by Q-FISH. A significant difference ($P<0.05$; Mann-Whitney test) was found between the telomere lengths of the controls and each of the six NBS-LCLs both at the beginning and after 6 passages (Fig. 47), this was also observed by Q-PCR as shown above. Telomere lengths have not shown reduction after 6 passages in the NBS and the control cell 06P0131.The NBS lines, however, exhibited some spontaneous aberrations, such as chromatid breaks and translocations. More interestingly, the cell line 94P0307 showed in 50 % of metaphases telomere fusions and had also the shortest telomere length of all NBS-LCLs.

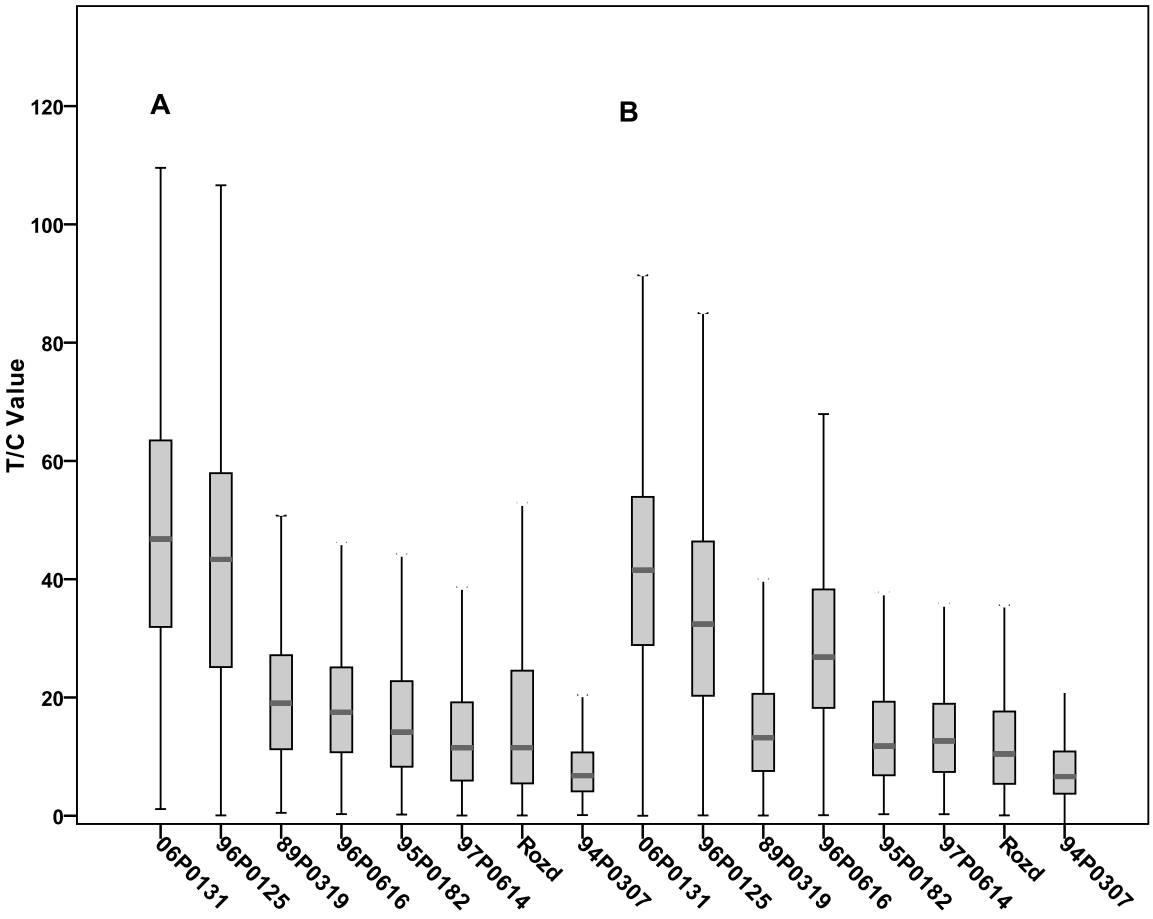

Figure 47: Boxplots of total telomere lengths (T/C values) of NBS-LCLs and two control lines 06P0131 and 96P0125 (A), and after 6 passages (B).

3.3.2.1. Telomere length of individual chromosomes in the lymphoblastoid NBS line 94P0307

This cell line showed a telomere fusion in 50 % of the metaphases, the fusion was between the p telomere of chromosome 2 and an undefined chromosome, which was difficult to identify (Fig. 48). The telomere length of this NBS-LCL was measured in both of its cell types: one with normal karyotype and one with this fusion (8 metaphases were analysed each). The latter cells with the marker chromosome showed a significantly longer telomere length (T/C value) than the normal ones ($P<0.05$; Mann-Whitney test) (Fig. 49).

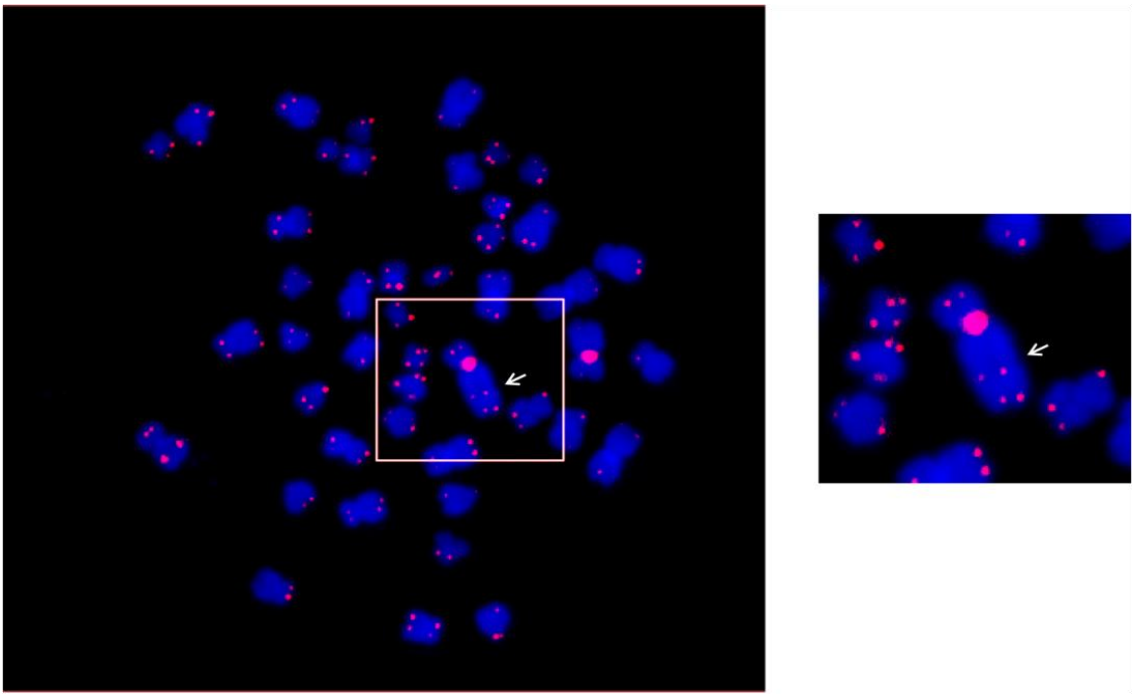

Figure 48: Metaphase of NBS-LCL 94P0307 after Q-FISH. The arrow points to the telomere fusion between p telomere of chromosome 2 and an undefined chromosome

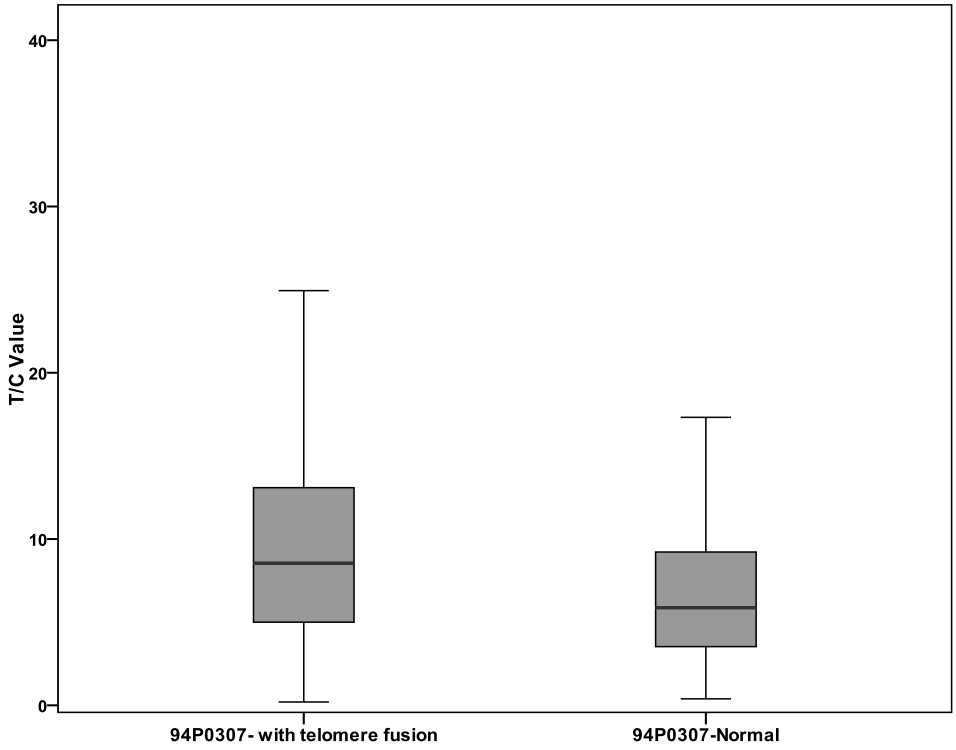

Figure 49: Boxplots of total telomere length (T/C Value) of two types of cells of the NBS-LCL 94P0307, one with normal karyotype and one with telomere fusion (8 metaphases were analysed each).

In addition to this, an extremely highly fluorescent telomere was observed on the p arm of one chromosome 19 in 70% of the metaphases in this lymphoblastoid cell line, while the other chromosomes 19 had only weak fluorescence intensity (Fig. 50). The ratio between their relative T/C values was about 11:1 (Fig. 50 (B); Table 14). Thus, this line was a mosaic with respect to chromosome. This is due to a spontaneous *in vitro* elongation of the chromosome 19 telomere. Telomere lengths (T/C values) of p and q arms of the chromosomes were also estimated by Q-FISH which showed the higher length of telomere in p arm of chromosome 19 (Fig. 51; Appendix 10). Its percentage was (13%) lower in cells analyzed at a later passage.

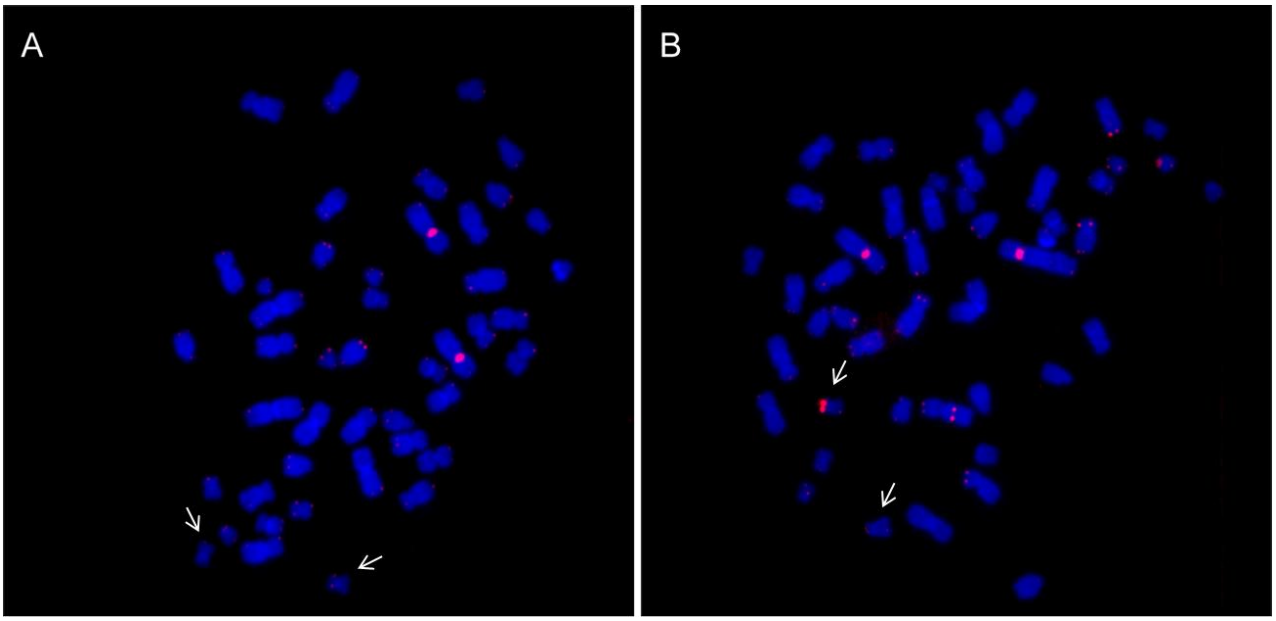

Figure 50: Metaphases of the NBS-LCL 94P0307 after Q-FISH showing a highly fluorescent telomere of the p-arm of one chromosome 19 and the other chromosomes 19 with weak fluorescence intensity (A; white arrows), and with the normal p arms of chromosome 19 (B; white arrows).

Table 14: T/C-FISH data on telomere lengths of p arm of chromosome 19 with high fluorescence intensity and p arm of the other chromosome 19 with weak fluorescence intensity of NBS-LCL 94P0307 (from 11 metaphases analysed)

Metaphase	**Median of p-arm (T/C value) of chromosome 19 with high fluorescence intensity**	**Median of p-arm (T/C value) of chromosome 19 with weak fluorescence intensity**
1	85.19	3.23
2	52.61	12.62
3	47.14	2.04
4	44.1	2.11
5	60.46	8.18
6	33.44	1.06
7	79.36	2.1
8	60.24	6.33
9	32.86	2.15
10	68.29	3.45
11	58.61	9.55
Average	**56.57**	**4.80**

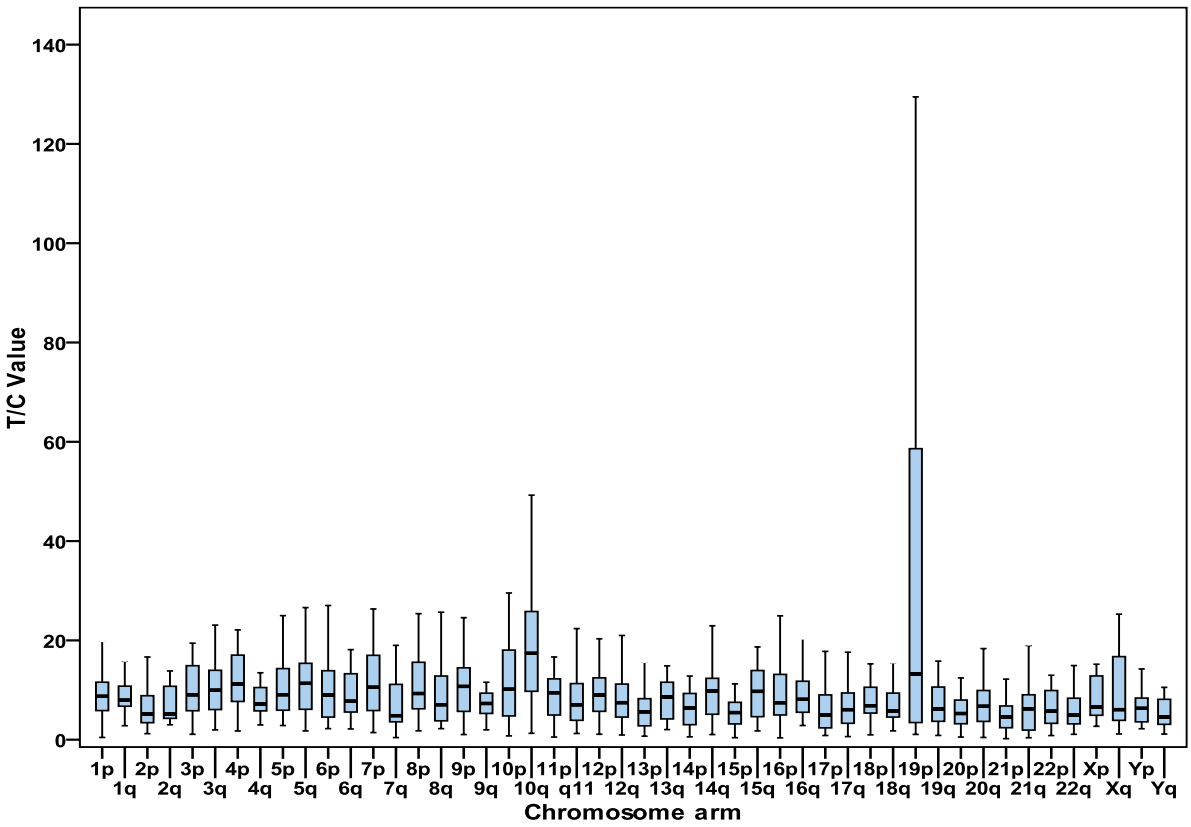

Figure 51: Boxplots of telomere lengths (T/C value) of p and q arms of autosomes 1-22 and sex chromosomes X and Y of the NBS-LCL 94P0307.

3.3.3. Estimation of telomere length in SV40 transformed cell lines after different passages

Telomere length was measured by Q-FISH in the SV40 transformed NBS cell line GMV7166, the same line transfected with the NBS wildtype gene GMV7166+nbs and the original diploid fibroblast line GMA7166 after different passages. The diploid line showed, as expected, a significant decrease in telomere length after subculturing ($P<0.05$; Wilcoxon test; Fig. 52). No significant difference was observed in this respect in the SV40 transformed line without and with the NBS wild type gene ($P>0.05$; Wilcoxon test; Fig. 53, 54). The telomere length of the diploid fibroblasts was longer than that of both SV40 transformed cell lines, confirming the Q-PCR analysis (see Fig. 40). The diploid cells stopped growth after 27 passages, while the SV40 transformed cells were fully transformed and proliferated rapidly, however, they showed different types of structural chromosome aberrations and were aneuploid (average chromosome number: 49).

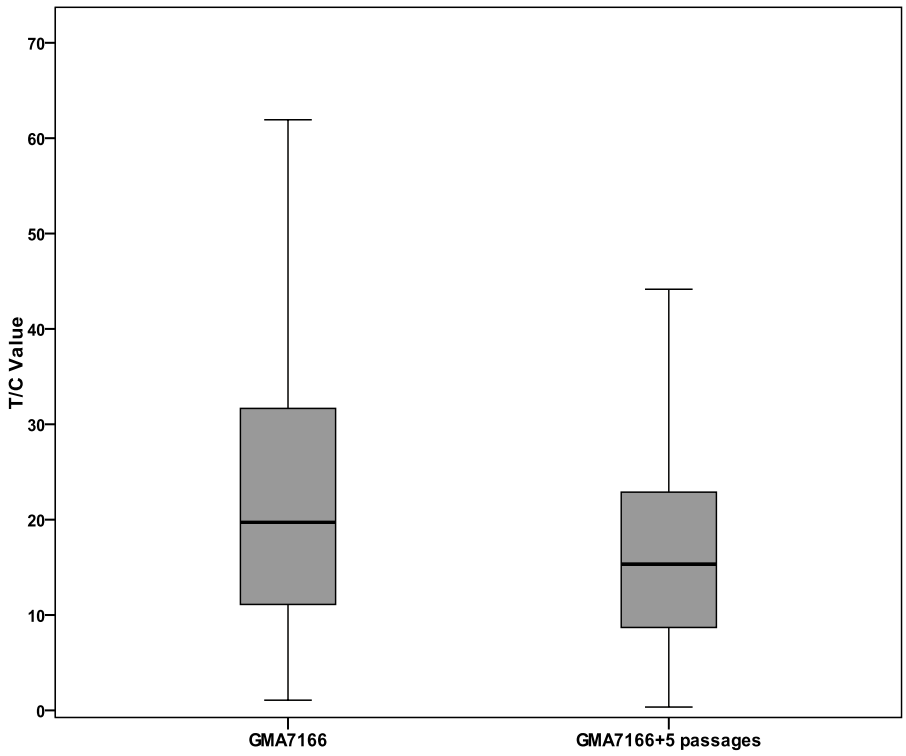

Figure 52: Boxplots of the total telomere length (T/C value) of NBS fibroblast cell line GMA7166 (NBS patient) after two different passages (15 metaphases were analysed each).

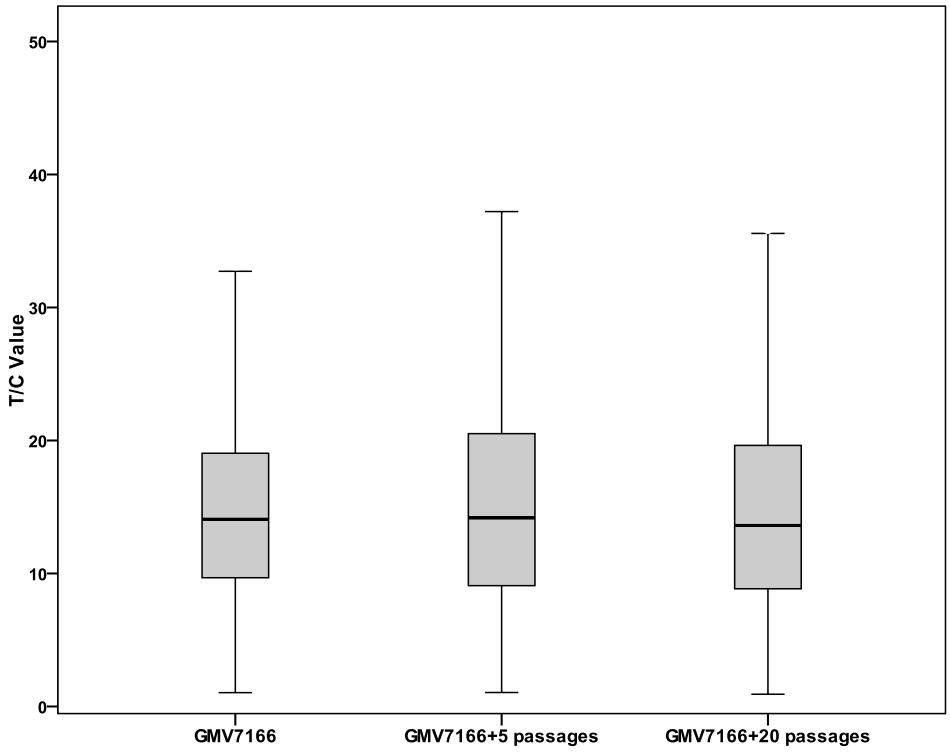

Figure 53: Boxplots of the total telomere length (T/C value) of SV40 transformed NBS fibroblast cell line GMV7166 at three different passages (15 metaphases were analysed each).

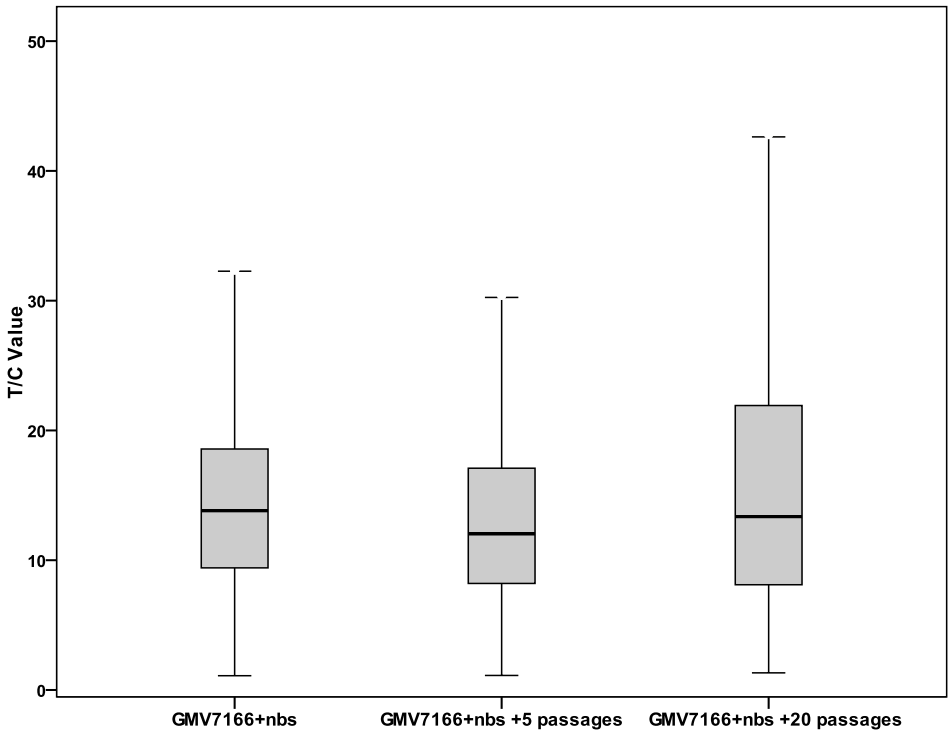

Figure 54: Boxplots of the total telomere length (T/C value) of SV40 fibroblast cell line transfected with the NBS wildtype gene GMV7166+nbs at three different passages (15 metaphases were analysed each).

3.3.4. Estimation of telomere length of individual chromosomes

Telomere length (T/C value) of individual chromosomes was measured in the control fibroblast cell line 09P0285 at passage 7 and 24 (Fig. 55, 56). A significant decrease in telomere length (T/C values) was observed in all chromosomes, the median T/C value dropped from 88.7 to 56.1 ($P<0.05$). Chromosomes 8 and 14 showed the longest telomere lengths with median T/C values of 106.7 and 100.6 at P7 and 76.2 and 78.4 at P24, respectively. The shortest telomere length was observed in chromosome 19 in both passages with median T/C values of 66.4 and 37.0.

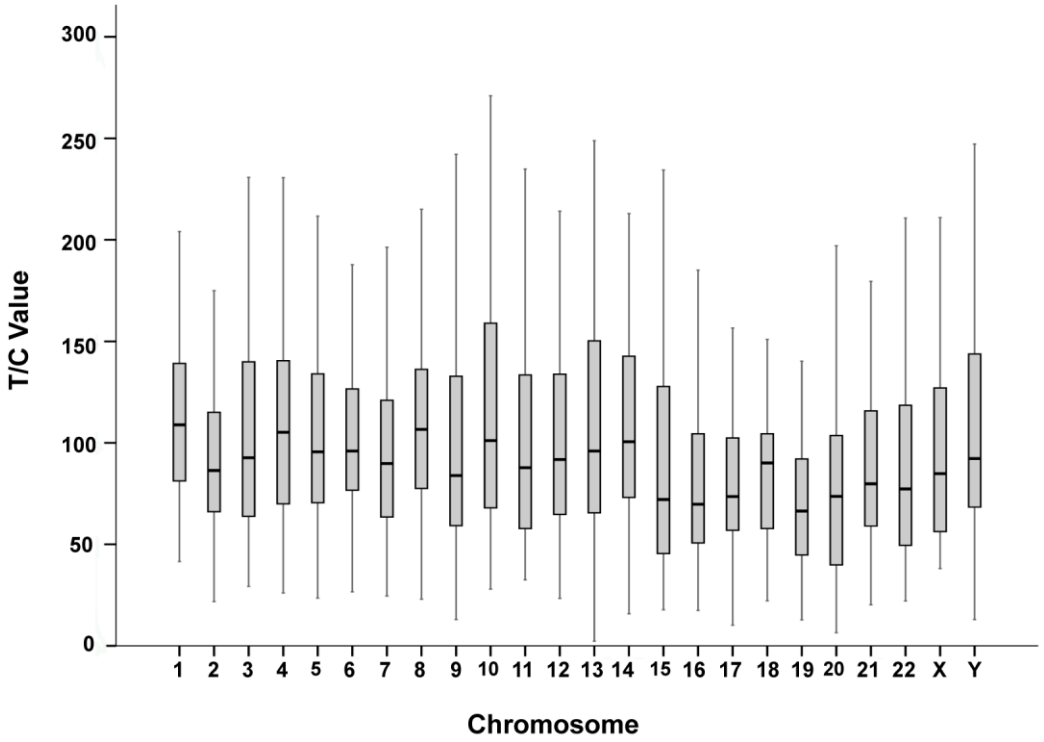

Figure 55: Boxplots of telomere lengths (T/C value) of all chromosomes (autosome 1-22 and sex chromosomes X and Y) of fibroblast line 09P0285 at passage 7.

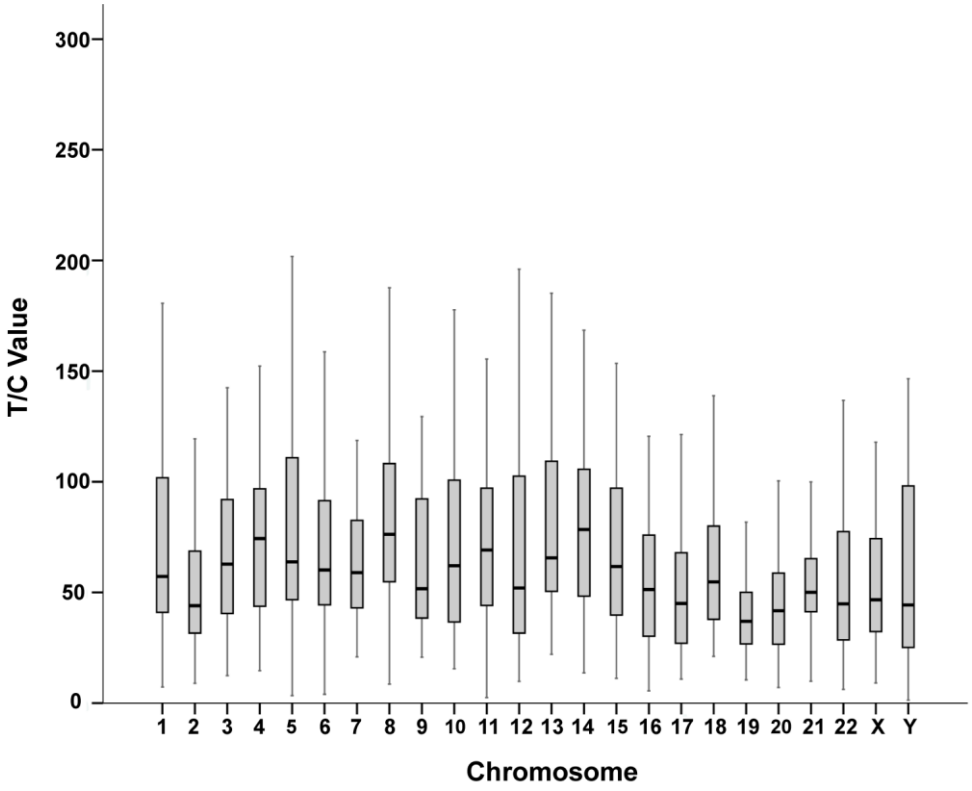

Figure 56: Boxplots of telomere lengths T/C value of all chromosomes (autosome 1-22 and sex chromosomes X and Y) of fibroblast line 09P0285 at passage 24.

Telomere length was also estimated in the NBS-fibroblast line 94P0496 for all individual chromosomes (Fig. 57). Here, chromosome 4 showed the longest telomere length (median T/C value: 51.8) and chromosome 22 the shortest length (median T/C value: 19.5). Telomere lengths (T/C values) of chromosomes of the control were significantly longer for each telomere than that of the NBS chromosomes (P<0.05).

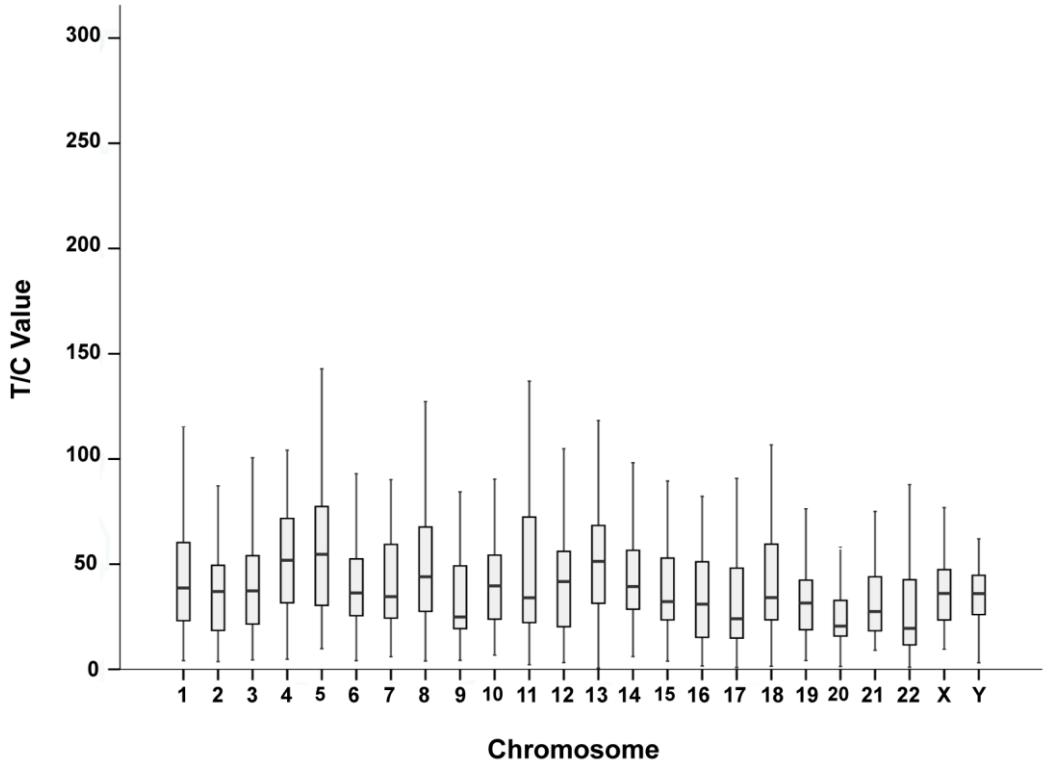

Figure 57: Boxplots of telomere lengths (T/C value) of all chromosomes (autosome 1-22 and sex chromosomes X and Y) of NBS-fibroblast line 94P0496.

3.3.4.1. Estimation of telomere length in p and q arms of individual chromosomes

Telomere length of p and q arms of autosomes and sex chromosomes was estimated by Q-FISH in three lymphoblastoid cell lines, one control (06P0131), and two NBS-LCLs (97P0614 and 95P0182, Fig. 58, 59). Telomere lengths (T/C values) of p and q chromosome arms of the control were significantly longer for each telomere than that of the NBS chromosomes (P<0.05). The longest telomere lengths in the control were 4p (median T/C value 70.1) and 3q (median T/C value 62.8), while shortest lengths were 19p (median T/C value 29.8) and 22q (median T/C value 29.9). The longest telomere lengths in NBS chromosomes were still shorter than the shortest of the controls. In 97P0614 it was 3p (median T/C value 21) and 4q (median T/C value 17.1) and in 95P0182 it was 14p (median T/C value 24.8) and 4q (median T/C value 23.5). The shortest NBS telomeres were in

97P0614 12p (median T/C value 4.9) and 20q (median T/C value: 5.6), and in 95P0182 it was, as in the control, 19p (T/C value 7.7) and 17q (median T/C value 5.9).

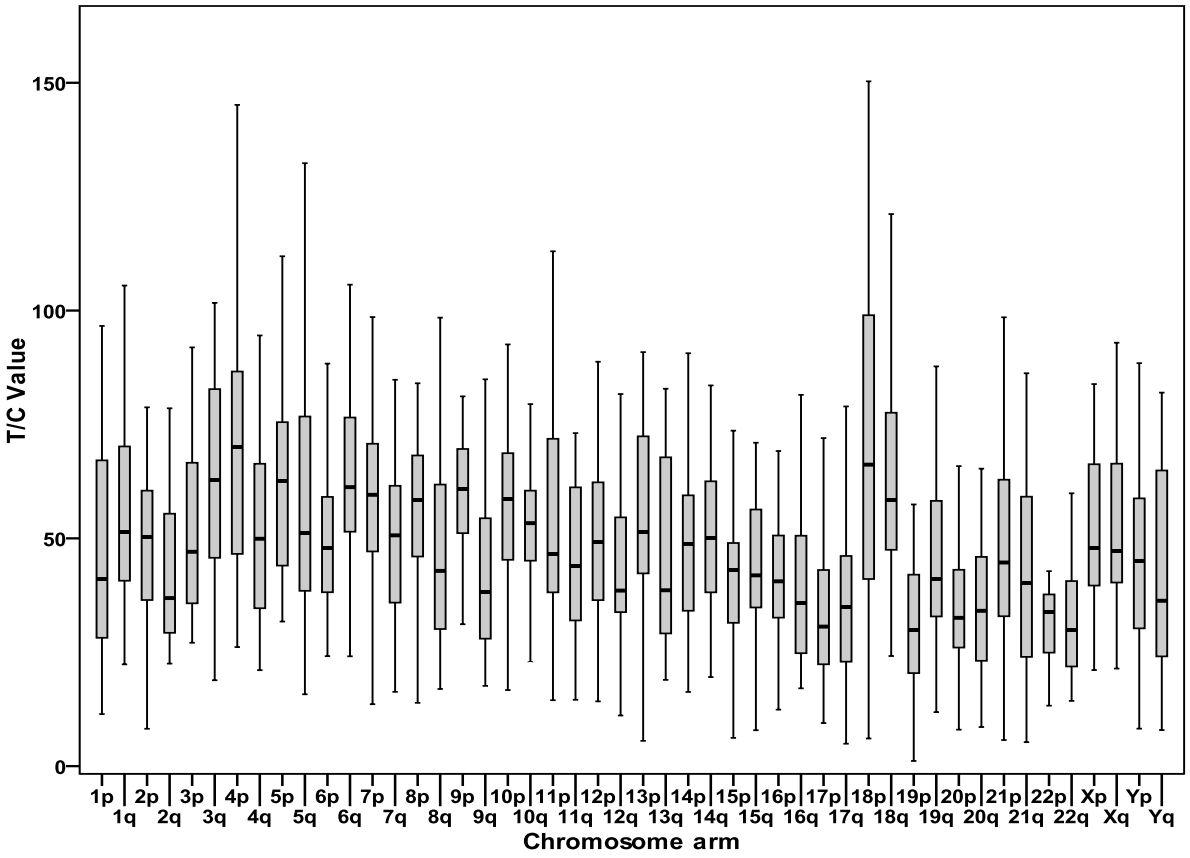

Figure 58: Boxplots of telomere lengths (T/C value) of p and q arms of all chromosomes (autosomes 1-22 and sex chromosomes X and Y) of the control-LCL 06P0131.

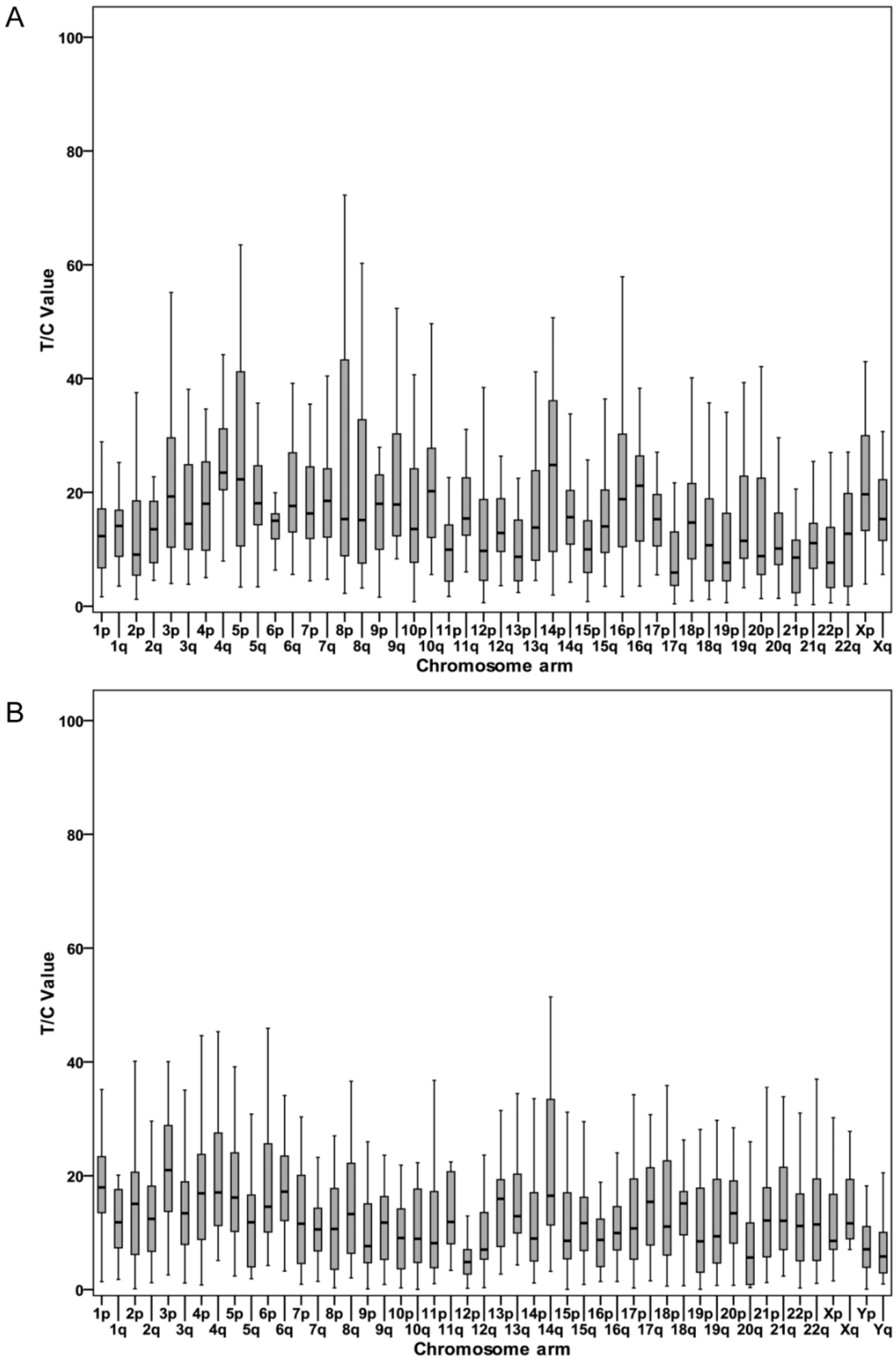

Figure 59: Boxplots of telomere lengths (T/C value) of p and q arms of all chromosomes (autosomes 1-22 and sex chromosomes X and Y) of the NBS-LCL 96P0182 (A) and 97P0614 (B).

3.3.4.1.2. Estimation of telomere length in p and q arms of chromosomes 1, 17, 19 and the X

Telomere lengths of p and q arms of autosome chromosomes 1, 17 and 19 and sex chromosome X were measured by Q- FISH in lymphocyte metaphases of two females 01P0614, 07P0370 and one male 10P0287 who served as controls throughout this study and were of same age with 32 years. In all three cases, the telomere lengths (T/C values) of p and q arms of chromosome 1 were the longest of the autosomes while p and q arms of chromosome 19 had the shortest telomere lengths. On the other hand, telomere length of the X p arm was longer than that of the q arm in all three samples (Fig. 60).

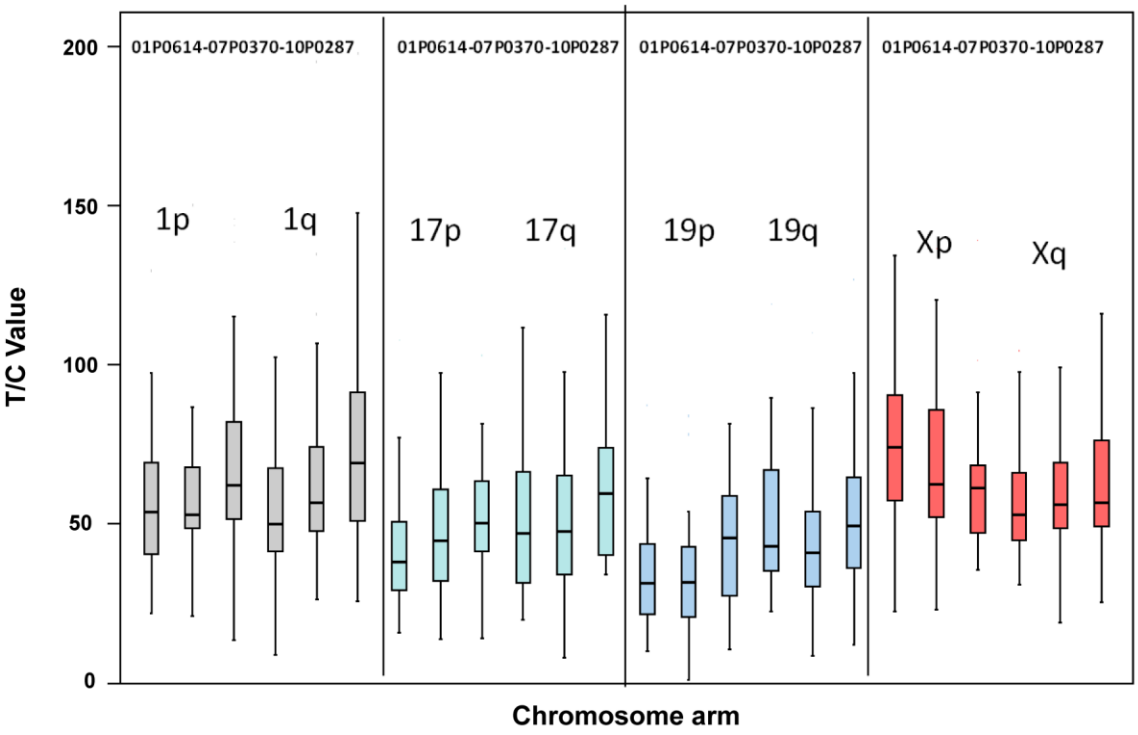

Figure 60: Boxplots of telomere lengths (T/C value) of p and q arms of autosomes 1, 17, 19 and the X in lymphocyte metaphases of the control individuals 01P0614, 07P0370 and 10P0287.

3.3.4.2. Estimation of telomere length of X and Y chromosomes

In order to test if the parental origin of the chromosomes has an influence on telomere length (T/C values) the X and Y telomeres were estimated by Q-FISH in lymphoblastoid and fibroblast cell lines of two NBS males and one control, each. The X is of maternal, the Y chromosome of paternal origin. It was observed that in the LCLs the X telomeres were longer than the Y telomeres, however, the difference was significant only in the NBS line 97P0614 ($P<0.05$) (Fig. 61). Likewise, in the three male fibroblast cell lines the X telomeres were only in one NBS line longer, in the two other lines, however, shorter than those of the Y chromosomes (Fig. 62). The difference in the latter cases was not significant

(P>0.05). Thus, no clear correlation was found between the parental origin of the telomeres.

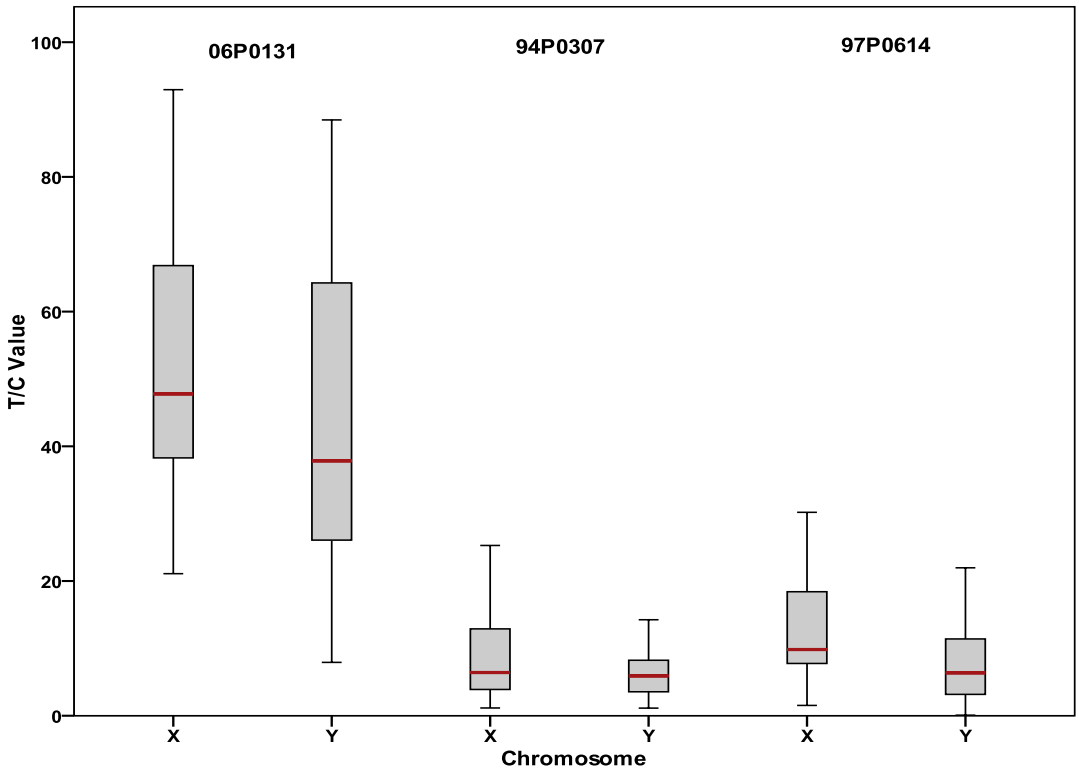

Figure 61: Boxplots of telomere lengths (T/C value) of the X and Y chromosomes in three male cell lines: NBS-LCLs 94P0307, 97P0614 and the control 06P0131.

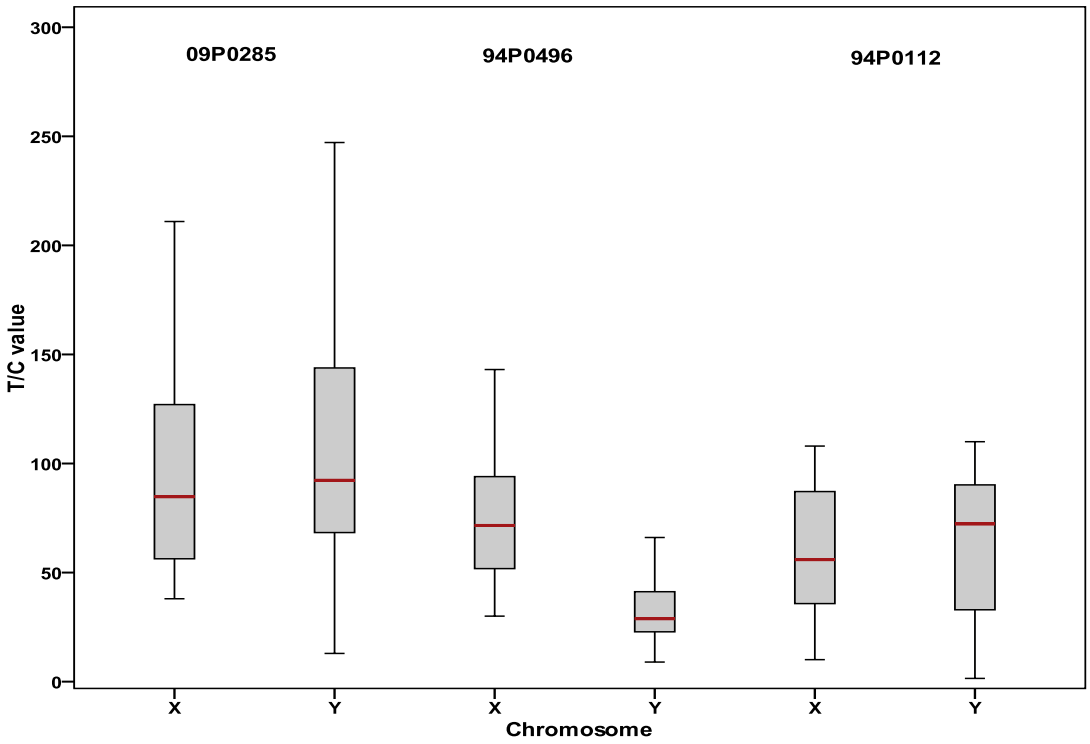

Figure 62: Boxplots of telomere lengths (T/C value) of the X and Y chromosomes in three male cell lines: NBS-fibroblasts 94P0112, 94P496 and the control 09P0285.

3.4. Comparison of telomere length measurements between Q-PCR, Q-FIH, and TRF analysis.

3.4.1. Correlation between Q-PCR and Q-FISH

Total telomere length was estimated by Q-FISH and by Q-PCR in seven lymphoblastoid cell lines, five NBS and two controls, at two different passages. A highly positive correlation was found between both approaches. The correlation coefficient was r = 0.97 at the early passage (Fig. 63), and r=0.87 after six further passages (Fig. 64). Likewise, a highly positive correlation was shown between the Q-FISH and Q-PCR data of telomere length in the diploid NBS line GMA7166 and the derived SV40 transformed lines GMV7166, and GMV7166+nbs (transfected with the NBS wildtype gene) with a correlation coefficient of r = 0. 96. (Fig. 65). Thus, the Q-FISH and Q-PCR data, which both represent relative telomere lengths, show a tight linear relationship.

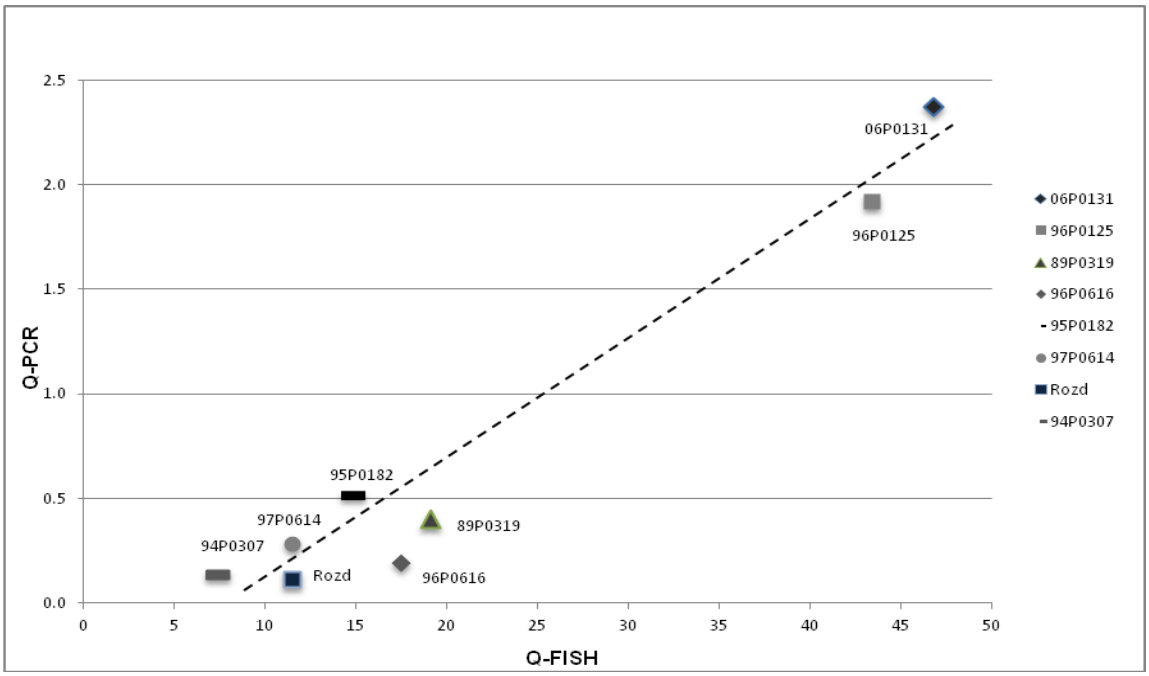

Figure 63: Correlation between Q-PCR and Q-FISH in NBS- and control-LCLs at an early passage. The corresponding correlation coefficient is r = 0.97.

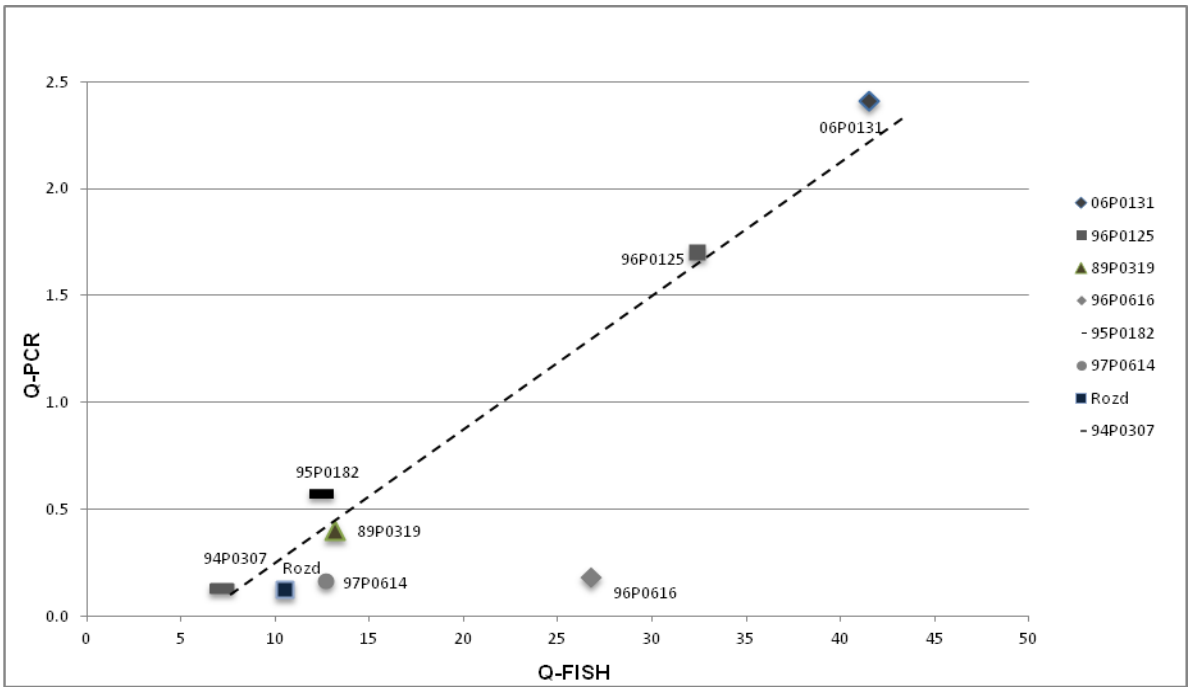

Figure 64: Correlation between Q-PCR and Q-FISH in NBS- and control-LCLs after 6 passages. The corresponding correlation coefficient is r = 0.87.

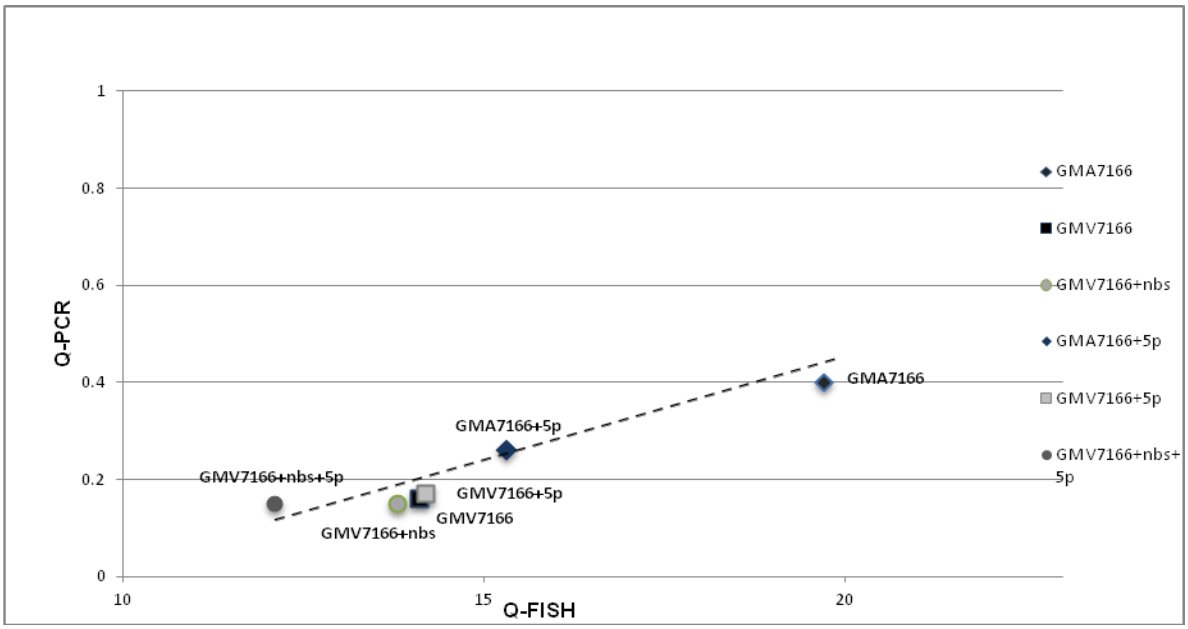

Figure 65: Correlation between Q-PCR and Q-FISH in SV40 transformed cell line GMV7166, GMV7166+nbs and the NBS patient GMA7166 after different passages. The corresponding correlation coefficient is r = 0. 96.

3.4.2. Correlation between Q-PCR and TRF analysis

Telomeric restriction fragments (TRF) analysis measures the average absolute telomere length and was compared with the relative length estimated by Q-PCR in the same seven DNA probes, derived from peripheral blood, lymphoblastoid cell lines, and fibroblasts. There was a positive correlation with a correlation coefficient of r= 0.64 (Fig. 66).

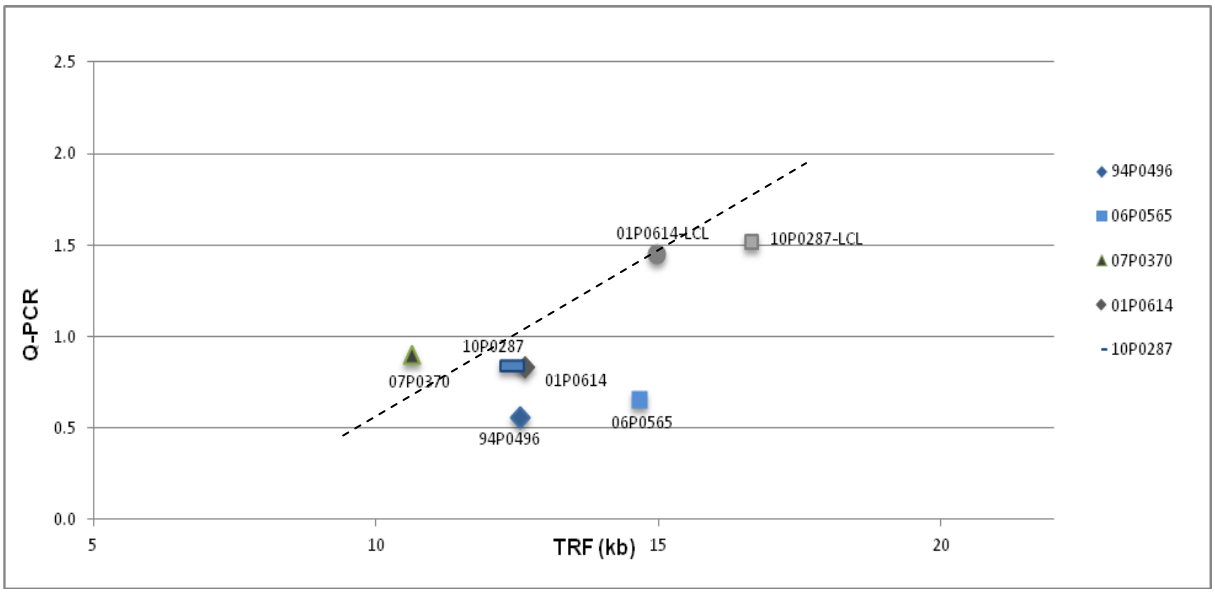

Figure 66: Correlation between Q-PCR and TRF in NBS-fibroblast 94P0496 and 05P0565, peripheral blood cells: 07P0370, 01P0614 and 10P0287, LCLs: 01P0614 and 10P0287. The corresponding correlation coefficient is r = 0.64.

3.5. Characterization of the mosaic NBS fibroblast cell line 94P0496

The fibroblast cell line 94P0496 was derived from a 9 years old NBS patient with the founder mutation (657del5). In cells with the wild type allele the nucleotide sequence ACAAA is found on chromosome 8q21 at position 657 in exon 6 of the *NBS* gene, while these five bases are deleted in NBS patients (Fig. 67).

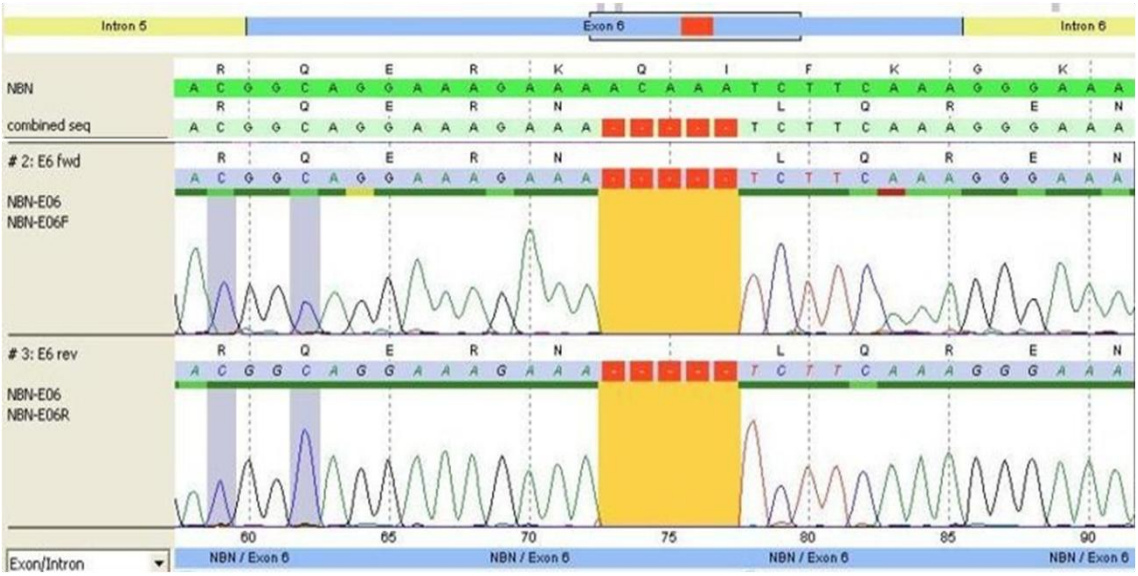

Figure 67: Sequence analysis of exon 6 of the *NBS* gene from patient 94P0496, homozygous for the founder mutation 657del5. The bases ACAAA are deleted.

After chromosome analysis two cell lines, one with 46 the other with 45 chromosomes, could be identified. The latter was due to a complex, unbalanced translocation. Interestingly, this aberrant line increased during subcultivation, from 50 % at passage 3 to about 90% at passage 7 (Table 15). Based on Fisher´s exact test, the two-tailed P value for this increase is highly significant (P< 0.0001). After Giemsa banding, one chromosome 6 and 13 were missing and a marker chromosome added (Fig 68, 69). The diploid line had a normal male karyotype 46, XY.

Table 15: The percentage of aberrant cells during subcultivation,

Passage	Metaphase analyzed	Normal cells	Aberrant cells	Percentage of aberrant cells
3	46	23	23	50 %
5	60	20	40	66 %
7	48	5	43	90 %

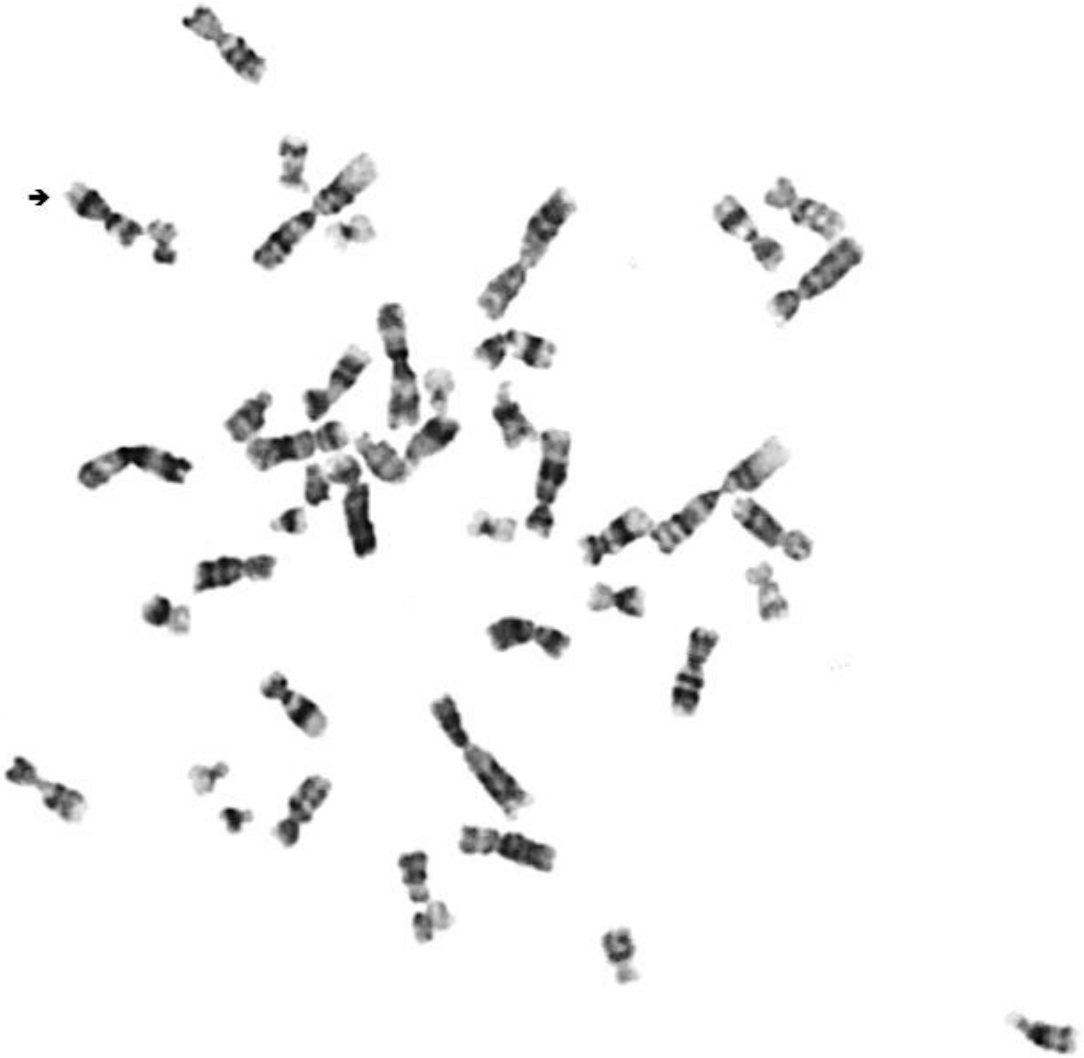

Figure 68: Metaphase of the NBS line 94P0496 with a marker chromosome (arrow) after G-banding.

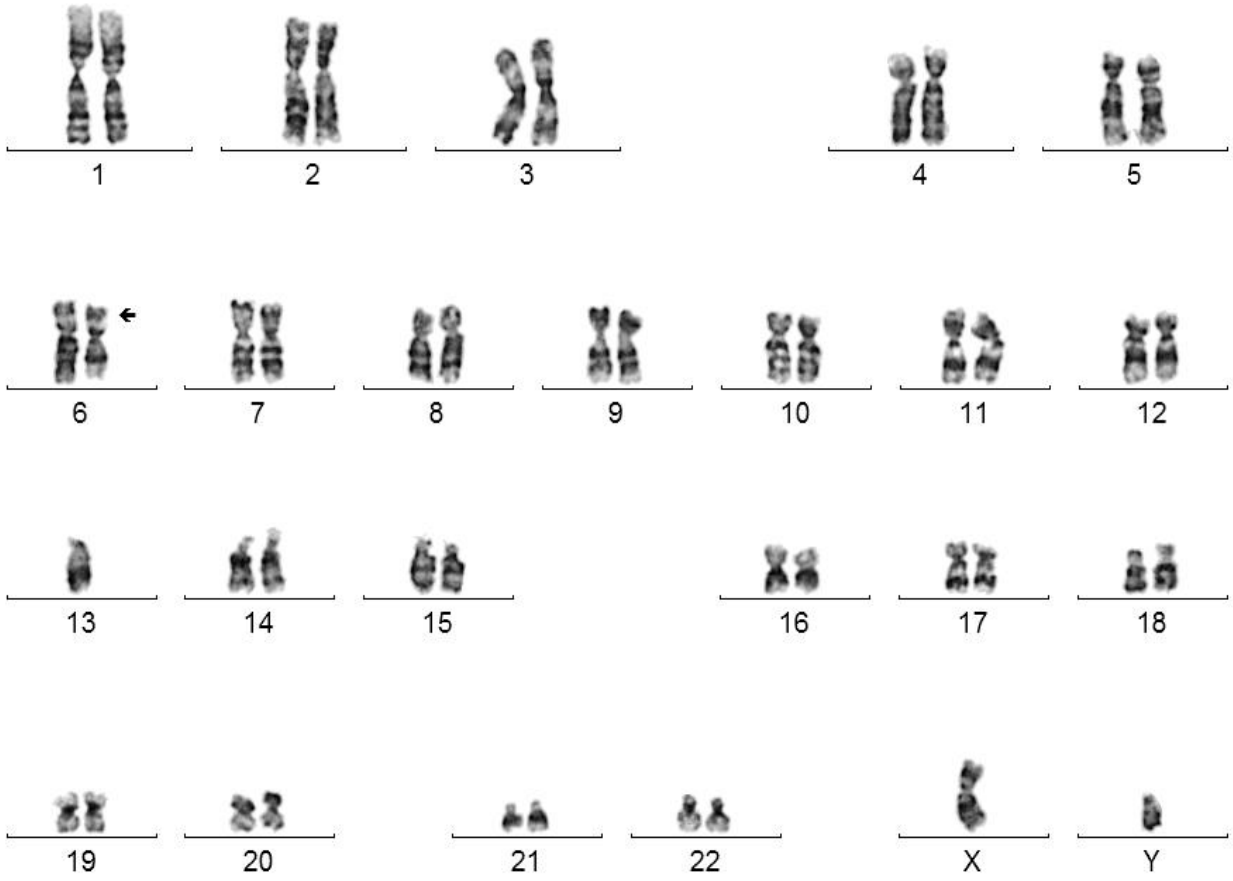

Figure 69: karyotype of the NBS line 94P0496 with a marker chromosome (arrow) after G-banding.

Comparative genomic hybridization (CGH) was applied to further characterize this aberration (Fig. 70). In this case the test DNA (94P0496) was labeled with a green, the control DNA with a red fluorochrome. Both were hybridized on normal metaphase chromosomes. The green to red fluorescence ratio (F/R) profiles along each chromosome were measured and depicted in an ideogram. The centre line in the CGH profiles represents the balanced state (1: 1 ratio of red and green fluorescence signals). An upper threshold of >1.25 was used to define a gain of chromosomal material (green line), while a lower threshold of <0.80 was used to interpret a loss of chromosomal material (red line). The low FR values of chromosomes 6 and 13 indicate partial monosomy, the high F/R ratio of chromosome 20 partial trisomy. The break points are defined as the point of inflexion (s. arrows in Fig.71). According to this, the breakpoints are: 6q12, 13q21.1, and 20q11.2.

In addition, whole chromosome painting for chromosomes 6, 13, and 20 was also performed to identify the aberrant chromosome. The short arm of the marker chromosome

including the centromere is from chromosome 6, the proximal part of the long arm is from chromosome 13. As no telomeres are visible, it is assumed that the distal break point is in the last band 13q34. To this part of the q-arm of chromosome 20 is attached (Fig. 72). The karyotype according to the international nomenclature is: 45,XY, der(6)(6pter→6q12 :: 13q21.1→13q34 :: 20q11.2→20qter), -13, ISCN 2009.[160]

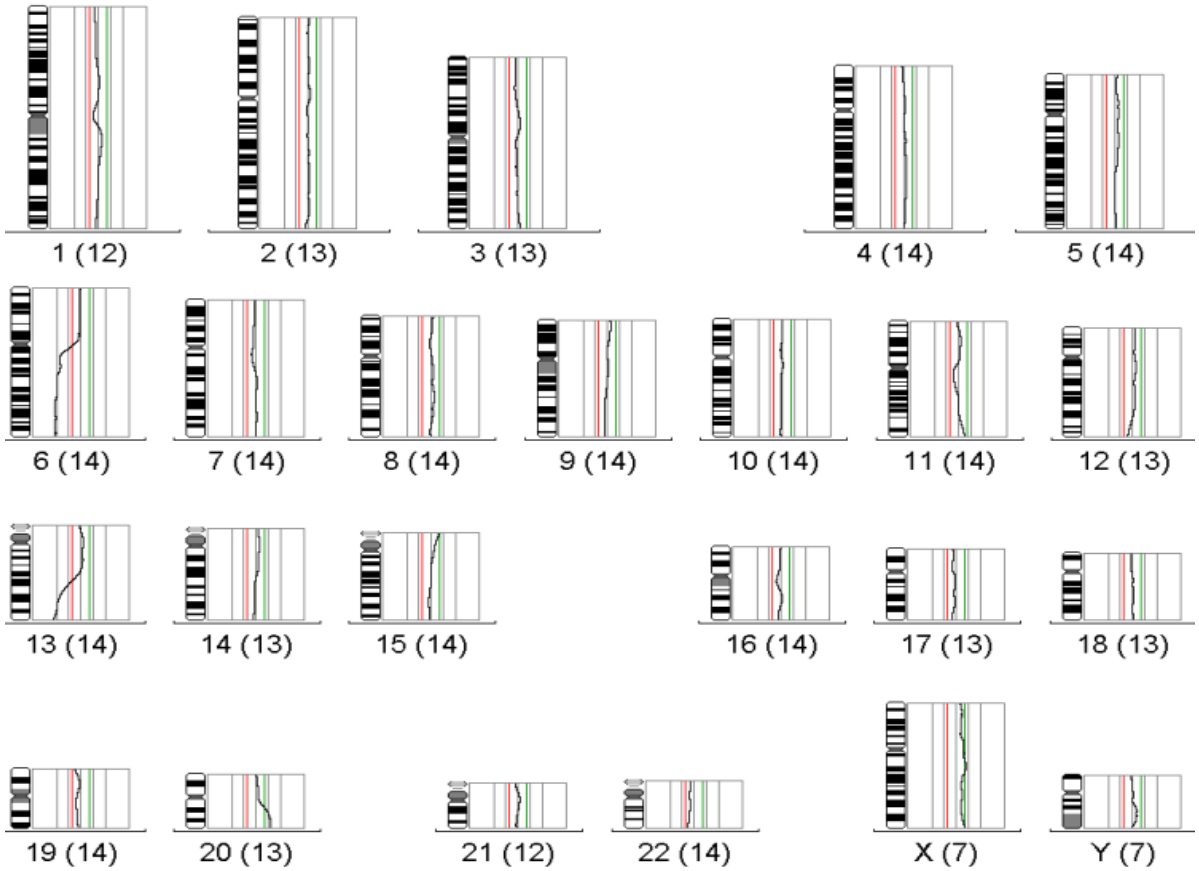

Figure 70: CGH analysis of NBS-patient 94P0496 showing partial monosomy for the q arms of chromosome 6 (6pter→6q12) and 13(q21.1→q34), and partial trisomy for chromosome 20 (q11.2→qter). The first figure beneath the ideogram designates the chromosome number, the second figure the number of chromosomes analysed to obtain the average profiles shown. The centre line in the CGH profiles represents the balanced state of the chromosomal copy number (ratio 1.0). Note the straight profiles along fluorescence ratio 1:1 for the unaffected chromosomes. An upper threshold of >1.25 was used to define a gain of chromosomal material, while a lower threshold of <0.80 was used to interpret a loss of chromosomal material. The high FR values of chromosome 20 indicate partial trisomy 20. Heterochromatic chromosomal regions are excluded from evaluation.

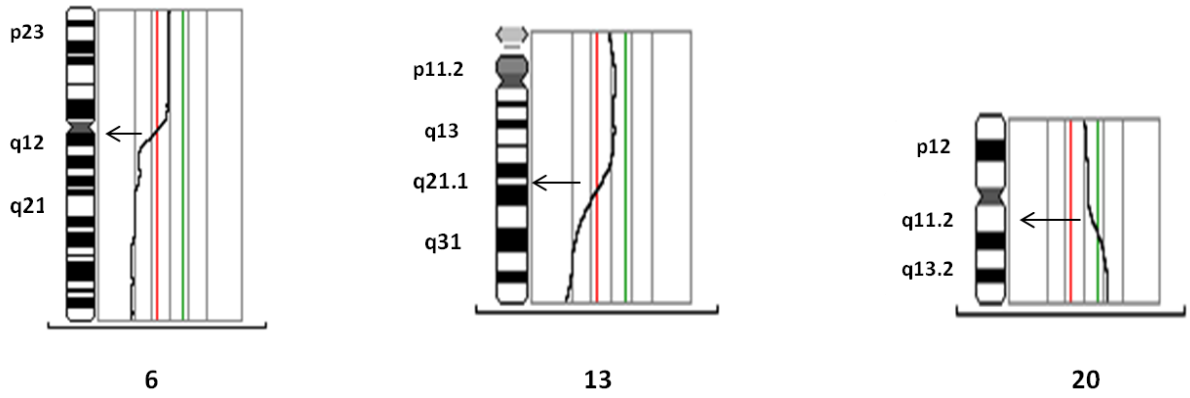

Figure 71: CGH analysis for chromosomes 6, 13 and 20 in the NBS patient 94P0496. The idiogram showing the G-banding pattern for normal human chromosomes 6 , 13 , and 20 at different bands resolution, arrows indicate the breakpoints positions on chromosomes (reproduced from ISCN 2009).

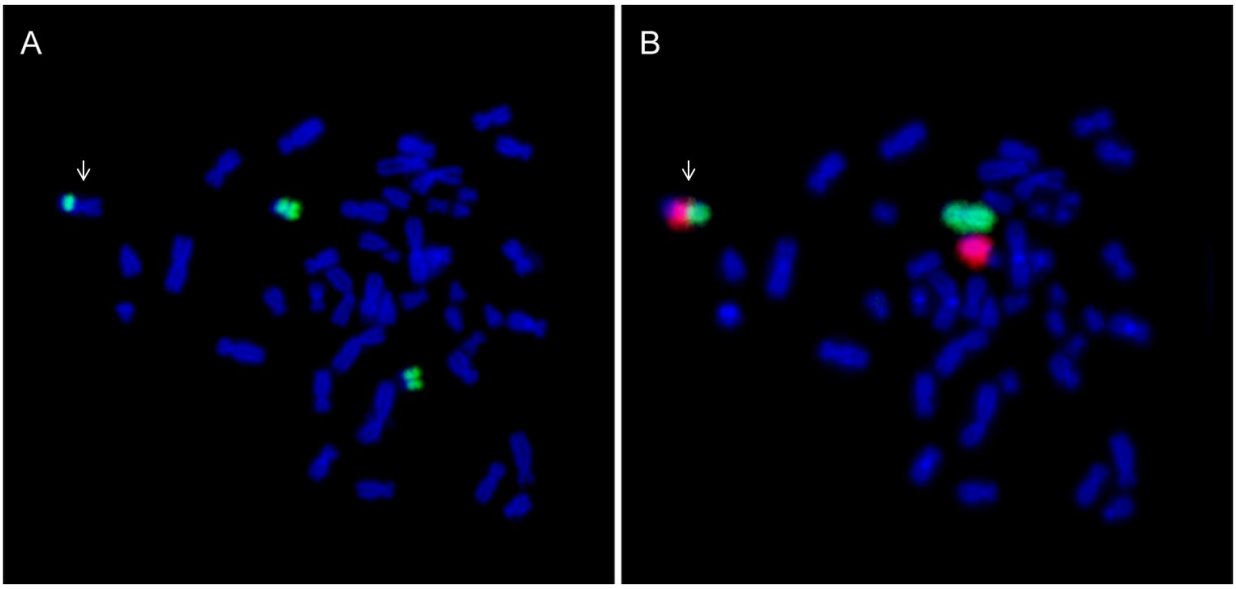

Figure 72: Metaphase of the NBS cell line 94P0496 with marker chromosome (white arrow) after WCP analysis, chromosome 20 in green (A), and chromosomes 13 in red and 6 in green (B).

3.5.1. Estimation of the cell cycle length after BrdU labelling

The cells were labelled with BrdU for 36 and 72 hours. This allowed the differentiation of metaphases, which had passed one, two or three S-phases after labelling. Metaphase chromosomes in the first mitosis after labelling show uniformly stained chromatids, those in the second mitosis (M2) exhibit differentially stained sister chromatids (Fig. 73), and third mitosis (M3) metaphases are characterized by a mixture of chromosomes with uniformly light stained sister chromatids, differentially stained sister chromatids and

chromosomes composed of both patterns (Fig 74). It was observed that the number of M2 cells after 36h and of M3 cells after 72h was higher in case of the aberrant cells in comparison with the normal ones. Accordingly, the cell cycle of the aberrant cells was shorter than that of the normal cells. The difference is significant (Fisher ´exact test, $P < 0.05$; Table 16).

Table 16: Analysis of metaphases of the 94P0496 cell line after 36 and 72 hours of BrdU labelling,

BrdU incubation	Mitoses after BrdU labelling	Metaphases analysed	aberrant metaphases	normal metaphases
36 hours	M1	5	3	2
	M2	50	48	2
72 hours	M1	0	0	0
	M2	16	13	3
	M3	34	34	0

Figure 73: Metaphase of the NBS cell line 94P0496 after BrdU labelling for 36 hours. The chromosomes show the labeling pattern of M2 mitoses.

Figure 74: Metaphase of the NBS cell line (94P0496) after BrdU labelling for 72 hours. The chromosomes show the labeling pattern of M3 mitoses.

3.5.2. Estimation of chromosomal aberrations (in the NBS cell line 94P0496) after X-irradiation

The cells were analyzed for chromosomal aberrations after irradiation with 0 Gy, 0.5 Gy and 1.0 Gy. About 20 normal and 40 aberrant cells were analysed each. The chromosomes were harvested four hours after irradiation. Accordingly, the irradiation was applied during G2-phase of the cell cycle. Different types of aberrations were identified, such as chromatid breaks, chromosome or isochromatid breaks and chromatid translocation (Fig 75), the latter are due to two breakage events and were counted twice. The aberrant cells were identified by their lower number of D-group (chromosomes 13-15) chromosomes, five instead of six in the normal cells (Fig 76). In order to calculate chromosomal breaks per cell the total number of all types of breaks was divided by the total number of analyzed metaphases. The number of chromosomal aberrations was significantly higher in the aberrant cells than in the normal ones after irradiation ($P < 0.05$; Chi-square test, Table 17, Fig 77).

Figure 75: Metaphase of the NBS cell line 94P0496 after irradiation with 1.0 Gy showing one chromatid translocation (black arrow) three chromatid breaks (ctb) and one achromatic lesion (ctg, chromatid gap).

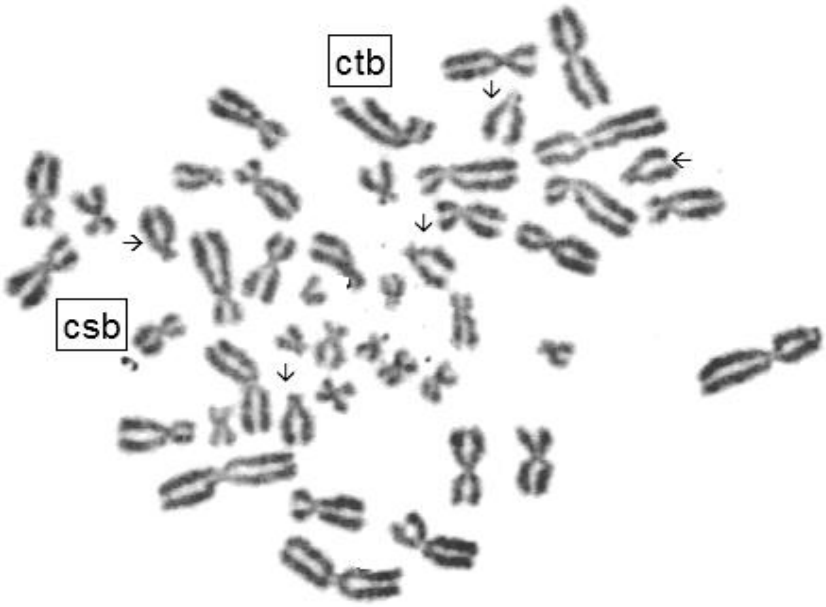

Figure 76: Metaphase of the NBS cell line 94P0496 after irradiation with 0.5 Gy showing a chromatid break (ctb) and a chromosome or an isochromatid break (csb). Here, one chromosome 13 is missing. Arrows refer to the five normal D-group chromosomes (13–15).

Table 17: Analysis of chromosomal breaks in normal and aberrant cells of the 94P0496 cell after irradiation,

Dose	94P0496 cells	Metaphases analyzed	Chromatid breaks	Chromatid translocation	Chromosome breaks	Total Breaks	Breaks per metaphase
0 Gy	Normal	23	5	-	-	5	0.22
	Aberrant	42	10	-	2	12	0.29
0.5 Gy	Normal	20	23	-	6	29	1.45
	Aberrant	42	53	4	9	66	1.57
1.0 Gy	Normal	21	39	-	10	49	2.3
	Aberrant	43	125	6	13	144	3.4

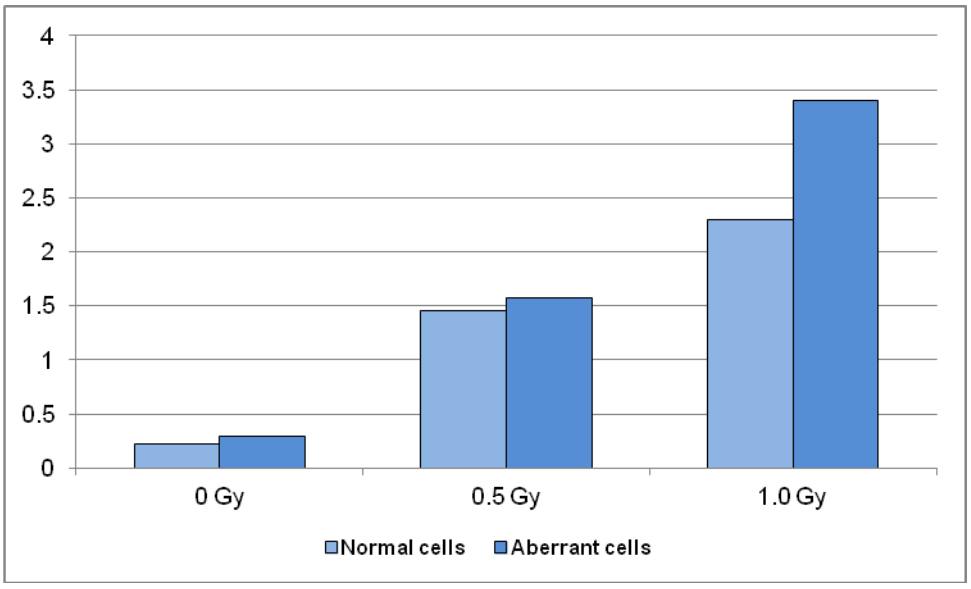

Figure 77: Breaks per cell in normal and aberrant cells of the NBS fibroblast cell line 94P0496 after irradiation with 0 Gy, 0.5 Gy and 1.0 Gy.

3.5.3. Estimation of telomere length (in NBS cell line 94P0496)

Telomere length (T/C value) was measured by Q-FISH in the normal and aberrant cells of the NBS line 94P0496 (8 metaphases were analyzed for each group). The total telomere length was significantly longer in aberrant than that in the normal cells ($P<0.05$) (Fig 78).

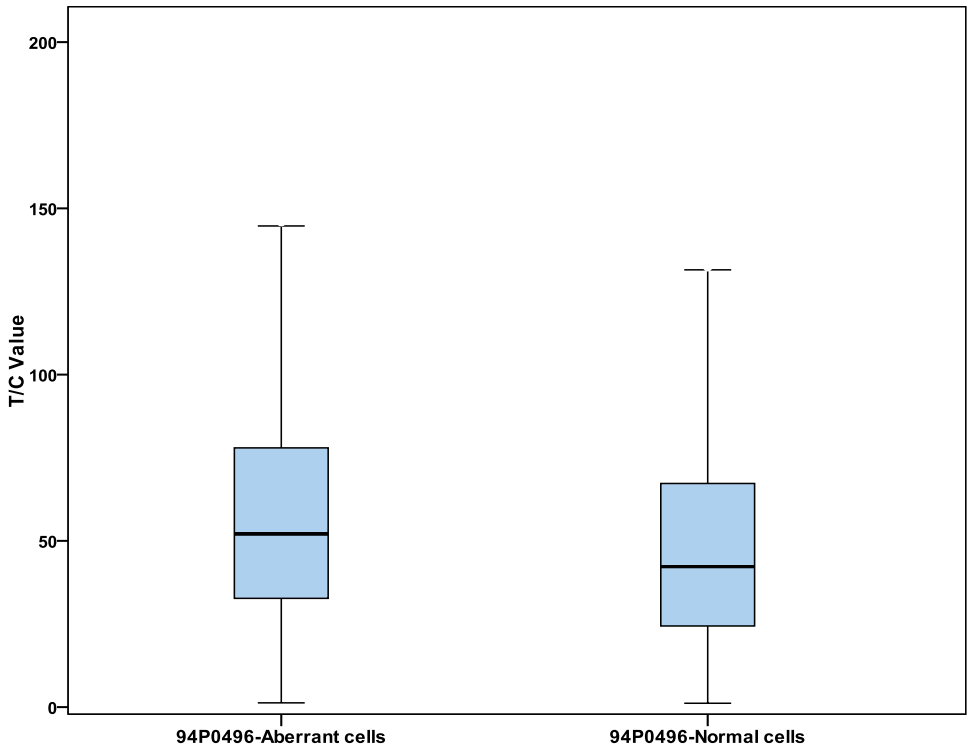

Figure 78: Boxplots of telomere lengths (T/C values) of normal and aberrant cells of the NBS-fibroblast cell line 94P0496.

However, There was no *hTERT* expression in this NBS cell line 94P0496 (Fig. 79). In conclusion, the aberrant cells of this NBS cell line had a significant growth advantage, correlated with higher telomere length and a higher mutation rate after X-irradiation. This may represent a first step in malignant transformation.

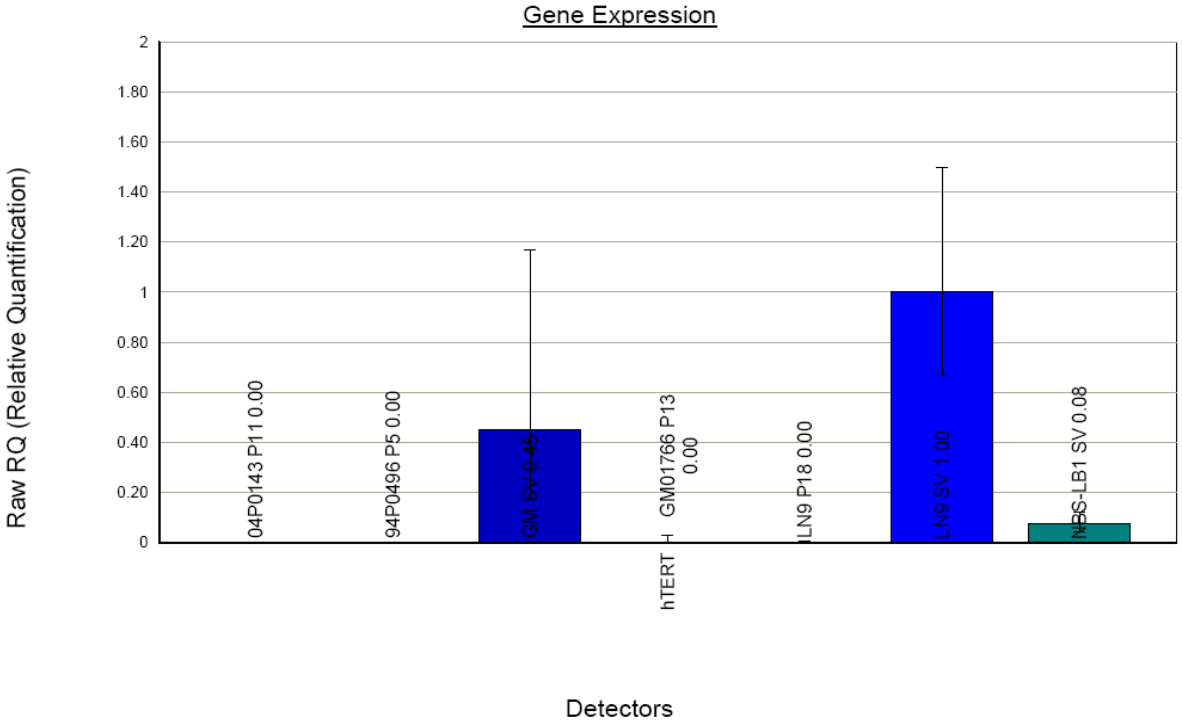

Figure 79: *hTERT* expression in NBS-fibroblast cell lines 94P0496 and 04P0143 and GM01766 (negative expression 0.00) and SV40 transformed NBS cell lines: GM SV and NBS-LB1SV (positive expression) in comparison to the control LN9 SV (performed by J. Radszewski).

4. Discussion

4.1. Estimation of telomere length by different techniques

Each technique that measures telomere length has specific advantages and disadvantages. It is important to realize what is actually being measured by each technique. For example the subtelomeric region is only detected by TRF analysis, which, however, also includes the variant repeat region and the telomere repeats, Q-PCR detects only the latter [161] (Fig. 80). Accordingly, the combination of different methods that measure telomere length is necessary to validate the results and compare them with other studies. Thus, a comprehensive review by Horn et al. in 2010 illustrated that the relationship between relative length, measured by Q-PCR, and the absolute telomere length in kb, measured by TRF analysis, was not constant among different studies,[162] although other studies reported a high correlation between results obtained by Q-PCR and TRF, and between Q-FISH and TRF.[163,164]

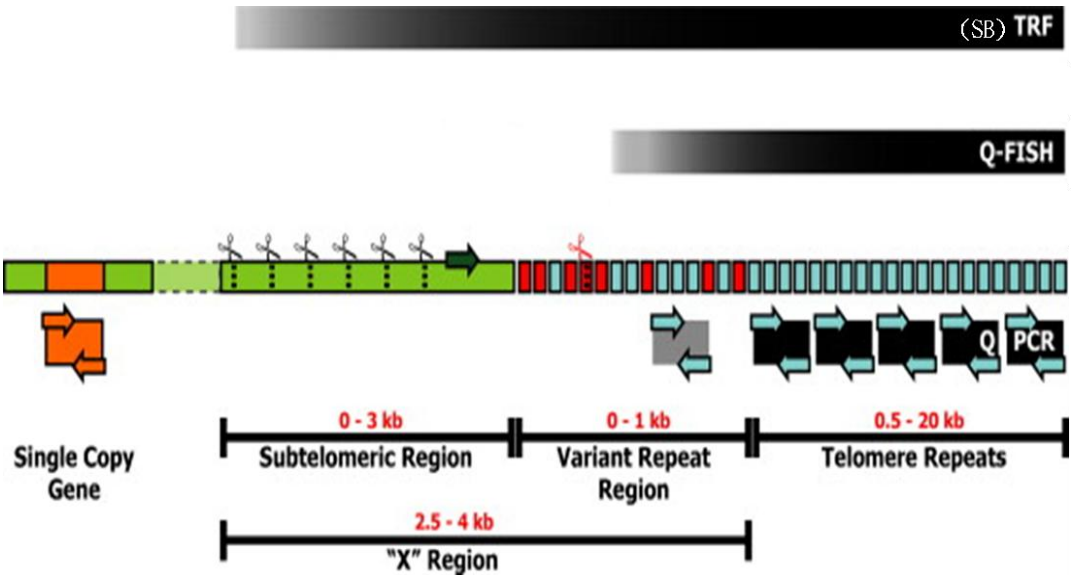

Figure 80: Telomeric regions detected by different techniques. Telomere length measured by Southern blot (SB), TRF analysis, includes subtelomeric DNA (green bar) and telomere variant repeats (red bars) which can occupy up to 2 kb. The measured length of this "X" region depends on the restriction enzymes used (represented as scissors). Some restriction enzymes will cut a particular common variant repeat (red scissor), and these restriction sites can differ between chromosomes and individuals. Q-FISH detects pure telomeric repeats (blue bars) and an unknown fraction of repeats in the variant region. Q-PCR measures the pure telomere repeats, using telomeric primers (blue arrows), in comparison to a single copy locus (orange) amplified with a second primer set (orange arrows). (after Aubert, Hills, and Lansdorp, 2011)[165]

In this thesis a high correlation has been shown between the relative telomere lengths measured by Q-PCR and Q-FISH. In addition, a good correlation was found between Q-PCR and the absolute length estimated by TRF analysis. This is a vital step to compare results obtained by these two different techniques. Q-PCR and TRF are expected to provide similar results, even if small differences might occur due to subtelomeric sequences detected only with TRF analysis.[166] To transform the Q-PCR data into absolute length a regression analysis was applied (Fig. 81). The formula is y= 3.4 x X +10.11, where y is the predicted TRF value in kb, X the Q-PCR value, 3.4: the slope and 10.11 the y-intercept, a constant. In this case, to each Q-PCR an equivalent in kb of absolute length can be assigned, e.g. if the T/S value according to Q-PCR is 1.0, the absolute length, y, is 3.4 x 1 + 10.11=13.51 kb. Accordingly, the TRF values of telomere length in fibroblasts and blood cells were estimated here from their Q-PCR values by using this formula. Due to the high correlation between Q-PCR and Q-FISH it is now also possible to transform the T/S values after Q-FISH into absolute lengths.

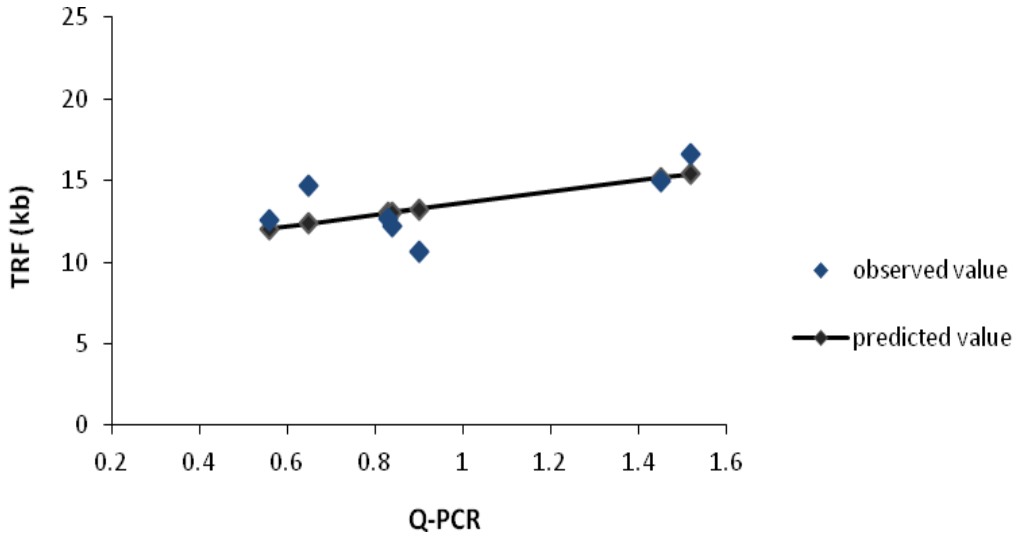

Figure 81: Regression analysis of telomere lengths of 7 samples measured by both Q-PCR and TRF analysis. The equation of the computed regression line, which is used to correlate the T/S Q-PCR values with the TRF data, is y= 3.4 x X +10.11 with a correlation coefficient of r= 0.64.

4.2. Telomere length in NBS-cell lines (*in vitro* studies)

The results presented in this thesis showed that telomere loss occurs during *in vitro* culture in both control and NBS-cell lines. One characteristic structural DNA change of most dividing cells, *in vivo* and *in vitro*, is the shortening of telomeres, which is consistent with the ”end replication problem” of telomeres and cell ageing.[167,168] Telomere attrition with

each division is an important aspect of the ageing theory, especially in chromosomal instability syndromes such as NBS, which is a focal point in this thesis, due to the role of the NBN protein in telomere maintenance.[169,170,171] The present findings confirmed the significant difference in telomere lengths between NBS and control cell lines, which was already described previously.[172,173] Here, NBS fibroblasts yielded a mean telomere length of 12.55 kb compared to 17.06 kb for control cell lines (calculated by the formula on p.113). In accordance with this, it has been reported that telomere repeats of DNA sequences at chromosome ends are shortened by 33-120 bp with each cell division in normal human fibroblasts,[174] but by approximately 220-260 bp/replication in NBS fibroblasts.[175]

In addition, an increased frequency of spontaneous and X-ray induced chromosomal aberrations was observed, confirming the spontaneous chromosomal instability of NBS cells and their sensitivity to ionizing radiation. This is due to defective DNA repair, cell cycle checkpoint control, and failure to activate p53 protein. [176, 177,178,179,180]

NBS lymphoblastoid cell lines also exhibited significantly shorter telomeres than control cell lines, however, in contrast to diploid fibroblasts there was no further reduction in length after different passages. The same was observed in SV40 transformed NBS cell lines: GMV7166 and GMV7166+nbs. It has been reported that telomerase activity or alternative lengthening of telomeres (ALT) is activated in SV40-transformed fibroblasts[181,182] and EBV-transformed LCLs, which may thus be a common step in the immortalization of somatic cells by viruses. [183,184]

Here, it was observed that telomerase activity was present, as expected, in both SV40 transformed NBS cell lines and in some, but not all EBV transformed LCLs. Variability in hTERT expression and telomere length has been found in immortal cells such as tumor cells.[185,186] It is possible that a telomere maintenance pathway such as alternative lengthening of telomeres (ALT) was activated in the telomerase-negative immortal cells as our hTERT negative LCLs.[187]

Furthermore, a significant difference in telomere length was observed between individual chromosome arms, both in NBS and control cells. In agreement with previous studies, heterogeneity in telomere lengths among homologous chromosomes could be also observed.[188] In most cases the shortest telomeres were found on the p arm of chromosome 19, and the q arms of chromosomes 19, 17 and 20. A study of der-Sarkissian et al. (2004) also showed that the shortest telomeres were found on the p arm of chromosome 19 and the q arms of chromosomes 19 and 20, in addition to the q arms of chromosomes 6 and 18.[189]

In a previous study it was suggested that the telomere on 17p is the shortest of all telomeres in normal human cells.[190] This was criticized by Perner et al, who reported that the 17p telomere is among the shorter ones, but not the shortest.[191] Thus, these studies on normal diploid human cells are compatible with the present findings in NBS cells. Obviously, the genetic defect has no significant influence on the relative telomere length between individual chromosomes.

However, there was one completely unexpected finding. In the lymphoblastoid cell line 94P0307, which had the shortest total telomere length after Q-PCR and Q-FISH, the telomeres of the p arm of one chromosome 19 was brightly fluorescent in 70 % of the metaphases, while the other chromosome 19 had only weak fluorescence intensity. The ratio between their relative T/C values was about 11:1. In later passages the percentage of cells with this unusual chromosome 19 decreased to 13%. In a recent study on chromosome arm-specific telomere length in chronic myelogenous leukemia cells some chromosomes had relatively long telomeres which might even be further elongated during malignant transformation. This has been explained by the assumption that chromosomal specific factors contribute in individual telomere length regulation with a special affinity for shorter telomeres. As underlying mechanisms, a telomerase-dependent or a recombination-based process were discussed.[192, 193] In accordance with this, line 94P0307 has extremely short telomeres and hTERT is weakly expressed. Nonetheless, the enormous elongation of one telomere only is completely different to the situation in the leukemic cells, has not been described before in human chromosomes, and therefore might depend on a different mechanism. In this respect the detailed studies on telomere dynamics in yeast could be of interest, in which novel mechanisms, such as rolling circle replication of telomeres, have been described by Bhattacharyya and Lustig (2006).[194] The first step is the formation of telomeric circles, so called "T-circles", which have also been found in vertebrate cells. Perhaps the further molecular characterization of this specific chromosome 19 telomere could give insight into its origin.

Interestingly, a telomere fusion was also observed in this NBS-LCL 94P0307 between the p arm of chromosome 2 and an undefined chromosome. This cell line had the shortest telomere lengths among all NBS-LCLs and it is well known that short telomeres have a tendency to fusion. [195,196,197] Hemann et al.(2001) suggested that loss of telomere function occurs preferentially on chromosomes with critically short telomeres.[198] This finding is consistent with studies showing that cells from NBS-patients exhibit high levels of chromosome breakage including end to end fusion (telomere fusion).[199, 200] However, the

mechanism of this fusion between critically shortened telomeres in human cells is still not clearly understood. A recent study suggests that NBN deficiency simultaneously affects ATM-dependent DNA damage signaling and TRF2-regulated telomere maintenance, which lead to these chromosomal abnormalities.[201]

4.3. Telomere length in NBS-patients (*in vivo* studies)

Telomere length in blood cells from 108 healthy individuals became shorter with age. The age group of 1-10 years had the longest telomeres with a mean of 16.19 kb, telomere lengths declined to 14.53 kb in the next age group (11-20 years). Telomere length reaches a plateau around 21-45 years with a mean of 13.62 kb followed by a decline between 50 and 80 years with a mean of 11.91 kb (calculated by the formula on p.113). Many studies showed a significant negative correlation between telomere lengths in peripheral blood cells and donor age. [202,203] *In vivo* telomere shortening occurs at different rates throughout life. It has been reported that the rate of telomere loss is highest from birth to 4 years, with gradually decreasing rates between 4 and 39 years. However, the shortening rate is low between the ages of 40 and 95.[204] Frenck et al. (1998) found that the rates of telomere attrition in blood cells are highly variable at different ages, occurring at a rapid rate in blood cells of young children, then at a decreased rate between the ages of 4 and 20 years, and at a relatively constant rate through the rest of adult life. He also found that mean telomere length declined from a mean of 16.4±1.2 kb in newborn, to 11.6±1.2 kb in their parents, and to 9.6±0.8 kb in the grandparents. [205] Iwama et al. (1998) demonstrated that telomeres in human blood cells shorten with approximately14-80 bp per year.[206]

NBS patients also showed reduction in telomere lengths from 13.54 kb in the age group of 1-10 years to 12.32 kb in the next age group (11 to 20 years). This was also reported by Ranganathan et al. (2001). In their study the telomeric DNA of NBS patients was significantly shorter with a mean length of 7.77 kb compared to 10.32 kb in the control.[207]

Cawthon et al. (2003) found that telomere length in the blood cells showed an inverse relationship to mortality in 60-75 years old humans. The telomere length in blood cells ranges from 8.0 kb at birth to 3.0 kb as people age and to 1.5 kb in elderly people. Additionally, when people were divided into groups based on their telomere lengths, the half with longer telomeres lived five years longer than those with shorter telomeres.[208] Moreover, a relationship between telomere shortening and the evolution of cardiac disease was found.[209,210] Shorter telomeres in blood cells show an association with an increase of mortality from infection or heart disease.[211] This could be explained, at least in part, by the higher rate of hematopoietic stem cell proliferation due to the production of

immunocompetent cells. It was reported by Njajou et al. that telomere length may be a biomarker of healthy aging. Self-reported health status and longer healthy life are strongly related to longer telomere length.[212]

In principle, this observation is in agreement with the findings presented in this thesis as healthy donors of different ages showed significantly longer telomeres than NBS patients or patients with other chromosomal instability syndromes. The reduced telomere length is already manifest before birth and thus, cannot be related to infectious diseases. It must be due to the underlying genetic defect. The inherent defect in the telomere biology is due to mutation in the *NBN* gene, which leads to the replacement of the p95 (NBN) protein by the p70 protein. As has been outlined above, the p95 (NBN) protein plays an important role in telomere maintenance and DNA repair. Thus, the elevated rate of telomere shortening in patients with chromosomal instability, NBS patients included, cannot be explained by the "end replication problem" alone. In addition, an S-phase-specific exonuclease, exacerbating the 3´-overhang length, has been proposed to explain an elevated rate of telomere shortening, as well as deficient DNA repair of lesions induced by oxidative stress at telomeres, and epigenetic factors.[213,214]

In this thesis, corresponding values of telomere lengths were observed in blood and lymphoblastoid cells of healthy individuals of the same age. Surprisingly, the telomere lengths in the CD3 and CD19 cells (T and B cells) isolated from peripheral blood were shorter than those determined from blood DNA of the same three individuals. It cannot be excluded that the isolation procedure of the B- and T-cells could have an influence on the Q-PCR assay. However, if the granulocytes and killer cells of the peripheral blood had longer telomeres than the B- and T-cells, this would be an alternative explanation. Indeed, telomere length measurements in subsets of blood leukocytes found a higher length in granulocytes and natural killer cells compared to naive T- and B-cells.[215]

Furthermore, it was observed that the blood DNA of a one year old healthy individual showed very long telomeres. Moreover, a large variability in telomere length was observed within control individuals and especially in NBS patients up to 20 years of age. Epidemiological studies indicated that there is a large interindividual variation both in telomere loss and telomere length.[216] An earlier study indicated that telomere length variation is to a large extent genetically determined.[217] Later studies found that telomere length is by 36-84% inherited but the mode of inheritance and the genes involved are unknown. [218,219] Based on the comparison between monozygotic (MZ) and dizygotic twins (DZ) the pattern of chromosome-specific variations in telomere length seems to be

conserved throughout life and is at least partially inherited.[220,221] However in an elderly cohort of MZ and DZ male twins (war veterans) telomere length was largely associated with shared environmental factors. [222] Interestingly, the telomere lengths in sperm actually increase with age. In other words, the telomere lengths in the zygote might influence telomere length in blood cells later in life.[223,224]

In addition to blood cells, many studies have demonstrated that telomeres shorten significantly with ageing in most human tissues. [225,226] On the other hand, the brain and heart tissue, in which cells do not continually divide and renew, do not show significant telomere shortening.[227] Cameron has reported receding rates of telomere lengths in human tissues of about 30-60 bp per year. Neurons and myocardium are exceptional in this study because their telomeres were relatively static.[228] Another study showed telomere reduction rates of 29-60 bp per year in the liver, renal cortex and spleen tissues but no such decrease in the cerebral cortex and myocardium. Furthermore, the longest telomeres were observed in myocardium, while the shortest telomeres were observed in liver and renal cortex.[229]

In this thesis, telomere lengths were measured in various tissues of a NBS-fetus terminated at 34 weeks of gestation. It was shown that spinal cord and brain tissues had the longest telomeres with a mean of 30.20 kb and 21.05 kb, respectively, followed by heart and lungs tissues, 19.69 kb and 18.33 kb, respectively (calculated by the formula on p.113). Telomere lengths in fibroblast and skin were the shortest, 14.08 kb and 12.32 kb, respectively. Telomere lengths in the other tissues were: 16.97 kb in stomach, 16.87 kb in colon 16.77 kb in kidney, 16.67 kb in umbilical cord, 16.43 kb in small intestine, 15.89 kb in thymus, 15.75 kb in adrenal gland and 14.56 kb in liver. In line with these observations, Youngren et al. studied telomere lengths in different tissues from human fetuses of gestational ages between 15–19 weeks. Apart from a significant variation between the fetuses, telomere length ranged from 9.9 to 11.5 kb in heart, 10 to 12.7 kb in liver, 11.1 to 12.9 in skin, 10.1 to 12.6 kb in kidney, 10.3 to 12.3 in spleen and from 10.3 to 12.2 kb in lung. The authors found a synchrony in telomere length in different tissues of the human fetus. This synchrony was apparently lost during extra uterine life.[230] Butler et al. (1998) also found that among the shortest telomere lengths in fetus was skin tissue with 4.3 ± 0.9 kb.[231] A minor difference in telomere length only was observed between fibroblasts taken from NBS patients (7 year and 1 year of age at skin biopsy) with 12.67 kb, and the NBS fetus with 12.32 kb.

Allsopp et al. (1995) demonstrated that telomere length in brain tissue is stable during *in vivo* ageing. In addition, there is no significant loss of telomeres in adult and fetal brain tissues. This could be explained by the fact that nerves and brain cells stop dividing after birth.[232] The stable or increasing telomere length in reproductive cells as well as in stem cells is explained by the expression of telomerase. [233,234] It was revealed that telomere lengths in different organs and tissues are characteristic for each individual. [235]

Clearly, the pathway by which short telomeres affect ageing *in vivo* is still not fully understood. Telomere shortening may induce apoptosis or cell cycle arrest *in vivo*, which results in cell loss and tissue dysfunction. It may also impair the ability of stem cells to regenerate tissues which leads to tissue failure.[236] On the other hand, Epel et al. (2004) suggested a link between cigarette-smoking, oxidative stress and telomere attrition. It has been shown that the psychological stress, both perceived and chronic, was associated with higher oxidative stress, lower telomerase activity and shorter telomere lengths.[237] Interestingly, it was shown that each year of smoking results in shortening of telomeres equal to 5 bp. Smoking is one of the main reasons for oxidative stress. However, increased body mass and obesity in women may also be associated with telomere shortening. [238,239] Altogether, there is an association between diet, lifestyle and telomere length.[240]

4.4. Sex-related differences in telomere length

It has been observed that healthy women have a longer lifespan compared to healthy men. However, the primary cause for this is still unknown.[241] It has also been shown that long telomeres are positively correlated with human lifespan. [242,243,244] In some studies women have been shown to actually exhibit longer telomeres and males to lose telomeric sequences faster than females. [245,246] In agreement with these reports, the analysis of telomere length in our control (all age groups) showed that the mean relative telomere length of females (average age 24.5 years) was significantly longer than that of males (average age 31.4 years) ($P<0.05$). However, this difference was no longer significant if a more uniform age cohort of 20-30 years old males and females was compared. Telomere length was 13.48 kb for males and slightly longer in females with 13.68 kb. Also NBS females had slightly longer telomeres than NBS males, with 13.23 versus 13.01 kb. The difference is not significant, but in all cases it is the same tendency. Both Mayer et al. and Möller et al. found shorter telomere lengths in males compared to females, associated with a higher rate of telomeric loss in males.[247, 248]

Perner et al. showed that there are no differences between males and females in the telomere lengths of autosomes, however, a significant difference was detected with respect to q-arms of sex chromosomes.[249] The Xq telomeres of male newborn were significantly shorter than that of females. In males, the X chromosome is of maternal and the Y chromosome of paternal origin. Perner explained the longer Xq telomeres in male by a possible epigenetic effect in the female germ line, e.g. recombination between subtelomeres. In this thesis, telomere lengths of the X chromosome were longer than those of the Y chromosome in two NBS males and one control in lymphoblastoid cell lines, while no clear correlation was found in telomere lengths between the X chromosome and the Y chromosome in male fibroblasts, except for one cell line.

The situation, however, might be more complex. Njajou et al. observed a positive correlation between daughter's telomere length and paternal lifespan ($P < 0.001$), but not between daughter's telomere length and maternal lifespan.[250] In another study the role of paternal age on telomere length and its variability in the offspring was pointed out.[251] Furthermore, a high correlation was shown between fathers and sons and daughters, but not between mothers and offspring.[252] Nawrot et al. found a significant association of telomere lengths between mother and daughter, mother and son, and father and daughter, but not between father and son.[253]

4.5. Telomere length in a humanized NBS mouse

Previous studies suggested that telomeres in mice are significantly longer than human telomeres in spite of the fact that mice lifespan is much shorter than the human lifespan.[254] Mark et al. found that the total telomere length in mice was heterogeneous, ranging from 20 to 150 kb. [255] The role of Nbs1 in mouse development and DNA repair has been already studied. [256,257] The Nbs mutant mice, which were described in this thesis, represent a mouse model to study the mechanisms of pathogenesis in this human disease, with a focus on the role of Nbs in the telomere maintenance.

This is the first time that telomere length has been studied in Nbs mice. As control served Nbs null mice transfected with the human wild type *NBS* allele. All specimens had about the same age. Generally, the two control mice had longer telomeres in all four tissues analysed than the three mice with the mutant allele. However, the difference was rather high towards one control (no 98) and only marginal to the control (no. 95). This fits well with the general observation that the disease phenotype in the Nbs mouse models is less severe than in NBS patients.[258] In addition, it was observed in the control mice the longest telomeres were present in brain and heart tissues as compared to liver and kidney. This

observation is in agreement with studies of telomere lengths in human tissues as discussed above. Cheng et al. suggested that during the processes of neurogenesis and neuronal maturation telomere repeat-binding factor 2 (TRF2) and telomerase function together within special mechanisms for telomere protection. Thus, newly generated neurons could be more sensitive sensors for errors and damages in telomeres.[259] The Nbs mice did not show any consistent pattern of telomere lengths between the four different tissues. Also in the NBS fetus, the telomere length between brain, heart and lung were rather similar, as well as telomere lengths between stomach, colon, kidney, umbilical cord, small intestine and thymus.

This similarity in telomere length among different tissues was also found in newborn mice, whereas it differed between tissues in adult mice.[260] Altogether, the findings indicate that Nbs mice have dysfunctional telomeres and hence shortened telomere length. However, from the beginning of life these mice start with much longer telomeres than human embryos and this might be one explanation for the mild expression of the mutant NBS allele.

4.6. Telomeres and cancer risk related to NBS

The role of telomere biology in cancer has been extensively discussed in several recent reviews.[261,262] Xu et al. demonstrated that short telomeres, which were named "T-stumps“ have been found in human cancer cell lines,[263] confirming previous studies from Hastie et al. who reported already in 1990 that telomeres in human tumors were shorter than telomeres in the normal surrounding tissues.[264]

Telomere shortening contributes to genetic instability which is responsible for the wide repertoire of chromosomal aberrations found in malignomas, especially in solid tumors.[265] Patients with Nijmegen breakage syndrome are characterized by their high cancer risk, especially for lymphoid malignancies but also for solid tumors. [266,267,268,269,270,271,272,273]

As has been stated before, the NBN protein plays an important role in telomere maintenance, DNA-damage repair and cell cycle control. The NBN protein has both caretaker and gatekeeper functions and thus prevents cells from malignant transformation.[274] Interestingly, also heterozygotes for the NBN founder mutation (657del5) exhibit an increased cancer risk,[275,276,277,278] including an increased risk for breast cancer. [279,280,281,282] This was first described by Seemanova in blood relatives of NBS patients.[283]

The genomic instability in all cells from NBS patients leads to a large number of genetically unique cells from which those capable of continual proliferation will be

selected. Mutation and selection are the driving forces of cancerogenesis. In this context the NBS fibroblast cell line (94P0496) is of special interest. It consisted of two cell types: one with a normal diploid karyotype and the other with an unbalanced translocation, with partial trisomy for 20q11.2-20qter, and monosomy for 6pter-6q12 and 13q21.1-13q34. This aberrant line increased from 50% in passage 3 to 90% in passage 7 which is, at least partially, explained by its shorter cell cycle compared to the diploid cells. Clearly, this line had a selective advantage in tissue culture. Generally, (partial) aneuploidy of single chromosomes is detrimental to diploid cells, but could be beneficial in cancer cells. Most solid cancer show large scale chromosomal alterations and it is generally accepted that some are functionally important (cancer drivers) whilst others represent only random changes. Thus, this aberrant line has obviously a driver aberration which might represent an early (first) step in malignant transformation. Moreover, one can speculate that this specific combination of gain and losses of genetic material may reflect a mechanism for balancing the dosage of the affected genes.

Gain of chromosome 20 is frequently observed in colorectal carcinomas and malignant epithelial tumors. [284,285] Moreover, the combination of gains of 20q and losses of 6q and 13q is common in oral squamous cell carcinomas.[286] No information is available about this polish patient with respect to the fate of this cell type established from a skin biopsy at the age of 9, however, the patient was diagnosed with a thyroid carcinoma at the age of 20.

Based on the databank <www.ncbi.nlm.nih.gov/mapview/>, it is easy to identify the genes which are trisomic or monosomic in the aberrant cell line: The chromosomal region 6p11.1→6qter harbors 858 genes, the region 13q21.32→13q34 258 genes and the region 20q11.1 →20qter 575 genes. The later region contains the putative oncogenes *AURKA* and *ZNF217*, as well as the transcription factor E2F that is involved in DSB repair in association with the MRN complex.[287] Loss of the *IGF2R* on 6q increases the growth of human and murine tumors.[288] These few examples should only illustrate how gains or losses of specific genes could influence cell proliferation and malignant transformation.

At the end of this thesis it could be suggested that there is no standard telomere length throughout life. It was shown that telomere lengths of individuals of the same age are heterogeneous. Differences in telomere length could be found also between different tissues from the same individual. Understanding the genetic differences in the regulation of telomere lengths could help to explain the variation in human longevity. A new study

confirmed that telomere length correlated inversely with lifespan. [289] Moreover, telomere length measured at the end of the main growth period might be a predictor of lifespan.[290] The important role of telomere biology in the control of replicative capacity and in tumorigenesis is confirmed.[291] NBS patients showed significantly shorter telomeres than control individuals. This supports the role of NBN in telomere maintenance. The NBN studies shed light on DSB-induced genetic instability. The chromosome instability inherent in NBS affects all cells and increases the risk for haematological malignancies and solid tumours. Moreover, NBS patients are sensitive towards exogenous and endogenous mutagens. In this respect, free oxygen radicals generated during energy metabolism may pose a particular threat, especially if the short telomeres are affected.

These findings have had immediate therapeutical consequences. The standard therapy for lymphoreticular malignancy included radiotherapy and led to rapidly progressive organ insufficiency and death in NBS patients. After identification of the *NBN* gene and proper diagnosis, the affected children were treated by modified protocols completely avoiding ionising radiation and radiomimetics. Survival is now for several years after diagnosis and some patients have survived more than one malignancy. Thus, confirmed homozygotes can be appropriately protected from mutagens, and particularly from ionizing radiation. Prior to identification of the *NBS* gene, the mean age at diagnosis was 7 years and was made solely on the basis of microcephaly, lymphoreticular malignancy, and toxic complications of standard tumor therapy. Since 1998, the mean age at diagnosis in the Czech Republic has dropped to 4 months (range 2–5 months) due to the routine analysis of the *NBS* gene in all infants with congenital microcephaly.[292]

Altogether, the present findings underline the role of the *NBN* gene in telomere maintenance and shed new light on the chromosome instability inherent in NBS which increases their risk for haematological malignancies and solid tumors.

5. Refferences

[1] Shammas M.A. 2010. Telomeres, lifestyle, cancer, and aging. Curr Opin Clin Nutr Metab Care. 14(1):28-34

[2] Ye J, Wu Y and Gilson E. 2010. Dynamics of telomeric chromatin at the crossroads of aging and cancer. Essays Biochem. 48(1):147-64

[3] Minamino T. 2010. Role of cellular senescence in lifestyle-related disease. Circ J. 74(12):2527-33

[4] Takubo K et al., 2010. Changes of telomere length with aging. Geriatr Gerontol Int. 10 (1): 197-206

[5] Muler H.J. 1938. The remaking of chromosomes. Collecting Net. 13:181-198

[6] Muller H.J and Hersowikz I. 1954. Concerning the healing of chromosome ends produced by breaking in drosophila melanogaster. American Naturalist. 88:177-208

[7] CHuaire L. 2006. Telomere and Telomerase: brief review of a history initiated by Hermann Muller and Barbara McClintock. Colombia Médica. 336-337

[8] McClintock B. 1940. The Stability of Broken Ends of Chromosomes in Zea Mays. Genetics. 26(2):234-282

[9] McClintock B. 1939. The Behavior in Successive Nuclear Divisions of a Chromosome Broken at Meiosis. Proc Natl Acad Sci . 25(8):405-416

[10] Blackburn E.H and Gall J.G . 1977. A tandemly repeated sequence at the termini of the extrachromosomal ribosomal RNA genes in Tetrahymena. Journal of Molecular Biology 120(1):33-53

[11] Szostak .J and Blackburn E.H. 1982. Cloning yeast telomeres on linear plasmid vectors. Cell. 29(1):245-55

[12] Shampay J, Szostak J.W and Blackburn E.H. 1984. DNA sequences of telomeres maintained in yeast. Nature. 310:154-157

[13] Greider C.W and Blackburn E.H. 1989. A telomeric sequence in the RNA of Tetrahymena telomerase required for telomere repeat synthesis. Nature. 337(6205):331-7

[14] Madonna R et al., 2010. Biologic function and clinical potential of telomerase and associated proteins in cardiovascular tissue repair and regeneration. Eur Heart J. 32 (10): 1190-1196

[15] Moyzis R.K et al., 1988. A highly conserved repetitive DNA sequence, (TTAGGG)n, present at the telomeres of human chromosomes. Proc Natl Acad Sci U S A. 85:6622-6626

[16] de Lange T et al., 1990. Structure and variability of human chromosome ends. Mol Cell Biol. 10:518-527

[17] Makarov V.L, Hirose Y and Langmore J.P. 1997. Long G tails at both ends of human chromosomes suggest a C strand degradation mechanism for telomere shortening. Cell. 88:657-666

[18] Sfeir A.J et al., 2005. Telomere-end processing the terminal nucleotides of human chromosomes. Molecular Cell. 18:131-138

[19] Griffith J.D et al., 1999. Mammalian telomeres end in a large duplex loop. Cell. 97:503-514

[20] Stansel R.M, de Lange T and Griffith J.D. 2001. T-loop assembly in vitro involves binding of TRF2 near the 3' telomeric overhang. EMBO J. 20:5532-5540

[21] Liu D et al., 2004. PTOP interacts with POT1 and regulates its localization to telomeres. Nature Cell Biol. 6:673-680

[22] Houghtaling B.R et al, 2004. A dynamic molecular link between the telomere length regulator TRF1 and the chromosome end protector TRF2. Curr Biol. 14,1621-1631

[23] De Lange T. 2005. Shelterin the protein complex that shapes and safeguards human telomeres. Genes Dev. 19(18):2100-10

[24] Elwood N.J. 2004. Telomere Biology of Human Hematopoietic Stem Cells. Cancer Control. 11(2):77-85

[25] Young N.S. 2010. Telomere biology and telomere diseases: implications for practice and research. Hematology Am Soc Hematol Educ Program. 30-35

[26] Watson J.D and Crick F.H. 1953. Molecular structure of nucleic acids; a structure for deoxyribose nucleic acid. Nature. 171(4356):737-8

[27] Ogawa T and Okazaki T. 1980. Discontinuous DNA Replication. Annual Review of Biochemistry. 49:421-457

[28] Watson J.D. 1972. Origin of concatemeric T7 DNA. Nature New Biol. 1239(94):197-201

[29] Olovnikov AM. 1973. A theory of marginotomy. The incomplete copying of template margin in enzymic synthesis of polynucleotides and biological significance of the phenomenon. J Theor Biol. 41(1):181-90

[30] Hayflick L and Moorhead P.S. 1961. The serial cultivation of human diploid cell strains. Exp Cell Res. 25(3):585-621

[31] Deng Y Chan S.S and Chang. S. 2008. Telomere dysfunction and tumour suppression: the senescence connection. Nat Rev Cancer. 8(6):450-8

[32] Levy M.Z et al., 1992. Telomere end-replication problem and cell aging. J Mol Biol .225(4):951-60

[33] Cookson J.C and Laughton C.A. 2009. The levels of telomere-binding proteins in human tumors and therapeutic implications. Eur J Cancer. 45(4):536-550

[34] Wie C et al., 2002. Effects of double-strand break repair proteins on vertebrate telomere structure. Nucleic Acids Res. 30(13):2862-2870

[35] Neumann A.A and Reddel R.R. 2002. Telomere maintenance and cancer ? look, no telomerase. Nature Reviews Cancer. 2(11):879-884

[36] Wright WE et al., 1996. Telomerase activity in human germline and embryonic tissues and cells. Dev Genet. 18(2):173-9

[37] Hiyama E and Hiyama K. 2007. Telomere and telomerase in stem cells. British Journal of Cancer .96, 1020–1024

[38] Kouniavsky G and Zeiger M.A. 2010. The role of telomeres and telomerase in endocrine tumors. Discov Med. 10(53):340-7

[39] Greider C and Blackburn B. 1989. A telomeric sequence in the RNA of Tetrahymena telomerase required for telomere repeat synthesis. Nature. 337(6205):331-7

[40] Greider C.W and Blackburn E.H.1987. The telomere terminal transferase of tetrahymena is a ribonucleoprotein enzyme with two kinds of primer specificity. Cell. 51(6):887-898

[41] Cohen S.B et al., 2007. Protein composition of catalytically active human telomerase from immortal cells. Science. 315 (5820): 1850–3

[42] Weinrich S.l et al., 1997. Reconstitution of human telomerase with the template RNA component hTR and the catalytic protein subunit hTRT. Nat Genet. 17(4):498-502

[43] Smogoryeweska A and de Lang T. 2004. Regulation of telomerase by telomeric proteins. Annu Rev Biochem. 73:177-208

[44] Callen E and Surralles J. 2004.Telomere dysfunction in genome instability syndromes. Mutat Res. 567(1):85-104

[45] Fleisig H.B and Wong J.M.Y. 2006. Telomerase as a clinical target: current strategies and potential applications. Exp Gerontol. 42(1-2):102-12

[46] Wong J.M.Y and Collins K. 2003. Telomere maintenance and disease. The Lancet. 362(9388):983-8

[47] Biessmann H and Mason J.M. 2003.Telomerase-independent mechanisms of telomere elongation. Cell Mol Life Sci. 60(11):2325-33

[48] Sheng Cong Yu, Wright W.E, and Shay J.W. 2002. Human telomerase and its regulation. Microbiol Mol Biol Rev. 66(3):407-25

[49] Poole J.C, Andrews L.G and Tollefsbol T.O. 2001. Activity, function, and gene regulation of the catalytic subunit of telomerase (hTERT). Gene. 269(1-2):1-12

[50] Kyo S et al., 2008. Understanding and exploiting hTERT promoter regulation for diagnosis and treatment of human cancers. Cancer Sci. 99(8):1528-1538

[51] Belair C.D, et al, 1997. Telomerase activity: A biomarker of cell proliferation, not malignant transformation. Proc. Natl. Acad. Sci. 94(25):13677–13682

[52] Wong J.M and Collins K. 2003. Telomere maintenance and disease. Lancet. 362(9388):983-8

[53] Wright W.E and Shay J.W. 2000. Telomere dynamics in cancer progression and prevention: fundamental differences in human and mouse telomere biology. Nat Med. 6(8):849-51

[54] Herbert B.S et al., 1999. Inhibition of human telomerase in immortal human cells leads to progressive telomere shortening and cell death. Proc Natl Acad Sci. 96(25):14276-81

[55] Halvorsen T.L, Leibowitz G and Levine F. 1999. Telomerase activity is sufficient to allow transformed cells to escape from crisis. Mol Cell Biol. 19(3):1864-70

[56] Lengauer C, Kinzler K.W and Vogelstein B. 1998. Genetic instabilities in human cancers. Nature. 396 (6712):643–649

[57] Bayani J et al., 2007. Genomic mechanisms and measurement of structural and numerical instability in cancer cells. Semin Cancer Biol. 17(1):5-18

[58] Callen E and Surralles J. 2004. Telomere dysfunction in genomic instability syndromes. Mutat Res. 567(1):85-104

[59] Wai L.K. 2004. Telomeres, Telomerase, and Tumorigenesis. MedGenMed. 6(3): 19

[60] Hahn W.C et al., 1999. Inhibition of telomerase limits the growth of human cancer cells. Nat. Med. 5(10):1164-1170

[61] Burger A.M et al., 2005. The G-quadruplex-interactive molecule BRACO-19 inhibits tumor growth, consistent with telomere targeting and interference with telomerase function. Cancer Res. 65(4):1489-1496

[62] Shay J.W and Keith W.N. 2008. Targeting telomerase for cancer therapeutics. Br. J Cancer. 98:677-683

[63] De Cian A et al., 2008. Targeting telomeres and telomerase. Biochimie. 90: 131-155

[64] Efrat .S. 2004. Generation of insulin-producing cells from stem cells for cell replacement therapy of type 1 diabetes. Isr Med Assoc J. 6(5):265-7

[65] Bodnar A.G et al., 1998. Extension of life-span by introduction of telomerase into normal human cells. Science. 279(5349):349-52

[66] Bryan T.M, Reddel R.R, 1997. Telomere dynamics and telomerase activity in in vitro immortalised human cells. European Journal of Cancer. P 767-773

[67] Henson J.D et al, 2002. Alternative lengthening of telomeres in mammalian cells. Oncogene. 21(4):598-610

[68] Fasching C.L et al., 2007. DNA Damage Induces Alternative Lengthening of Telomeres (ALT)–Associated Promyelocytic Leukemia Bodies that Preferentially Associate with Linear Telomeric DNA. Cancer Res. 67(15):7072-7

[69] Draskovic I et al., 2009. Probing PML body function in ALT cells reveals spatiotemporal requirements for telomere recombination. Proc Natl Acad Sci. 106(37):15726-31

[70] Caser A.J and Reddel R.R. 2010. Alternative lengthening of telomeres: models, mechanisms and implications. Nat Rev Genet. 11(5):319–30

[71] Roger R.R. 2002. Alternative lengthening of telomeres, telomerase, and cancer. Cancer Lett. 194(2):155-62

[72] Anthony J, Cesare A. J and Roger R.R. 2008. Alternative Lengthening of Telomeres in Mammalian Cells. From the book :Origin and Evolution of Telomeres by Jozef Nosek and Lubomir Tomaska. Landes Bioscience. Bookshelf ID: NBK6486

[73] Murray J.M and Carr A.M. 2008. Smc5/6: a link between DNA repair and unidirectional replication?. Nature Reviews Molecular Cell Biology. 9,177-82

[74] Vundinti B.R and Ghosh K. 2009. Chromosomal instability and cancer: An insight into the rhythm of life, Indian J Hum Genet. 15(1):1-2

[75] Michor F et al., 2005. Can chromosomal instability initiate tumorigenesis?. Semin Cancer Biol. 15(1):43-9

[76] Surrallés J et al., 2004. Molecular cross-talk among chromosome fragility syndromes Genes Dev. 18(12): 1359–1370

[77] Callén E and Surrallés J. 2004.Telomere dysfunction in genome instability syndromes. Mutat Res. 567(1):85-104

[78] Saar K et al.,1997. The gene for the ataxia-telangiectasia variant, Nijmegen breakage syndrome, maps to a 1-cM interval on chromosome 8q21. Am J Hum Genet. 60(3): 605-610

[79] Weemaes C.M.1981. A new chromosomal instability disorder: the Nijmegen breakage syndrome. Acta Paediatr Scand. 70(4):557-64

[80] Antoccia A et al., 2006. Nijmegen breakage syndrome and functions of the responsible protein. Genome Dyn. 1:191-205

[81] Seemanova E et al., 1985. Familial microcephaly with normal intelligence, immunodeficiency, and risk for lymphoreticular malignancies: a new autosomal recessive disorder. Am J Med Genet. 20(4):639-48

[82] Seemanova E.1990. An increased risk for malignant neoplasms in heterozygotes for a syndrome of microcephaly, normal intelligence, growth retardation, remarkable facies, immunodeficiency and chromosomal instability, Mutat Res. 238(3):321-4

[83] Chrzanowska K.H et al., 2010. High prevalence of primary ovarian insufficiency in girls and young women with Nijmegen breakage syndrome: evidence from a longitudinal study. J Clin Endocrinol Metab. 95(7):3133-40

[84] Michałkiewicz J et al., 2003. Abnormalities in the T and NK lymphocyte phenotype in patients with Nijmegen breakage syndrome. Clin Exp Immunol.134(3):482-90

[85] García-Pérez M.A et al., 2001. Role of Nijmegen Breakage Syndrome Protein in Specific T-Lymphocyte Activation Pathways. Clin Diagn Lab Immunol. 8(4): 757-761

[86] Digweed M, Reis A and Sperling K. 1999. Nijmegen breakage syndrome: consequences of defective DNA double strand break repair. Bioessays. 21(8):649-56

[87] Saar K et al., 1997.The gene for the ataxia-telangiectasia variant, Nijmegen breakage syndrome, maps to a 1-cM interval on chromosome 8q21. Am J Hum Genet. 60(3): 605-610

[88] Karen M et al., 1998. Fine Localization of the Nijmegen Breakage Syndrome Gene to 8q21:Evidence for a Common Founder Haplotype. Am J Hum Genet. 63(1):125-134

[89] Genetic home information, NBN gene http://ghr.nlm.nih.gov/gene/NBN ; Gene cards http://www.genecards.org/cgi-bin/carddisp.pl?gene=NBN

[90] Desai-Mehta A, Cerosaletti K.M and Concannon P. 2001. Distinct functional domains of nibrin mediate Mre11 binding, focus formation, and nuclear localization. Mol Cell Biol. 21(6):2184-91

[91] Cerosaletti K.M, Concannon P. 2003. Nibrin forkhead-associated domain and breast cancer C-terminal domain are both required for nuclear focus formation and phosphorylation. J Biol Chem. 278(24):21944-51

[92] Falck J, Coates J and Jackson S.P. 2005. Conserved modes of recruitment of ATM, ATR and DNA-PKcs to sites of DNA damage. Nature. 434:605-611

[93] Lloyd J et al., 2009. A super-modular FHA/BRCT-repeat architecture mediates Nbs1 adaptor function in response to DNA-damage. Cell. 139(1): 100-111

[94] http://www.uniprot.org/uniprot/O60934 (last time checked on 03.04.2012)

[95] Varon R et al., 1998. Nibrin, a novel DNA double-strand break repair protein, is mutated in Nijmegen breakage syndrome. Cell. 93(3):467-76

[96] Resnick I.B et al., 2002. Nijmegen breakage syndrome: clinical characteristics and mutation analysis in eight unrelated Russian families. J Pediatr. 140(3):355-61

[97] Maraschio P et el., 2001. A novel mutation and novel features in Nijmegen breakage syndrome. J Med Genet. 38:113-117

[98] Seemanova E et al., 2007. Cancer Risk of Heterozygotes With the NBN Founder Mutation. JNCI J Natl Cancer Inst. 99(24):1875-1880

[99] Varon R et al., 2006. Mild Nijmegen breakage syndrome phenotype due to alternative splicing. Hum Mol Genet. 15(5):679-89

[100] Seemanova E et al., 2006. Nijmegen breakage syndrome (NBS) with neurological abnormalities and without chromosomal instability. J Med Genet. 43(3):218-224

[101] Gennery A.R et al., 2004.The clinical and biological overlap between Nijmegen Breakage Syndrome and Fanconi anemia. Clin Immunol. 113(2):214-219

[102] New H.F et al., 2005. Nijmegen breakage syndrome diagnosed as Fanconi anaemia. Pediatr Blood Cancer. 44(5):494-9

[103] Digweed M and Sperling K .2004. Nijmegen breakage syndrome: clinical manifestation of defective response to DNA double-strand breaks. DNA Repair (Amst). 3(8-9):1207-17

[104] D'Amours D and Jackson S.P .2002. The Mre11 complex: at the crossroads of DNA repair and checkpoint signalling. Nat Rev Mol Cell Biol. 3(5):317-27

[105] Zhang Y, Zhou J and Lim ˙C.U. 2006. The role of NBS1 in DNA double strand break repair, telomere stability, and cell cycle checkpoint control. Cell Res. 16(1): 45-54

[106] Jackson S.P .2002. Sensing and repairing DNA double-strand breaks. Carcinogenesis. 23(5):687-96

[107] Pardo B, Gómez-González B and Aguilera A. 2009. DNA repair in mammalian cells: DNA double-strand break repair: how to fix a broken relationship. Cell Mol Life Sci. 66(6):1039-56

[108] Collis S.J et al., 2005. The life and death of DNA-PK. Oncogene. 24(6):949-61

[109] Koch C.A et al., 2004. Xrcc4 physically links DNA end processing by polynucleotide kinase to DNA ligation by DNA ligase IV. EMBO J. 23(19):3874-85

[110] Li X and Heyer W.D.2008. Homologous recombination in DNA repair and DNA damage tolerance. Cell Res. 18(1):99-113

[111] Lee J and Paull T.2004. Direct Activation of the ATM Protein Kinase by the Mre11/Rad50/Nbs1 Complex. Science. 304(5667):93-96

[112] Lavin M.F . 2007. ATM and the Mre11 complex combine to recognize and signal DNA double-strand breaks Recognition and signalling of DNA DSB. Oncogene. 7749-7758

[113] Shiloh Y . 2006. The ATM-mediated DNA-damage response: taking shape. Trends Biochem Sci. 31(7):402-10

[114] Shiloh Y. 2003. ATM and related protein kinases: safeguarding genome integrity. Nat Rev Cancer. 3(3):155-8

[115] Celeste A et al., 2003.Histone H2AX phosphorylation is dispensable for the initial recognition of DNA breaks. Nat Cell Biol. 5(7):675-9

[116] Dupré A, Boyer-Chatenet L and Gautier J .2006. Two - step activation of ATM by DNA and the Mre11-Rad50-Nbs1 complex. Nat Struct Mol Biol. 13(5):451-7

[117] Paull T.T and Gellert M.1999. Nbs1 potentiates ATP-driven DNA unwinding and endonuclease cleavage by the Mre11/Rad50 complex. Genes Dev. 13(10):1276-88

[118] Tauchi H. 2002. Nijmegen breakage syndrome gene, NBS1, and molecular links to factors for genome stability. Oncogene. 21(58):8967-80.

[119] Yeo T.C et al., 2000. V(D)J rearrangement in Nijmegen breakage syndrome. Mol Immunol. 37(18):1131-9

[120] Petersen S et al., 2001. AID is required to initiate Nbs1/gamma-H2AX focus formation and mutations at sites of class switching. Nature. 414(6864):660-5

[121] Van Engelen B.G .2001. Decreased immunoglobulin class switching in Nijmegen Breakage syndrome due to the DNA repair defect. Hum Immunol. 62(12):1324

[122] Tauchi H et al., 2002.Nbs1 is essential for DNA repair by homologous recombination in higher vertebrate cells. Nature. 420(6911):93-8

[123] Sakamoto S et al.,2007. Homologous recombination repair is regulated by domains at the N- and C-terminus of NBS1 and is dissociated with ATM functions NBS1 and ATM in homologous recombination. Oncogene. 26(41):6002-6009

[124] Czornak K, Chughtai S and Chrzanowska K.H .2008.Mystery of DNA repair: the role of the MRN complex and ATM kinase in DNA damage repair. J Appl Genet. 49(4):383-96

[125] Houtgraaf J.H, Versmissen J and van der Giessen W.J. 2006. A concise review of DNA damage checkpoints and repair in mammalian cells. Cardiovasc Revasc Med. 7(3):165-72

[126] Shimada M and Nakanishi M .2006. DNA damage checkpoints and cancer. J Mol Histol. 37(5-7):253-60

[127] Ishikawa K, Ishii H, Saito T. 2006. DNA damage-dependent cell cycle checkpoints and genomic stability. DNA Cell Biol. 25(7):406-11

[128] Kobayashi J et al., 2004. NBS1 and its functional role in the DNA damage response. DNA Repair (Amst). 3(8-9):855-61

[129] Wu L et., 2008. MDC1 regulates intra-S-phase checkpoint by targeting NBS1 to DNA double-strand breaks. Proc Natl Acad Sci U S A. 105(32):11200-5

[130] Horejsí Z et al., 2004.Distinct functional domains of Nbs1 modulate the timing and magnitude of ATM activation after low doses of ionizing radiation. Oncogene. 23(17):3122-7

[131] Girard P.M et al., 2002. Nbs1 promotes ATM dependent phosphorylation events including those required for G1/S arrest. Oncogene. 21(27):4191-9

[132] Antoccia A et al., 1999. Impaired p53-mediated DNA damage response, cell-cycle disturbance and chromosome aberrations in Nijmegen breakage syndrome lymphoblastoid cell lines. Int J Radiat Biol. 75(5):583-91

[133] Jongmans W et al., 1997. Nijmegen breakage syndrome cells fail to induce the p53-mediated DNA damage response following exposure to ionizing radiation. Mol Cell Biol. 17(9):5016-22

[134] Buscemi G et al., 2001. Chk2 activation dependence on Nbs1 after DNA damage. Mol Cell Biol. 21(15):5214-22

[135] Gerard P.M et al., 2000. Radiosensitivity in Nijmegen Breakage Syndrome Cells Is Attributable to a Repair Defect and not Cell Cycle Checkpoint Defects. CANCER RESEARCH. 60(17):4881-4888

[136] Digweed M and Sperling K .2004. Nijmegen breakage syndrome: clinical manifestation of defective response to DNA double-strand breaks. DNA Repair (Amst). 3(8-9):1207-17

[137] Bailey S.M et al., 1999. DNA double-strand break repair proteins are required to cap the ends of mammalian chromosomes. Proc Natl Acad Sci U S A. 96(26):14899-904

[138] Hsu H.L et al., 1999. Ku is associated with the telomere in mammals. Proc Natl Acad Sci U S A. 96(22):12454-12458

[139] Bailey S.M et al., 2004. The kinase activity of DNA-PK is required to protect mammalian telomeres. DNA Repair (Amst). 3(3):225-33

[140] Hsu HL et al., 2000. Ku acts in a unique way at the mammalian telomere to prevent end joining. Genes Dev. 14 (22):2807-12

[141] Kass-Eisler A and Greider C.W. 2000. Recombination in telomere-length maintenance. Trends Biochem Sci. 25(4):200-4

[142] Zhu Xu et al., 2000. Cell-cycle-regulated association of RAD50/MRE11/NBS1 with TRF2 and human telomeres. Nature Genetics. 25, 347-352

[143] Ranganathan V et al., 2001. Rescue of a telomere length defect of Nijmegen breakage syndrome cells requires NBS and telomerase catalytic subunit. Curr Biol. 11(12):962-6

[144] Zhang Y, Zhou J and Lim C.U. 2006. The role of NBS1 in DNA double strand break repair, telomere stability, and cell cycle checkpoint control. Cell Res. 16(1):45-54

[145] Naka K, Ikeda K and Motoyama N.2002. Recruitment of NBS1 into PML oncogenic domains via interaction with SP100 protein. Biochem Biophys Res Commun. 20;299(5):863-71

[146] Jiang WQ et al., 2005. Suppression of alternative lengthening of telomeres by Sp100-mediated sequestration of the MRE11/RAD50/NBS1 complex. Mol Cell Biol. 25(7):2708-21

[147] Verma R.S and Babu. A Human Chromosomes-Manual of basic techniques. Pergamon Press 1989.

[148] Perner .S et al., 2003. Quantifying telomere lengths of human individual chromosome arms by centromere-calibrated fluorescence in situ hybridization and digital imaging. Am J Pathol. 163(5):1751-6

[149] Hirai M, Suto Y and Kanoh M. 1994. A method for simultaneous detection of fluorescent G-bands and in situ hybridization signals. Cytogenet Cell Genet. 66:149-151

[150] Tönnies H. 2002. Modern molecular cytogenetic techniques in genetic diagnostics. Trends Mol Med. 8(6):246-50

[151] Tönnies H et al., 2001. Comparative genomic hybridization based strategy for the analysis of different chromosome imbalances detected in conventional cytogenetic diagnostics. Cytogenet. Cell Genet. 93(3-4):188-94

[152] Sanger F, Nicklen S and Coulson A.R. 1977. DNA sequencing with chain-terminating inhibitors. Proc Natl Acad Sci U S A. 74(12):5463-7

[153] Ishmael F.T and Stellato C. 2008. Principles and applications of polymerase chain reaction: basic science for the practicing physician. Ann Allergy Asthma Immunol. 101(4):437-43

[154] Cawthon R.M. 2002. Telomere measurement by quantitative PCR. Nucleic Acids Res. 30(10): e47

[155] Aubert G, Hills M and Lansdor P.M. 2011.Telomere length measurement-Caveats and a critical assessment of the available technologies and tools. Mutation Research. 730 (2012):59-67

[156] Wilson SE et al., 1993. Extended life of human corneal endothelial cells transfected with the SV40 large T antigen. Invest Ophthalmol Vis Sci. 34(6):2112-23

[157] Numora T et al., 2008. Basic concept of development and practical application of animal models for human diseases. Curr Top Microbiol Immunol. 324:1-24

[158] Devoy A et al., 2011.Genomically humanized mice: technologies and promises. Nat Rev Genet. 13(1):14-20

[159] Difilippantonio S et al., 2005. Role of Nbs1 in the activation of the Atm kinase revealed in humanized mouse models. Nature Cell Biology. 7,675-685

[160] Shaffer L.G, Slovak M.L and Campbell J.L. eds:ISCN 2009, An International System for Human Cytogenetic Nomenclature. S.Karger, Basel.

[161] Aubert G, Hills M and Lansdorp P.M. 2011. Telomere length measurement-Caveats and a critical assessment of the available technologies and tools. Mutat Res. 730(1-2):59-67

[162] Horn T, Robertson B.C and Gemmell N.J. 2010. The use of telomere length in ecology an evolutionary biology. Heredity (Edinb). 105(6):497-506

[163] Cawthon R.M . 2002. Telomere measurement by quantitative PCR. Nucleic Acids Res. 30(10): e47

[164] Perner S et al., 2003.Quantifying telomere lengths of human individual chromosome arms by centromere-calibrated fluorescence in situ hybridization and digital imaging. Am J Pathol .163(5):1751-6

[165] Aubert G, Hills M and Lansdorp P.M. 2011. Telomere length measurement-Caveats and a critical assessment of the available technologies and tools. Mutat Res. 730(1-2):59-67

[166] Horn T, Robertson B.C and Gemmell N.J. 2010. The use of telomere length in ecology an evolutionary biology. Heredity (Edinb). 105(6):497-506

[167] Levy MZ et al.,1992.Telomere end-replication problem and cell aging. J Mol Biol. Jun 225(4):951-60

[168] Oeseburg H et al., 2010. Telomere biology in healthy aging and disease. Pflugers Arch - Eur J Physiol. 459:259-268

[169] Bailey S.M and Murnane J.P. 2006. Telomeres, chromosome instability and cancer. Nucleic Acids Research. 34(8):2408-2417

[170] Bai Yand Murnane J.P.2003.Telomere instability in a human tumor cell line expressing NBS1 with mutations at sites phosphorylated by ATM. Mol Cancer Res. 1(14):1058-69

[171] Lamarche BJ, Orazio N.I and Weitzman M.D. 2010.The MRN complex in double-strand break repair and telomere maintenance. FEBS Lett. 584(17):3682-95

[172] Allsopp R.C, Harley C.B., 1995. Evidence for a critical telomere length in senescent human fibroblasts. Exp Cell Res. 219(1):130-6

[173] Ranganathan V et al., 2001. Rescue of a telomere length defect of Nijmegen breakage syndrome cells requires NBS and telomerase catalytic subunit. Curr Biol. 11(12):962-6

[174] Harley C.B et al., 1990. Telomeres shorten during ageing of human fibroblasts. Nature. 345(6274):458-60

[175] Tauchi H et al., 2002. Nijmegen breakage syndrome gene, NBS1, and molecular links to factors for genome stability. Oncogene. 21(58):8967-80

[176] Taalman R.D et al., 1983. Hypersensitivity to ionizing radiation, in vitro, in a new chromosomal breakage disorder, the Nijmegen Breakage Syndrome. Mutat Res. 112(1):23-32.

[177] Matsuura S. 1997. Genetic mapping using microcell-mediated chromosome transfer suggests a locus for Nijmegen breakage syndrome at chromosome 8q21-24. Am J Hum Genet. 60(6):1487-94

[178] Taalman R.D et al., 1989. Further delineation of the Nijmegen breakage syndrome. Am J Med Genet. 32(3):425-31

[179] Antoccia A et al., 1999. Impaired p53-mediated DNA damage response,cell-cycle disturbance and chromosome aberrations in Nijmegen breakage syndrome lymphoblastoid cell lines. International journal of radiation biology. 75(5):583-591

[180] Girard P.M et al., 2000. Radiosensitivity in Nijmegen Breakage Syndrome cells is attributable to a repair defect and not cell cycle checkpoint defects. Cancer Res. 60(17):4881-8

[181] Counter C.M. 1992. Telomere shortening associated with chromosome instability is arrested in immortal cells which express telomerase activity. EMBO J. 11(5):1921-9

[182] Counter C.M et al., 1998. Dissociation among in vitro telomerase activity, telomere maintenance, and cellular immortalization. Proc Natl Acad Sci U S A.8;95(25):14723-8

[183] Kamranvar S.A and Masucci M.G. 2011. The Epstein–Barr virus nuclear antigen-1 promotes telomere dysfunction via induction of oxidative stress. Leukemia. 25(6):1017-25

[184] Counter CM et al., 1994. Stabilization of short telomeres and telomerase activity accompany immortalization of Epstein-Barr virus-transformed human B lymphocytes. J Virol. 68(5):3410-4

[185] Savre-Train I, Gollahon L.S and Holt S.E. 2000. Clonal heterogeneity in telomerase activity and telomere length in tumor-derived cell lines. Proc Soc Exp Biol Med. 223(4):379-88

[186] Eiso Hiyama et al., 2001. Immunohistochemical Detection of Telomerase (hTERT) Protein in Human Cancer Tissues and a Subset of Cells in Normal Tissues. Neoplasia. 3(1):17–26

[187] Bryan T.M et al., 1997. The telomere lengthening mechanism in telomerase-negative immortal human cells does not involve the telomerase RNA subunit. Human Molecular Genetics. (6):921-6

[188] Lansdorp P.M et al., 1996. Heterogeneity in telomere length of human. Hum Mol Genet. 5(5):685-91

[189] der-Sarkissian H et al., 2004.The shortest telomeres drive karyotype evolution in transformed cells. Oncogene. 23(6):1221-8

[190] Martens U.M et al., 1998. Short telomeres on human chromosome 17p. Nat Genet. 18, 76 -80

[191] Perner S et al., 2003. Quantifying telomere lengths of human individual chromosome arms by centromere-calibrated fluorescence in situ hybridization and digital imaging. Am J Pathol. 163(5):1751-6

[192] Londoño-Vallejo J.A et al., 2001. Differences in telomere length between homologous chromosomes in humans. Nucl Acids Res. 29(15): 3164-3171

[193] Samassekou O et al., 2011. Chromosome Arm-Specific Long Telomeres: A New Clonal Event in Primary Chronic Myelogenous Leukemia Cells. Neoplasia. 13(6): 550-560

[194] Bhattacharyya M.K and Lustig A.J. 2006. Telomere dynamics in genome stability. Trends Biochem Sci. 31(2):114-22

[195] Saltman D et al., 1993. Telomeric structure in cells with chromosome end associations. Chromosoma. 102(2):121-8

[196] Rebeca C et al., 2007. The nature of telomere fusion and a definition of the critical telomere length in human cells. Genes Dev. 21(19): 2495-2508

[197] Lin T.T et al., 2010. Telomere dysfunction and fusion during the progression of chronic lymphocytic leukemia: evidence for a telomere crisis. Blood. 116(11):1899-907

[198] Hemann M.T et al., 2001. The shortest telomere, not average telomere length, is critical for cell viability and chromosome stability. Cell. 107(1):67-77

[199] Stumm M et al., 20001. High frequency of spontaneous translocations revealed by FISH in cells from patients with the cancer-prone syndromes ataxia telangiectasia and Nijmegen breakage syndrome. Cytogenet Cell Genet. 92(3-4):186-91

[200] Zhu X.D et al., 2000. Cell-cycle-regulated association of RAD50/MRE11/NBS1 with TRF2 and human telomeres. Nature Genetics 25(3):347-352

[201] Hou Y.Y, Toh M.T and Wang X. 2011. NBS1 deficiency promotes genome instability by affecting DNA damage signaling pathway and impairing telomere integrity. Cell Biochem Funct. 30(3):233-42

[202] Hastie N.D et al., 1990. Telomere reduction in human colorectal carcinoma and with ageing. Nature. 346(6287):866 - 868

[203] Bozzau C et al., 2011. Analysis of telomere dynamics in peripheral blood cells from patients with Lynch syndrome. Cancer. 117(18):4325-35

[204] Iwama H et al., 1998. Telomeric length and telomerase activity vary with age in peripheral blood cells obtained from normal individuals. Hum Genet. 102(4):397-402

[205] Frenck R.W , Blackburn E.H and Shannon K.M. 1998. The rate of telomere sequence loss in human leukocytes varies with age. Proc Natl Acad Sci U S A. 95(10):5607-10

[206] Iwama, H et al., 1998. Telomeric length and telomerase activity vary with age in peripheral blood cells obtained from normal individuals. Hum. Genet. 102, 397-402

[207] Ranganathan V et al., 2001. Rescue of a telomere length defect of Nijmegen breakage syndrome cells requires NBS and telomerase catalytic subunit. Curr Biol;11(12):962-6.

[208] Cawthon R et al, 2003. Association between telomere length in blood and mortality in people aged 60 years or older. Lancet. 361(9355):393-5

[209] Brouilette S.W et al., 2007. telomere length ,risk of coronary heart disease, and stain treatment in the west of Scotland primary prevention study. Lancet. 369(9556):107-14

[210] Serrano A.L and Vicente A. 2004.Telomeres and Cardiovascular Disease Does Size Matter?. Circ Res. 94(5): 575-584

[211] Benetos A et al., 2001. Telomere length as an indicator of biological aging: the gender effect and relation with pulse pressure and pulse wave velocity. Hypertension. 37(2):381-5

[212] Najajou O.T et al., 2009. Association between telomere length, specific causes of death, and years of healthy life in health, aging, and body composition, a population-based cohort study. J Gerontol A Biol Sci Med Sci. 64(8):860-4

[213] Callén E and Surrallés J. 2004. Telomere dysfunction in genome instability syndromes. Mutat Res. 567(1):85-104

[214] Blasco M.A. 2004. Telomere epigenetics: a higher-order control of telomere length in mammalian cells. Carcinogenesis. 25 (7): 1083-1087

[215] Baerlocher G.M and Lansdorp P.M. 2003. Telomere length measurements in leukocyte subsets by automated multicolor flow-FISH. Cytometry A. 55(1):1-6

[216] Jeffery P et al., 2005. Rise in Insulin Resistance Is Associated With Escalated Telomere Attrition. Circulation. 111(17):2171-2177

[217] Slagboom P. E, Droog S and Boomsma D.I. 1994. Genetic determination of telomere size in humans: a twin study of three age groups. Am J Hum Genet. 55(5): 876–882

[218] Jeanclos E et al., 2000. Telomere length inversely correlates with pulse pressure and is highly familial. Hypertension. 36(2):195-200

[219] Vasa-Nicotera M et al., 2005. Mapping of a Major Locus that Determines Telomere Length in Humans. The American Journal of Human Genetics. 76(1):147-151

[220] Graakjaer et al., 2003. The pattern of chromosome-specific variations in telomere length in humans is determined by inherited, telomere-near factors and is maintained throughout life. Mech Ageing Dev.124(5):629-40

[221] Graakjaer J et al., 2006. Allele-specific relative telomere lengths are inherited. Hum Genet. 119(3):344-50

[222] Huda N et al., 2007. Shared environmental factors associated with telomere length maintenance in elderly male twins. Aging Cell. 6(5):709-13

[223] Allsopp R.C et al., 1992. Telomere length predicts replicative capacity of human fibroblasts. Proc. Natl. Acad. Sci. U. S. A. 89(21):10114-10118

[224] Baird D.M et al., 2006. Telomere instability in the male germline. Hum Mol Genet. 15(1):45-51

[225] Aikata H et al., 2000. Telomere Reduction in Human Liver Tissues with Age and Chronic Inflammation. Exp Cell Res. 256(2):578-582

[226] Jiang H Ju Z and Rudolph K. L. 2007. Telomere shortening and ageing. Z Gerontol Geriat 40:314–324

[227] Djojosobroto MW et al., 2003. telomere and telomerase in ageing, regeneration and cancer. Mol cells. 15(2):164-175

[228] Cameron I.L., 1970. Cell renewal in the organs and tissues of the nongrowing adult mouse. Tex Rep Biol Med. 28(3):203-48

[229] Takubo K et al., 2002. Telomere lengths are characteristic in each human individual. Exp Gerontol. 37(49):523-531

[230] Youngren K et al., 1998. Synchrony in telomere length of the human fetus. Hum Genet. 102(6):640-643

[231] Butler M.G et al., 1998. Comparison of chromosome telomere integrity in multiple tissues from subjects at different ages. Cancer Genet Cytogenet. 105(2):138-44

[232] Allsopp R.C et al.,1995. Telomere shortening is associated with cell division *in vitro* and *in vivo*. Exp Cell Res. 220(1):194-200

[233] Liu L et al., 2007.Telomere lengthening early in development Nat Cell Biol. 9(12):1436-41

[234] Hiyama E and Hiyama K. 2007.Telomere and telomerase in stem cells. Br J Cancer. 96(7):1020-1024

[235] Takubo K et al., 2002. Telomere lengths are characteristic in each human individual. Exp Gerontol. 37(4):523-31

[236] Flores I Benetti R and Balasco M.A. 2006. Telomerase regulation and stem cell behavior. Curr Opin Cell Biol. 18(3):254-60

[237] Epel E.S et al., 2004. Accelerated telomere shortening in response to life stress, Proc Natl A, cad Sci U S A. 101(49):17312-5

[238] Voldes A.M et al., 2005. Obesity, cigarette smoking, and telomere length. Lancet. 366(9486):662-4

[239] Babizhayev M.A et al., 2011. Telomere Length is a Biomarker of Cumulative Oxidative Stress, Biologic Age, and an Independent Predictor of Survival and Therapeutic Treatment Requirement Associated with Smoking Behavior. Am J Ther. 18(6):209-26

[240] Cassidy A et al., 2010. Associations between diet, lifestyle factors, and telomere length in women. Am J Clin Nutr. 91(5):1273-80

[241] "Why is life expectancy longer for women than it is for men?". Scientific American. http://www.scientificamerican.com/article.cfm?id=why-is-life-expectancy-lo

[242] Cawthon RM et al., 2003. Association between telomere length in blood and mortality in people aged 60 years or older. Lancet. 361(9355):393-5

[243] Kimura,M et al., 2008.Telomere length and mortality: a study of leukocytes in elderly Danish twins. Am. J. Epidemiol. 167(7):799-806

[244] Honig L.S et al., 2006. Shorter telomeres are associated with mortality in those with APOE epsilon4 and dementia. Ann Neurol. 60(2):181-187

[245] Benetos A et al., 2001. Telomere length as an indicator of biological aging: the gender effect and relation with pulse pressure and pulse wave velocity. Hypertension. 37(2):381-5

[246] Unryn B.M, Cook L.S and Riabowol K.T. 2005. Paternal age is positively linked to telomere length of children. Aging Cell. 4(2):97-101

[247] Mayer S et al., 2006. Sex-specific telomere length profiles and age-dependent erosion dynamics of individual chromosome arms in humans. Cytogenet Genome Res. 112(3-4):194-201

[248] Möller P et al., 2009. Sex-related differences in length and erosion dynamics of human telomeres favor females. Aging (Albany NY). 1(8):733-9

[249] Perner S et al., 2003. Quantifying telomere lengths of human individual chromosome arms by centromere-calibrated fluorescence in situ hybridization and digital imaging. Am J Pathol. 163(5):1751-6

[250] Njajou O.T et al., 2007. Telomere length is paternally inherited and is associated with parental lifespan. Proc Natl Acad Sci U S A. 104(29):12135-9

[251] Unryn B.M, Cook L.S and Riabowol K.T. 2005. Paternal age is positively linked to telomere length of children. Aging Cell. 4(2):97-101

[252] Nordfjäll K et al., 2005. Telomere length and heredity: Indications of paternal inheritance. Proc Natl Acad Sci U S A. 102(45):16374-8

[253] Nawrot T.S et al., 2004. Telomere length and possible link to X chromosome. Lancet. 363(9408):507-10

[254] Kipling D and Cooke H.J. 1990. Hypervariable ultra-long telomeres in mice. Nature. 347(6291):400-2

[255] Zijlmans G.M et al., 1997. Telomeres in the mouse have large inter-chromosomal variations in the number of T2AG3 repeats. Proc Natl Acad Sci U S A. 94(14):7423-8

[256] Kang J et al., 2002. Targeted disruption of NBS1 reveals its roles in mouse development and DNA repair. EMBO J. 21(6): 1447-1455

[257] Zhu J et al., 2001. Targeted disruption of the Nijmegen breakage syndrome gene NBS1 leads to early embryonic lethality in mice. Curr Biol. 11(2):105-9

[258] Williams B.R et al., 2002. A murine model of Nijmegen breakage syndrome. Curr Biol. 12(8):648-53

[259] Cheng A et al., 2007. Telomere Protection Mechanisms Change during Neurogenesis and Neuronal Maturation: Newly Generated Neurons Are Hypersensitive to Telomere and DNA Damage. The Journal of Neuroscience. 27(14):3722-3733

[260] Prowse K.R and Greider C.W. 1995. Developmental and tissue-specific regulation of mouse telomerase and telomere length. Proc Natl Acad Sci U S A. 92:4818-4822

[261] Blasco M.A. 2005. Telomeres and human disease: ageing, cancer and beyond. Nat Rev Genet. 6(8):611-22

[262] Perona R et al., 2009. Telomerase deficiency and cancer susceptibility syndromes. Clin Transl Oncol. 11(11):711-4

[263] Xu L and Blackburn E.H. 2007. Human cancer cells harbor T-stumps, a distinct class of extremely short telomeres. Mol Cell. 28(2):315-27

[264] Hastie N.D et al., 1990. Telomere reduction in human colorectal carcinoma and with ageing. Nature. 346(6287):866-868

[265] Ozery-Flato et al., 2011. Large-scale analysis of chromosomal aberrations in cancer karyotypes reveals two distinct paths to aneuploidy. Genome Biol. 12(6):R61

[266] Callén E and Surrallés J. 2004. Telomere dysfunction in genome instability syndromes. Mutat Res. 567(1):85-104

[267] Tauch H et al., 2002. Nijmegen breakage syndrome gene, NBS1, and molecular links to factors for genome stability. Oncogene . 21(58):8967-80

[268] Varon R et al., 2001. Mutations in the Nijmegen Breakage Syndrome Gene (NBS1) in Childhood Acute Lymphoblastic Leukemia (ALL). Cancer Res. 61(9):3570-2

[269] Plisiecka Halasa J et al.,2002.Nijmegen breakage syndrome gene (NBS1) alterations and its protein (nibrin) expression in human ovarian tumours. Ann Hum Genet. 66(Pt 5-6):353-9

[270] Seidemann K et al., 2000. Non-Hodgkin's lymphoma in pediatric patients with chromosomal breakage syndromes (AT and NBS): Experience from the BFM trials. Ann Oncol. 1:141-145

[271] Steffan J et al., 2006. Increased risk of gastrointestinal lymphoma in carriers of the 657del5 NBS1 gene mutation. Int J Cancer. 119(12):2970-3

[272] Gladkowska-Dura M et al., 2008. Unique morphological spectrum of lymphomas in Nijmegen breakage syndrome (NBS) patients with high frequency of consecutive lymphoma formation. J Pathol. 216(3):337-44

[273] Dembowska-Baginska B et al., 2009. Non-Hodgkin lymphoma (NHL) in children with Nijmegen Breakage syndrome (NBS) Pediatr Blood Cancer. 52(2):186-90

[274] Kinzler KW, Vogelstein B 1997. Cancer-susceptibility genes. Gatekeepers and caretakers. Nature. 386(6627):761-763

[275] Cybulski C et al., 2004. NBS1 Is a Prostate Cancer Susceptibility Gene. CANCER RESEARCH. 64(4):1215-1219

[276] Seemanova E at al., 2007. Cancer Risk of Heterozygotes with the NBN Founder Mutation. J Natl Cancer Inst. 99(24):1875-80

[277] Debniak T et al., 2003. Germline 657del5 mutation in the NBS1 gene in patients with malignant melanoma of the skin. Melanoma Res. 13(4):365-70

[278] Dzikiewicz-Krawczyk A et al., 2011. Impact of heterozygous c.657-661del, p.I171V and p.R215W mutations in NBN on nibrin functions. Mutagenesis. 10.1093.ger048

[279] Heikkinen K et al., 2006. RAD50 and NBS1 are breast cancer susceptibility genes associated with genomic instability. Carcinogenesis. 27(8):1593-9

[280] Gorski B et al., 2003. Germline 657del5 mutation in the NBS1 gene in breast cancer patients. Int J Cancer. 106(6):984

[281] Sokolenko A.P et al., 2007. Founder mutations in early-onset, familial and bilateral breast cancer patients from Russia. Fam Cancer. 6(3):281-6

[282] Desjardins S et al., 2009. Variations in the *NBN/NBS1* gene and the risk of breast cancer in non-*BRCA1/2* French Canadian families with high risk of breast cancer. BMC Cancer. 9:181

[283] Seemanova E .1990. An increased risk for malignant neoplasms in heterozygotes for a syndrome of microcephaly, normal intelligence, growth retardation, remarkable facies, immunodeficiency and chromosomal instability. Mutat Res. 238(3):321-4

[284] De Angelis et al., 2007. Chromosomal 20q gain in the DNA diploid component of aneuploid colorectal carcinomas. Int J Cancer. 120(12):2734-8

[285] Michael B. 2007. Genomic imbalances in 5918 malignant epithelial tumors: an explorative meta-analysis of chromosomal CGH data. BMC Cancer. 7:226

[286] Noutomi Y et al., 2006. Comparative genomic hybridization reveals genetic progression of oral squamous cell carcinoma from dysplasia via two different tumourigenic pathways. J Pathol. 210(1):67-74

[287] Biswas A.K and Johnson D.G. 2012. Transcriptional and nontranscriptional functions of E2F1 in response to DNA damage. Cancer Res. 72(1):13-7

[288] Hoyo C et al., 2012. IGF2R genetic variants, circulating IGF2 concentrations and colon cancer risk in African Americans and Whites. Dis Markers. 32(2):133-41

[289] Nuno M et al., 2011. Comparative biology of mammalian telomeres: hypotheses on ancestral states and the roles of telomeres in longevity determination. Aging Cell. 10(5)761-768

[290] Heidinger B.J et al., 2012. Telomere length in early life predicts lifespan. Proc Natl Acad Sci U S A. 109(5):1743-8

[291] Morin GB., 2003. Telomere control of replicative lifespan. Exp Gerontol. 32(4-5):375-82

[292] Chrzanowska K.H, Digweed M, Sperling K and Seemanova E. 2009. DNA-Repair Deficiency and Cancer: Lessons from Lymphoma. In: Allgayer H, Rehder H, Fulda S (Hrsg) Hereditary Tumors. S. 377-391; Wiley-Blackwell.

6. Summary

Telomeres are located at the ends of chromosomes and have an essential role in the maintenance of genome stability in all eukaryotes. The length of the telomeric DNA, an evolutionary highly conserved repetitive sequence, plays a crucial role both in cellular senescence and in carcinogenesis. In addition, a number of human genetic disorders have been identified which are characterized by dysfunctional telomeres, a defective DNA damage response, limited cell proliferation capacity in vitro and a highly increased cancer risk. Thus, telomere biology is directly linked to basic biological phenomena such as aging, tumorigenesis, maintenance of DNA integrity and chromosomal instability.

Here, telomere length was analysed in various chromosomal instability syndromes, particularly in Nijmegen Breakage Syndrome (NBS) and a NBS mouse model. Three different complementary methods to measure telomere length were applied: (1) Quantitative-PCR (Q-PCR), based on the simultaneous amplification of telomeric repeats and a single copy gene, (2) Quantitative fluorescence in situ hybridization of telomere repeats (Q-FISH) in which the fluorescence intensity of single telomeres is measured relative to a constant repetitive sequence in the centromeric region of chromosome 2, allowing calculation of the relative length of individual telomeres, and (3)Terminal Restriction Fragment length analysis by Southern blot (TRF analysis) to measure the absolute average length of telomeric DNA.

The results show that comparison of total telomere length, estimated by Q-FISH and Q-PCR in the same probes, resulted in a highly positive correlation with a correlation coefficient of $r > 0.9$. Thus, the Q-FISH and Q-PCR data, which both represent relative telomere lengths, show a tight linear relationship. Telomeric restriction fragment (TRF) analysis measures the average absolute telomere length. Here, absolute telomere length was compared with the relative length estimated by Q-PCR in the same seven DNA probes. There was a positive correlation with a correlation coefficient of $r= 0.64$. Based on this comparison, it was then possible to roughly convert the relative telomere lengths after Q-PCR into absolute lengths.

Telomere length , measured in blood DNA of individuals less than 10 years of age, are significantly shorter in NBS-, NBS-like, AT and FA patients compared to controls and NBS-heterozygotes. Telomeres become shorter with age in normal individuals although at different rates throughout an individuals lifetime. Despite originally shorter telomeres, the

shortening rate from birth to 20 years is almost the same in NBS patients and controls. The mean relative telomere length of females was slightly longer than in males, both in NBS patients and controls. This difference was, however, not significant, when a homogenous age cohort was compared.

Estimation of telomere length in 14 different tissues of a NBS-fetus, terminated at 34 weeks of gestation, showed that the spinal cord, brain and heart had the longest telomeres, skin the shortest. Telomere length in 4 different tissues of a humanized Nbs mouse showed that in general the two control mice with the human wild type allele had slightly longer telomeres in all four tissues than the three mice with the mutant allele. Also here, telomeres in brain were the longest in two controls and one Nbs mouse, while almost no difference was found in the two other Nbs mice. These findings fit well with the general observation that the disease phenotype in Nbs mice is less severe than in NBS patients.

Telomere lengths in diploid NBS and control fibroblasts decreased as a function of subculturing. As expected, the telomere lengths of the controls were much longer than those of the NBS fibroblasts. However in NBS and control lymphoblastoid cell lines the telomere lengths remained almost constant during cultivation. The same was observed in SV40 transformed NBS fibroblasts, however, telomeres were significantly shorter than in the original diploid fibroblasts. The human telomerase reverse transcriptase (*hTERT*) was highly expressed in the SV40 transformed NBS cell lines but not in the original diploid lines. Great variability of *hTERT* gene expression was found in the lymphoblastoid cell lines, ranging from high expression to no detectable mRNAs.

Estimation of total telomere length by Q-FISH in NBS and control cell lines confirmed the results obtained by Q-PCR. The cell line with the shortest telomeres showed in some metaphases telomere fusions. In addition, the estimation of telomere length of individual chromosomes by Q-FISH showed a significant difference in telomere length between individual chromosome arms, both in NBS and control cells. In most cases the shortest telomeres were found on the p arm of chromosome 19, and the q arms of chromosomes 19, 17 and 20. In the lymphoblastoid cell line with the shortest total telomere length, the telomere of the p arm of one chromosome 19 was brightly fluorescent in 70 % of the metaphases, while the other chromosomes 19 displayed only weak fluorescence. The difference in relative T/C value (Telomere fluorescence/Centromere fluorescence) was about 11: 1 for the two chromosomes 19. To the best of our knowledge such an enormous elongation of a single telomere has not been described before in human chromosomes and

might depend on a hitherto unknown mechanism. *hTERT* was only weakly expressed in this line.

Another completely unexpected observation was made after Q-FISH in a fibroblast cell line, derived from a 9 years old NBS patient with the founder mutation (c.657_661del5). After chromosome analysis, two cell lines, one with 46 the other with 45 chromosomes, could be identified. The latter was due to a complex, unbalanced translocation. Interestingly, this aberrant line increased during subcultivation, from 50 % at passage 3 to about 90% at passage 7. Based on comparative genomic hybridization (CGH) and whole chromosome painting the aberrant karyotype is: 45,XY, der(6)(6pter→6q12 :: 13q21.1→13q34 :: 20q11.2→20qter), -13, ISCN 2009.

Estimation of the cell cycle length after BrdU labelling illustrated that the cell cycle of the aberrant cells was shorter than that of the normal cells. In addition, after X-irradiation with 0.5 and 1.0 Gy the aberrant line had more chromosomal aberrations than the diploid line. Thus, the high radiosensitivity of the original NBS line was further increased. Moreover, the total telomere length was significantly longer in aberrant than that in the normal cells. Clearly, this line had a selective advantage in tissue culture and might represent an early (first) step in malignant transformation. Moreover, one can speculate that this specific combination of gain and losses of genetic material may reflect a mechanism for balancing the dosage of the affected genes.

Altogether, the present findings underline the role of the *NBN* gene in telomere maintenance and shed new light on the chromosome instability inherent in NBS which increases their risk for haematological malignancies and solid tumours.

7. Zusammenfassung

Telomere stellen die natürlichen Chromosomenenden aller Eukaryoten dar. Ihnen kommt eine entscheidende Rolle bei der Aufrechterhaltung der genomischen Integrität zu. Es handelt sich um ein evolutionär hoch-konservierte repetitive Sequenzen, deren Länge insgesamt eine wichtige Rolle bei der zellulären Seneszenz und der Karzinogenese spielt. Es gibt es eine Reihe genetisch bedingter Krankheiten, die die Funktion der Telomere beeinträchtigen, die DNA Reparatur und die Zellproliferation einschränken sowie mit einem stark erhöhten Krebsrisiko einhergehen. Es besteht daher eine unmittelbare Verbindung zwischen der Biologie der Telomere und so grundlegenden biologischen Phänomenen, wie Alterung und Tumorgenese, Aufrechterhaltung der DNA Integrität und der chromosomalen Stabilität.

In dieser Arbeit wurde die Telomerlänge bei verschiedenen Syndromen mit Chromosomeninstabilität analysiert, insbesondere dem Nijmegen Breakage Syndrom (NBS) and einem NBS Mausmodell. Hierbei wurden drei sich ergänzende Methoden eingesetzt: (1) Quantitative-PCR (Q-PCR), sie basiert auf der gleichzeitigen Amplifikation telomerischer Repeats und eines Einzelkopie-Gens und gibt die durchschnittliche relative Länger aller Telomere an, (2) Quantitative Fluoreszenz in situ Hybridisierung telomerischer Repeats (Q-FISH), bei der die Fluoreszenzintensität einzelner Telomere in Bezug zu einer konstanten repetitiven Sequenz der centromerischen Region von Chromosom 2 gesetzt und dadurch die relative Länge individueller Telomere bestimmt wird und (3) die „Terminal Restriction Fragment length analysis by Southern blot“ (TRF Analyse), durch die die durchschnittliche absolute Länge der Telomere ermittelt wird.

Die Ergebnisse zeigen, dass die mittels Q-FISH und Q-PCR bestimmten Telomerlängen identischer Proben miteinander hoch korreliert sind. Der Korrelationskoeffizient ist $r > 0.9$. Das heißt, die Befunde nach Q-FISH und Q-PCR, die beide relative Telomerlängen widergeben, zeigen einen deutlichen linearen Bezug zueinander. Eine Vergleich der TRF Analyse und der Q-PCR derselben sieben Proben ergab ebenfalls eine positive Korrelation mit $r = 0.64$. Darauf gestützt, war es möglich, aus den mittels Q-FISH und Q-PCR ermittelten relativen Telomerlängen die absoluten Längen näherungsweise zu berechnen.

Die Telomerlängen, die aus DNA der Blutproben von Kindern (<10 Jahre) mit Chromosomeninstabilität (NBS, „NBS-like“, Ataxia telangiectasia und Fanconi Anämie) ermittelt wurden, sind signifikant kürzer als die gesunder Kontrollkinder und NBS-

Heterozygoter. Die Kontrollpersonen zeigten eine altersabhängige Verkürzung der Telomere, allerdings in unterschiedlichem Ausmaß zu verschiedenen Lebenszeiten. Bei den NBS-Patienten erfolgt die Verkürzung in den ersten 20 Lebensjahren ähnlich wie bei den Kontrollpersonen, wobei die Telomerlängen insgesamt wesentlich kürzer sind. Die Telomere weiblicher Personen waren etwas länger als die männlicher, sowohl bei den Kontrollen als auch bei den NBS-Patienten. Dieser Unterschied war jedoch nicht mehr signifikant, wenn homogene Alterskohorten verglichen wurden.

Die Bestimmung der Telomerlängen in 14 unterschiedlichen Geweben eines NBS-Feten, der in der 34. Schwangerschaftswoche abortiert wurde, zeigte, dass Rückenmark, Gehirn und Herz die längsten Telomere aufwiesen, Hautgewebe die kürzesten. Die Analyse der Telomerlängen in 4 unterschiedlichen Geweben der “humanized” Nbs-Mäuse ergab, dass die beiden Mäuse mit dem menschlichen wildtyp Gen etwas längere Telomere besaßen als die drei Mäuse mit dem mutanten Allel. Auch hier wies das Gehirn beider Kontrolltiere und einer Nbs-Maus die längsten Telomere auf, wobei bei den anderen Nbs-Mäusen praktisch kein Unterschied gefunden wurde. Diese Befunde bestätigen die allgemeine Beobachtung, dass der Krankheitsphänotyp bei Nbs-Mäusen deutlich geringer ausgeprägt ist als bei NBS-Patienten.

Die Telomerlänge in diploiden NBS- und Kontroll-Fibroblasten verkürzte sich in Abhängigkeit von der Zahl der Passagen. Auch hier waren erwartungsgemäß die Telomere der Kontrollzellen wesentlich länger als die der NBS-Zellen. In lymphoblastoiden NBS- und Kontroll-Zellen hingegen blieb die Telomerlänge während der Kultivierung praktisch konstant. Das Gleiche traf auch auf die SV40 transformierten NBS-Fibroblasten zu. In letzteren war jedoch die Länge der Telomere deutlich kürzer als in den ursprünglichen diploiden Fibroblasten. Die „human telomerase reverse transcriptase” (*hTERT*) war in den SV40 transformierten NBS-Zellen stark exprimiert, nicht jedoch in den Ursprungszellen. Eine erhebliche Variabilität der *hTERT* Expression wiesen die lymphoblastoiden Zellen auf, sie reichte von hoher bis nicht nachweisbarer Expression auf RNA-Ebene.

Die Bestimmung der gesamten Telomerlänge nach Q-FISH in den NBS- und Kontroll-Zellen bestätigte die Q-PCR Befunde. Die NBS-Zelllinie mit den kürzesten Telomeren wies in einigen Fällen Telomerfusionen auf. Darüber hinaus zeigten die Telomere einzelner Chromosomen signifikante Längenunterschiede, sowohl bei den NBS- als auch den Kontroll-Zellen. In der Mehrzahl der Fälle wiesen der p arm von Chromosom 19 und der q Arm der Chromosomen 19, 17 und 20 die kürzesten Telomere auf. In der

lymphoblastoiden NBS-Zelllinie mit den kürzesten Telomeren zeigte das Telomer des p Arms eines Chromosoms 19 in 70% der Metaphasen eine intensive Fluoreszenz, während die anderen Chromosomen 19 nur schwach fluoreszierende Telomere aufwiesen. Der Unterschied in der Fluoreszenzintensität betrug etwa 11 : 1. Nach unserer Kenntnis wurde eine derartige Verlängerung eines einzelnen Telomers bislang noch nicht für menschliche Zellen beschrieben und könnte auf einen neuen Mechanismus hinweisen. Die *hTERT* Expression war in dieser Zelllinie nur sehr gering.

Ein vollkommen unerwarteter Befund ergab die Q-FISH Analyse primärer Fibroblasten, die von einem 9 Jahre alten NBS Kind mit der Gründermutation (c.657_661del5) stammten. Die Chromosomenanalyse ergab ein Mosaik aus einer Line mit 46 und einer mit 45 Chromosomen. Letztere wies eine komplexe, unbalanzierte Translokation auf. Diese Zellen nahmen von 50 % bei Passage 3 auf etwa 90% bei Passage 7 zu. Mittels „comparative genomic hybridization" (CGH) und „whole chromosome painting" ergab sich für die aberrante Linie der Karyotyp: 45,XY, der(6)(6pter→6q12 :: 13q21.1→13q34 :: 20q11.2→20qter), -13, ISCN 2009.

Die Bestimmung der Zellzykluslänge nach BrdU Markierung ergab für die aberrante Linie einen kürzeren Zellzyklus als für die normal diploide. Zusätzlich zeigte sich nach Bestrahlung mit 0.5 und 1.0 Gy, dass die aberrante Linie mehr Chromosomenschäden als die diploide aufwies, das heißt, die hohe Strahlenempfindlichkeit der ursprünglichen NBS-Zelllinie wurde noch weiter verstärkt. Zudem war auch die Länge der Telomere gegenüber den diploiden Zellen signifikant erhöht. Zweifellos hat die aberrante Zellinie einen Selektionsvorteil in der Gewebekultur und könnte einen frühen (ersten) Schritt zu maligner Transformation repräsentieren. Darüber hinaus kann man vermuten, dass die spezifische Kombination von zusätzlichem und fehlendem Erbgut einen „Mechanismus" darstellt, um die Dosis-Unterschiede der betroffenen Gene auszugleichen.

Insgesamt unterstreichen die Befunde die Bedeutung des *NBN*-Gens für die Stabilisierung der Telomere und werfen ein neues Licht auf die Chromosomeninstabilität bei NBS-Patienten mit ihrem hohen Risiko für hämtologische und solide Tumore.

8. Acknowledgments

I would like to express my deepest thanks to my supervisor Prof. Dr. Karl Sperling for his support, attention, immense guidance and continued advices in addition to his humanely nice dealing.

I would like to thank Prof. Dr. Heidemarie Neitzel for her kind cooperation and suggestions.

Special thanks to Prof. Dr. Carsten Niemitz for helping and granting me admission at Frei University. Many thanks for Prof. Dr. Rupert Mutzel for reviewing my thesis.

I also thank Dr. Raymonda Varon-Mateeva for her advices and critical comments, and Dr. Ilja Demuth for his nice collaboration in TRF analysis.

I would like to thank Veronique Dutrannoy-Tönsing, Antje Gerlach, Britta Teubner, Traute Burmester, Reyk Richter, Marlies Schwanke, Marianne Plieth, Mohsen Karbasiyan, Janina Radszewski and Bastian Salewsky for technical and practical help in the laboratory. A special thank also to Rami Derbas for helping me in statistical tests.

I am extremely grateful to my friends, who supported and helped me a lot, my best friend Zeina Nicola, Kamila Czornak and Reham Fadl.

I am very grateful to my parents, my sisters, my brother and my lovely grandmother who gave me the strength, belief and support in my exile.

Finally, I deeply thank my husband Fadi for his understanding, patience, everlasting optimism and motivation.

9. Confirmation

Herewith I confirm that, I have done this thesis completely on my own and without impermissible help.

Raneem Habib

10. Appendix

Appendix 1: Telomere length in healthy individuals (controls)

DNA number	relative telomere length	Age(years)	Sex
04P0523	2.16	1	F
04P0862	3.41	1	F
05P0586	1.6	2	M
05P0509	1.12	2	F
04P0535	1.45	3	F
01P0888	0.9	3	M
02P01053	2.25	5	M
04P0216	1.42	9	M
112	1.37	11	F
204	1.29	11	F
166	1.83	12	F
17	1.94	13	F
443	1.93	14	F
444	1.36	15	M
210	0.98	16	F
365	1.51	17	F
247	1.23	18	F
47	1.17	19	F
293	1.58	19	-
193	0.74	20	M
390	1.41	20	M
431	1.25	20	M
423	0.79	20	M
11	1.2	20	M
161	1	20	F
420	0.73	20	F
o2	1	21	M
440	1	21	F
143	1.26	21	F
448	0.83	21	F
129	0.93	21	F
169	1.16	21	F
164	1.18	21	F
13	1.22	21	M
413	0.9	21	F
223	1	22	F
163	0.95	22	M
40	0.91	22	F

188	0.76	22	F
241	1	23	M
246	0.84	23	M
470	1	23	M
280	1.44	23	F
262	0.99	23	F
191	0.89	23	F
328	0.78	24	M
333	1.14	24	F
471	1.39	24	F
464	0.75	24	M
284	1	24	F
150	1	24	F
330	0.85	24	F
292	1.26	24	M
o1	0.97	25	F
425	0.81	25	F
49	1.65	25	F
165	0.99	25	F
189	0.92	25	M
323	1.33	25	M
90	0.84	26	F
320	1.23	26	F
93	1.72	26	F
41	1.52	26	F
388	0.78	27	F
147	0.75	27	F
303	1.34	27	F
445	0.88	27	F
430	0.84	27	F
102	1.3	27	F
32	1	28	M
313	1.54	28	F
160	0.94	28	M
472	0.73	28	F
347	1	28	F
146	0.74	28	M
222	1.1	28	F
Ra	1	28	F
305	1.51	29	F
383	0.92	29	F
207	1	29	F
37	0.81	29	M
73	1.12	29	M

187	0.96	29	M
104	0.74	29	F
23	0.71	29	-
31	0.92	30	F
269	0.84	30	F
1	0.88	30	M
271	1.23	30	F
372	0.93	30	M
27	0.75	30	-
595	1.71	35	M
188	1.21	37	M
596	0.88	38	M
192	0.78	39	M
597	0.94	40	-
194	1	43	F
584	0.79	45	-
591	0.53	60	F
592	0.51	60	M
579	0.4	64	M
590	0.47	66	M
570	0.56	67	M
574	0.5	74	M
588	0.51	75	F
572	0.61	78	F
580	0.61	78	M
587	0.61	80	M

Age groupe	**Number**	**Mean**	**Stdev.**	**Max**	**Min**
1--10	8	1.79	0.80	3.41	0.9
11 --20	18	1.30	0.37	1.94	0.73
21--30	65	1.03	0.24	1.72	0.71
31-45	7	1.04	0.33	1.71	0.78
46- 80	10	0.53	0.07	0.61	0.4

Appendix 2: Telomere length in healthy individuals (control) according to gender

Category (all ages)	**Number**	**Mean**	**Stdev.**	**Median**	**Mean of age (years)**
Females-control	63	1.15	0.45	1.0	24.5
Males-control	40	0.98	0.37	0.94	31.4

Category (20-30 years)	**Number**	**Mean**	**Stdev.**	**Median**	**Mean of age(years)**
Females-control	46	1.05	0.26	1.0	25.1
Males-control	24	0.99	0.19	0.95	25.0

Appendix 3: Estimation of telomere length between NBS-homozygotes and controls

DNA number	**Relative telomere lengths**	**Age (years)**	**Sex**
13720	1.62	1	M
12207	1.48	1	M
13424	1.29	1	F
6645	0.3	1	F
5342	0.21	1	M
6018	0.68	2	F
7105	0.44	2	F
3769	0.43	2	M
3772	0.43	2	F
7694	2.1	3	F
11766	2	3	F
8294	2.1	3	F
13607	0.98	5	F
13028	1.55	6	M
3426	1.35	6	F
8165	1	6	M
9990	1.3	6	M
11348	1.17	7	F
5202	0.67	7	F
3201	0.35	7	F
4530	0.22	7	F
8304	0.34	8	M
12557	1.13	8	-

5700	0.99	9	F
11154	1.73	10	M
7822	0.96	10	M
9028	0.78	10	F
5546	0.58	10	M
6023	1.3	12	F
13921	0.76	12	M
2552	0.69	13	M
3197	0.2	13	M
3205	1.3	14	M
3316	0.29	15	M
5567	0.64	15	M
5450	0.56	18	F
10376	0.46	19	F
5431	0.26	20	F

1-10 years:

Category	Number	Mean	Stdev.	Max	Min
Control	8	1.79	0.80	3.41	0.90
NBS-Homozygote	28	1.01	0.58	2.10	0.21

11-20 years

Category	Number	Mean	Stdev.	Max	Min
Control	18	1.30	0.37	1.94	0.73
NBS-Homozygote	10	0.65	0.39	1.30	0.20

Appendix 4: Comparison of telomere length in NBS-homozygotes according to gender

Category (all ages)	Number	Mean	Stdev.	Median	Mean of age (years)
Females NBS-homozygote	20	0.92	0.61	0.73	7.2
Males NBS-homozygote	17	0.88	0.53	0.76	8.4

Appendix 5: Estimation of telomere length between NBS-heterozygotes and controls

DNA number	Relative telomere lengths	Age (years)	Sex
5343	2	1	F
10130	1.51	2	M
4328	0.89	3	M
8296	1.68	3	M
3221	1	4	M
3223	2	5	F
10133	1.38	5	F
10131	0.99	5	M
10123	2.35	7	M
7234	1.56	8	F
6017	1.77	8	M
3224	1.49	10	M
10120	0.71	12	F
4787	1.31	19	M
8295	0.71	22	F
3222	1	25	F
10124	2	25	M
508	1	27	F
6024	1.3	30	F
466	1.3	30	M
7235	0.79	30	M
7824	0.75	33	M
7823	0.78	35	M
6025	0.32	40	M
4786	0.25	40	M
464	0.6	50	F
463	0.27	54	M

Age	Ctagory	Number	Mean	Stdev.	Max	Min
1 -- 10	Control	8	1.79	0.80	3.41	0.90
	NBS-Heterozygote	12	1.55	0.45	2.35	0.89
11 -- 30	Control	83	1.08	0.29	1.94	0.71
	NBS-Heterozygote	9	1.12	0.41	2.00	0.71
30 <	Control	17	0.74	0.33	1.71	0.40
	NBS-Heterozygote	6	0.50	0.24	0.78	0.25

Appendix 6: Estimation of telomere length in NBS-like patients and controls

DNA number	Relative telomere lengths	Age (years)	Sex
10703	1.26	1	M
12641	1.51	1	F
12755	1.73	1	F
12439	1.48	1	F
11694	1.21	2	M
11207	1.08	3	M
12446	0.89	3	F
11785	1.73	4	F
10889	1.23	5	F
11947	1.27	5	F
10462	1	5	M
7690	1.77	5	F
10362	1.2	6	M
11153	0.83	6	M
9414	0.93	7	M
11118	1	7	F
10603	0.71	9	M
10604	1.11	10	M
10116	0.92	11	M
12329	0.62	12	F

12129	0.66	14	M
56661	0.14	15	M
11170	1.54	27	M
06714	1.38	28	F
10272	0.64	30	F

Age	Ctagory	Number	Mean	Stdev.	Max	Min
<10	Control	8	1.79	0.80	3.41	0.90
	NBS-like	15	1.27	0.31	1.77	0.83
10 -- 30	Control	83	1.08	0.29	1.94	0.71
	NBS-like	7	0.69	0.33	1.11	0.14

Appendix 7: Estimation of telomere length in AT and FA patients and controls

DNA number	Relative telomere length	Age (years)	Sex	Syndrom
AT17	0.6	5	F	AT
L6	1.38	9	F	AT
L15	0.11	9	M	AT
88P0326	0.38	7	M	FA
I, G	0.82	7	F	FA
B, M	0.68	4	M	FA
HSC62	0.19	2	M	FA

Ctagory	Number	Mean	Stdev.	Max	Min
Control	8	1.79	0.80	3.41	0.9
AT	3	0.69	0.56	1.38	0.11
FA	4	0.52	0.29	0.82	0.19

Appendix 8: T/C-FISH data on telomere lengths of fibroblast cell lines at passage 7

Fibroblast cell line	Median of whole chromosomes (±SD)	Median of p arms (± SD)	Median of q-arms (±SD)
09P0285-control	87.9(±55.2)	91.7 (±56.1)	85.7(±58.1)
09P0752-control	87.5(±51.5)	87.5(±49.4)	88.9(±52.2)
96P0048-NBS	60.9(±37.8)	65.2(±41.5)	58.8(±37.4)
94P0112-NBS	53.7(±43.9)	53.5 (±44.7)	52.7(±43.8)
94P0496-NBS	48.5(±38.8)	51.9(±39.4)	43.3(±33.1)